

Two ABC transporters of the MRP subfamily contribute to azole tolerance and virulence of *Fusarium graminearum*

Dissertation
zur Erlangung des
Doktorgrades der Agrarwissenschaften (Dr. Agr.)

der
Naturwissenschaftlichen Fakultät III
Institut für Agrar- und Ernährungswissenschaften
der Martin-Luther-Universität Halle-Wittenberg

vorgelegt von
Herrn Reno Tryono
Geboren am 18.03.1982 in Jakarta, Indonesien

Gutachter / in:

Prof. Dr. Holger. B. Deising, Dr. Stefan G. R. Wirsal

Prof. Dr. Klaus Humbeck

Prof. Dr. Andreas von Tiedemann

Halle (Saale), 30 Mai 2016

Gedruckt mit Unterstützung des Deutschen Akademischen Austauschdienstes
Printed with support from the German Academic Exchange Service

Contents

Contents	i
Abbreviations	iv
List of figures	vii
List of tables	xii
I. Introduction	1
I.1. <i>Fusarium graminearum</i> is an important fungal species causing Fusarium Head Blight (FHB) in cereals	1
I.2. Control of <i>F. graminearum</i> using azole fungicides	5
I.2.1. Field application of azoles to control <i>F. graminearum</i>	7
I.2.2. Emergence of azole-resistant strains.....	9
I.3. Azole resistance mechanisms known in other fungi	10
I.3.1. CYP51 based mechanisms	12
I.3.2. ABC transporter based mechanisms	14
I.4. Fungal ABC transporters	15
I.4.1. Nomenclature	15
I.4.2. Biological functions of MRP transporters (ABC subfamily C)	17
I.5. Objectives of this study	19
II. Materials and methods	20
II.1. Fungal strains	20
II.2. Storage of fungal isolates.....	20
II.3. Culture media and buffers	21
II.3.1. Media	21
II.3.2. Buffers	22
II.4. Nucleic acid isolation	23
II.4.1. Small scale DNA preparation	23
II.4.2. Large scale DNA preparation	24
II.4.3. Total RNA preparation	24
II.4.4. DNA/RNA quantification	25
II.5. Nucleic acid analyses	25
II.5.1. Polymerase Chain Reaction (PCR)	25
II.5.1.1. Standard PCR	25
II.5.1.2. Double-Joint (DJ) PCR	26

II.5.1.3. Generation of Digoxigenin-labelled PCR fragments	27
II.5.2. Reverse transcription – quantitative PCR (RT-qPCR)	27
II.5.3. DNA digestion using restriction enzymes	28
II.5.4. Southern blot	29
II.5.5. DNA sequencing	30
II.6. Transformation	31
II.6.1. <i>E. coli</i> transformation	31
II.6.2. <i>F. graminearum</i> transformation	32
II.7. Fungal fitness assays	33
II.7.1. Vegetative growth	33
II.7.2. Conidia germination	33
II.8. Fungicide and plant metabolite sensitivity assay	33
II.9. Analysis of mycotoxins produced <i>in vitro</i>	34
II.10. Virulence assays	34
II.10.1. <i>Triticum aestivum</i>	34
II.10.2. <i>Zea mays</i>	35
II.10.3. <i>Hordeum vulgare</i>	35
II.11. Accession numbers	36
II.12. Vectors	36
II.13. Oligonucleotide sequences	36
III. Results	39
III.1. Verification of strains used in this study.....	39
III.1.1. Determination of the phylogenetic lineage within the <i>F. graminearum</i> species complex	39
III.1.2. Determination of the chemotype	41
III.2. Sequence analyses of <i>FgCyp51A</i> , <i>FgCyp51B</i> , <i>FgCyp51C</i> and <i>FgABC4</i> in azole resistant P1 and P2 mutants	42
III.3. Generation and characterization of deletion mutants for <i>FgABC1</i> and <i>FgABC4</i> in strains PH-1 and NRRL 13383	45
III.3.1. Generation and validation of deletion mutants	45
III.3.2. Vegetative fitness	50
III.3.3. Sensitivities against fungicides and plant metabolites	51
III.3.4. Transcript levels	53
III.3.5. Virulence levels on three host plants	54

III.3.6. Mycotoxin production	57
III.3.7. Complementation of deletion mutants with wild type alleles	58
III.4. Deletion of <i>FgABC4</i> in strain P1-11	61
III.4.1. Generation and validation of deletion mutants	61
III.4.2. Vegetative fitness	63
III.4.3. Fungicide sensitivities	64
III.4.4. Virulence levels	65
IV. Discussion	68
IV.1. The lineage and chemotype of the PH-1 and NRRL 13383 strains	68
IV.2. The role of <i>FgCYP51A</i> , <i>FgCYP51B</i> and <i>FgCYP51C</i> in azole resistance ..	71
IV.3. The role of <i>FgABC1</i> and <i>FgABC4</i> in azole resistance	74
IV.4. The role of <i>FgABC1</i> and <i>FgABC4</i> in virulence	77
V. Conclusions	81
VI. References	84
Acknowledgements	99
Curriculum vitae	100
List of publications	101
Declaration	102

Abbreviations

°C	degree Celsius
µg	microgram
A	adenine
ABC	ATP binding cassette
ADON	acetyldeoxynivalenol
ATP	adenosine triphosphate
BLAST	basic local alignment search tool
bp	base pair
C	cytosine
cDNA	complementary DNA
CRZ	calcineurin response zinc-finger protein
cv	cultivated variety
CYP51	cytochrome p450 14 α -sterol demethylase
DIG	digoxigenin
DJ-PCR	double joint - PCR
DMSO	dimethyl sulfoxide
DNA	deoxyribonucleic acid
DON	deoxynivalenol
dpa	days post anthesis
dpi	days post inoculation
EC ₅₀	effective concentration to suppress 50% of population
EDTA	ethylenediaminetetraacetic acid
ERG	ergosterol
EST	expressed sequence tags
FGSC	<i>Fusarium graminearum</i> species complex
FHB	Fusarium Head Blight
FRAC	Fungicide Resistance Action Committee
g	gravity in centrifugation
G	guanine
g/ha	gram per hectare
<i>hph</i>	hygromycin B phosphotransferase encoding gene

hpi	hours post inoculation
HPLC	high performance liquid chromatography
HSP	heat shock protein
kb	kilo base
LB/LBA	Luria Bertani / Luria Bertani Agar
M	molarity
m/s	meter per second
mg	milligram
mg/L	milligram per liter
mL	milliliter
mm	millimeter
mM	millimolar
MPa	Mega Pascal
MRP	multidrug-resistance-associated protein
<i>nat</i>	nourseothricin acetyltransferase encoding gene
NBD	nucleotide binding domain
NIV	nivalenol
NPS	non-ribosomal peptide synthetase
NRRL	northern regional research laboratory
ORF	open reading frame
P1	phenotype 1
P2	phenotype 2
PCI	phenol:chloroform:isoamyl alcohol (25:24:1)
PCR	polymerase chain reaction
PD/PDA	potato dextrose / potato dextrose agarbroth medium
PDR	pleiotropic drug resistance
pH	measure of the acidity or basicity of an aqueous solution
ppm	part per million
RF	resistance factor
RH	relative humidity
RM	regeneration medium
RNA	ribonucleic acid
RT	room temperature
RT-qPCR	reverse transcription – quantitative PCR

SBI	sterol biosynthesis inhibitor
SDS	sodium dodecyl sulfate
SNA	Spezieller Nährstoffarmer Agar
SNP	single nucleotide polymorphism
SSH	suppression subtraction hybridization
T	thymine
t/ha	ton per hectare
T _m	melting temperature
TMD	trans-membrane domain
<i>trpC</i>	tryptophan synthase C encoding gene of <i>Aspergillus nidulans</i>
U	uracil
USDA	United States Department of Agriculture
WT	wild type
ZEA	zearalenone

List of figures

- Figure 1. The life cycle of *F. graminearum* adopted from (Trail 2009). The fungus overwinters on plant debris as chlamydospores or perithecia. Mature perithecia discharge airborne ascospores that may land on flowers where they initiate infection after germination. Once the fungus successfully colonizes the head, it contaminates the grain with mycotoxins. Secondary infection may occur from dispersed conidia 2
- Figure 2. The infection pattern of *F. graminearum* in wheat adopted from (Brown et al. 2010). A) Schematic diagram of a longitudinal section of a partial wheat spike illustrating the individual parts. B) Photograph of a partial wheat spike. C - E) Progression of hyphal growth within an infected wheat spike during early, middle and late stages, respectively 4
- Figure 3. Classification of azole fungicides into five sub-classes and chemical structures of representative compounds (FRAC 2007) 7
- Figure 4. Mechanisms of azole resistance shown in *Candida albicans* adopted from (Cowen and Steinbach 2008). A) A mutation and/or an up-regulation of ERG11 or CYP51. B) A mutation and/or an up-regulation of a fungal transporter in the cell membrane. C) A mutation of ERG3 may prevent the accumulation of a toxic sterol intermediate. D) The general stress response activation by a molecular complex of calcineruin and HSP90 11
- Figure 5. Scheme of ergosterol biosynthesis in *S. cerevisiae* modified from (Lupetti et al. 2002; Onyewu et al. 2003). In the presence of azole, C14 α -demethylase encoded by *ERG11* (= *Cyp51*) is blocked. When *ERG3* is lost because of deletion or mutation, 14 α -methylfecosterol will accumulate in the plasma membrane and the fungus may survive 13
- Figure 6. Differentiation of fungal ABC transporter subfamilies based on the HUGO scheme adopted from (Kovalchuk and Driessen 2010). TMS, trans-membrane segment; NBD, nucleotide binding domain; NTE, N-terminal extension; R, ~120 amino acid residues 17
- Figure 7. Sequence analysis of *FgRED*. Top) an illustration of sequence reading. Gray boxes indicate exons, a white box an intron. Blue arrow points to the position of a SNP in NRRL 13383 differing from the PH-1 reference sequence. Bottom) phylogenetic tree of *RED* nucleotide sequences. The

- tree was obtained by the neighbor joining algorithm implemented in the software DNASTAR Lasergene MegAlign Version 7.0.0 40
- Figure 8. Sequence analysis of *FgTEF- α* . Top) an illustration of sequence reading. Gray boxes indicate exons, white boxes introns. Blue arrow points to the position of a SNP in NRRL 13383 differing from the PH-1 reference sequence. Bottom) phylogenetic tree of *FgTEF1- α* nucleotide sequences. The tree was obtained by the neighbor joining algorithm implemented in the software DNASTAR Lasergene MegAlign Version 7.0.0 41
- Figure 9. Multiplex PCR of *Tri3* (left) and *Tri12* (right) to determine the chemotypes of PH-1, NRRL 13383 and six adapted strains. Lane M: GeneRuler DNA ladder Mix; Lane 0: no-template control; Lane 1: PH-1; Lane 2: NRRL 13383; Lane 3: P1-1; Lane 4: P1-9; Lane 5: P1-11; Lane 6: P2-1; Lane 7: P2-4; Lane 8: P2-8 43
- Figure 10. A) Strategy to delete *FgABC1*. Blue arrows show the positions of primers used to detect the wild type locus by PCR and to generate a DIG-labelled hybridisation probe for the detection of the gene. Pink arrows indicate the respective primers to detect the hygromycin resistance cassette (*hph*) and to generate a *hph* probe. B) Results of PCR targeting the wild type locus in the PH-1 (left) and NRRL 13383 backgrounds (right). C) Results of Southern hybridisation detecting the wild type locus (blue) and the *hph* marker (pink) in the PH-1 (left) and NRRL 13383 backgrounds (right). Arrows indicate the expected band. Boxed lanes indicate clones used for subsequent analyses 47
- Figure 11. A) Strategy to delete *FgABC4*. Red arrows show the positions of primers used to detect the WT type locus by PCR and to generate a DIG-labelled hybridisation probe for the detection of the gene. Pink arrows indicate the respective primers to detect the nourseothricin resistance cassette (*nat1*) and to generate a *nat1* probe. B) Results of PCR targeting the wild type locus in the PH-1 (left) and NRRL 13383 backgrounds (right). C) Results of Southern hybridisation detecting the wild type locus (blue) and the *nat1* marker (pink) in the PH-1 (left) and NRRL 13383 backgrounds (right). Arrows indicate the expected band. Boxed lanes indicate clones used for subsequent analyses 49

- Figure 12. A) Kinetics of *in vitro* growth on PDA at 23⁰C during seven days. B) Percentages of conidia germination. Left and right panels provide data for strains having the PH-1 and NRRL 13383 backgrounds, respectively 51
- Figure 13. Azole sensitivity assay. A) PH-1 background, strains tested: 1. PH-1, 2. Δ FgABC1.PH.2, 3. Δ FgABC1.PH.3, 4. Δ FgABC4.PH.4, 5. Δ FgABC4.PH.15. B) NRRL 13383 background, strains tested: 1. NRRL 13383, 2. Δ FgABC1.NRRL.4, 3. Δ FgABC1.NRRL.7, 4. Δ FgABC4.NRRL.2, 5. Δ FgABC4.NRRL.3. Error bars represent SD. An asterisk indicates a significant difference between the wild type and a mutant. Significance level was determined using Student's T-Test ($P \leq 0.05$) 53
- Figure 14. Transcript levels of *FgABC1* (A) and *FgABC4* (B) as determined by RT-qPCR in NRRL 13383, Δ FgABC1-NRRL.4 and Δ FgABC4-NRRL.2. Strains were treated for 12 h with 5 mg/l tebuconazole, control cultures remained untreated. Error bars represent SD. A hashtag (#) indicates significant differences between 0 and 5 mg/l in the same strain. An asterisk (*) indicates a significant difference between wild type and a mutant for the same culture condition. Significance level was determined using Student's T-Test ($P \leq 0.05$) 54
- Figure 15. Virulence assays on three host plants. Left and right panels: strains of PH-1 and NRRL 13383 backgrounds, respectively. A) Wheat heads. B) Maize stems. C) Barley heads. An asterisk indicates a significant difference between wild type and a mutant. Significance level was determined using Student's T-Test ($P \leq 0.05$) 56
- Figure 16. Mycotoxin production of WT and the deletion mutants in PH-1 (A) and NRRL 13383 backgrounds (B). An asterisk (*) indicates a significant difference between wild type and a mutant. Significance level was determined using Student's T-Test ($P \leq 0.05$) 57
- Figure 17. PCR test of the complementation strains of *FgABC1*. A) PCR targeting the *nat1* marker. B) PCR targeting the *hph* marker. C) PCR targeting the WT allele. Whereas the WT and complementation strains show a band of 5,088 bp, the deletion strain shows a band of 4,573 bp. Lane M: GeneRuler DNA ladder Mix; lane 0: negative water control; lane 1: NRRL 13383; lane 2: Δ FgABC1.NRRL.4; lane 3-7 clones no. 5, 7, 8, 15,

18. Yellow, pink and blue arrows show primer positions to amplify *nat1*, *hph*, and WT genes, respectively. Black arrow heads point to the anticipated bands 59
- Figure 18. PCR test of the complementation strains of *FgABC4*. A) PCR targeting the *hph* marker. B) PCR targeting the *nat* marker. C) PCR targeting the WT allele. Whereas the WT and complementation strains show a band of 6,910 bp, the deletion strain shows a band of 3,864 bp. Lane M: GeneRuler DNA ladder Mix; lane 0: negative water control; lane 1: NRRL 13383; lane 2: Δ FgABC4.NRRL.2; lane 3-5 clones no. 3, 7, 8. Pink, yellow and red arrows show primer positions to amplify *hph*, *nat1* and WT genes, respectively. Black arrow heads point to the anticipated bands 60
- Figure 19. Fitness assays of complementation strains. A) The kinetics of *in vitro* growth on PDA at 23⁰C during seven days. B) Percentage of conidia germination 61
- Figure 20. Virulence assays of complementation strains on wheat heads (A) and maize stems (B). An asterisk (*) indicates a significant difference between NRRL 13383 and a mutant. Significance level was determined using Student's T-Test ($P \leq 0.05$) 62
- Figure 21. A) Strategy to delete *FgABC4* in the background of P1-11. Red arrows show the positions of primers used to detect the WT type locus by PCR and to generate a DIG-labelled hybridisation probe for the detection of the gene. Pink arrows indicate the respective primers to detect the nourseothricin resistance cassette (*nat1*) and to generate a *nat1* probe. B) Results of PCR targeting the WT locus (left) and *nat1* cassette (right). C) Results of Southern hybridisation detecting the WT locus (left) and *nat1* cassette (right). Arrows indicate the expected band. Boxed lanes indicate clones used for subsequent analyses. N=NRRL 13383, P = P1-11, 1 to 10= name of transformants 63
- Figure 22. A) Growth kinetics *in vitro* on PDA for seven days. B) Percentage of conidia germination of NRRL 13383, P1-11, three deletion mutants and one ectopic strain in the background of P1-11 64
- Figure 23. Azole sensitivity assay. A) Control treatment – no fungicide added. B) Prothioconazole 3 μ g/mL. C) Epoxyconazole 3 μ g/mL. D) Tebuconazole

3 µg/mL. E) Prochloraz 0.1 µg/mL. F) Fenarimol 3 µg/mL. Error bars represent SD. An asterisk indicates a significant difference between P1-11 against each tested strain. A hashtag indicates a significant difference between NRRL 13383 against each tested strain. Significance level was determined using Student's T-Test ($P \leq 0.05$)	66
Figure 24. Virulence assay of NRRL 13383, two <i>FgABC4</i> deletion mutants in NRRL 13383 background, adapted strain P1-11, three <i>FgABC4</i> deletion mutants in P1-11 background and one ectopic mutants in the P1-11 background on maize stem. No significant differences existed between NRRL 13383 and the other strains using Student's T-Test ($P \leq 0.05$)	67
Figure 25. Trichothecene biosynthetic pathway as proposed by (McCormick et al. 2011). The box highlights the type B trichothecenes	70
Figure 26. Model for the proposed roles of <i>FgABC1</i> in virulence and <i>FgABC4</i> in azole resistance	76

List of tables

Table 1. Components of standard PCR reaction	26
Table 2. Standard PCR program	26
Table 3. Components of DJ-PCR reaction	27
Table 4. DJ-PCR program	27
Table 5. Components of RT-qPCR reaction	28
Table 6. RT-qPCR program	28
Table 7. PCR sequencing program	31
Table 8. Vectors used in this study	36
Table 9. Oligonucleotides used in this study	37
Table 10. SNPs between PH-1 and NRRL 13383 in <i>FgCYP51A</i> , <i>FgCYP51B</i> , <i>FgCYP51C</i> and <i>FgABC4</i>	44
Table 11. List of xenobiotics used in the sensitivity assay of PH-1, NRRL 13383 and the deletion mutants	52
Table 12. List of fungicides used in the sensitivity test of mutants in P1-11 background	65

I. Introduction

I.1. *Fusarium graminearum* is an important fungal species causing Fusarium Head Blight (FHB) in cereals

Fusarium graminearum is a major fungal plant pathogen causing Fusarium Head Blight (FHB) disease in cereals. Even though, some other *Fusarium* species, alone and or together with *F. graminearum*, can also cause FHB, resulting in identical symptoms. These species form the *F. graminearum* species complex (FGSC). Back in earlier times, there were only two groups of *F. graminearum* differentiated based on the teleomorph. Group I represents a heterothallic species, which is infertile or poorly fertile, mostly unable to produce perithecia. It was later classified as *F. pseudograminearum*. Group II is homothallic and readily may form perithecia from a single culture. It was then classified as *F. graminearum* (Francis and Burgess 1977). Subsequently, it was discovered that group II is a complex of several *Fusarium* species, which were then referred to as *F. graminearum* sensu lato or FGSC. Six single copy nuclear genes encoding ammonia ligase, 3-*O*-acetyltransferase, phosphate permease, reductase, β -tubulin and translation elongation factor 1- α were used to distinguish seven lineages or species within the *F. graminearum* clade (O'Donnell et al. 2000). These species were designated as *F. austroamericanum* (lineage 1), *F. meridionale* (lineage 2), *F. boothii* (lineage 3), *F. mesoamericanum* (lineage 4), *F. acaciae-mearnsii* (lineage 5), *F. asiaticum* (lineage 6) and *F. graminearum* (lineage 7). Additional genes encoding histone H3 and four mating type genes (*Mat1-1-1*, *Mat1-1-2*, *Mat1-1-3*, *Mat1-2-1*) have uncovered an additional two species (O'Donnell et al. 2004). The species are *F. cortaderiae* (lineage 8) and *F. brasiliicum* (lineage 9). Later on, other new species were discovered i.e. *Fusarium* sp. NRRL 34461, *F. gerlachii* and *F. vorosii* (Starkey et al. 2007), *F. aethiopicum* (O'Donnell et al. 2008), *F. ussurianum* (Yli-Mattila et al. 2009), *F. nepalense* (Desjardins and Proctor 2011) and *F. louisianense* (Sarver et al. 2011). Therefore, in total there are currently 16 lineages representing 16 species of FGSC that had been identified worldwide (Aoki et al. 2012). *Fusarium graminearum* lineage 7 (= *F. graminearum* sensu stricto) kept the original name and it is this species that was used in this study.

Fusarium graminearum infects several cereal plants. Wheat, barley and maize are well known hosts (Bai and Shaner 2004; Scauflaire and Mahieu 2011). The fungus overwinters in plant debris as chlamydospores or perithecia that in spring forcibly discharge airborne

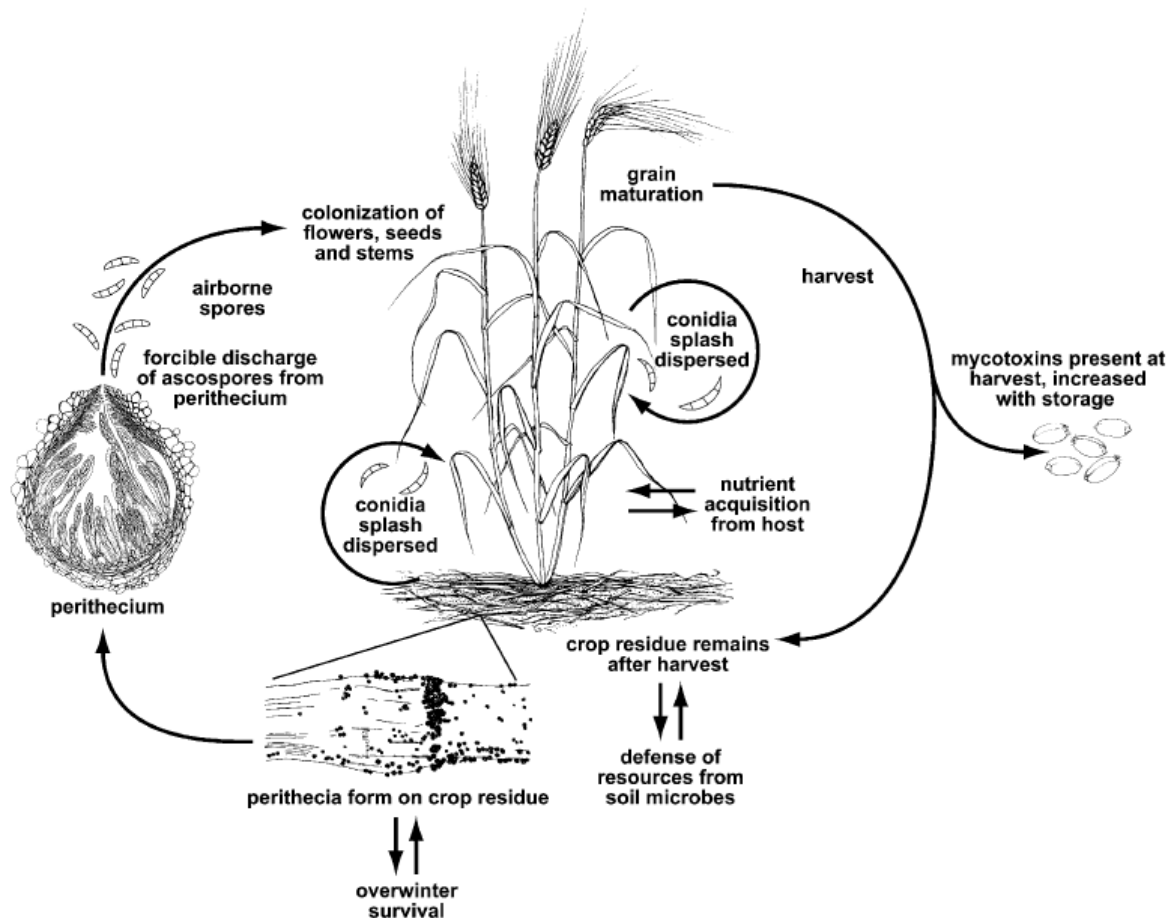


Figure 1. The life cycle of *F. graminearum* adopted from (Trail 2009). The fungus overwinters on plant debris as chlamydospores or perithecia. Mature perithecia discharge airborne ascospores that may land on flowers where they initiate infection after germination. Once the fungus successfully colonizes the head, it contaminates the grain with mycotoxins. Secondary infection may occur from dispersed conidia.

ascospores as the primary inoculum (Wegulo et al. 2008; Trail 2009) (Figure 1). Trail et al. (2005) studied the mechanical power of the perithecia that eject ascospores with a launch speed of more than 34.5 m/s. Such speed requires 1.54 MPa pressure and an acceleration of 870,000 g inside the ascus. This is the highest acceleration reported in a biological system. Wind and water splash assist ascospores to reach the florets where warm and humid conditions favour germination. The optimum conditions for ascospore germination are 20°C, 100% RH and pH 3.76. Light intensity is not a key factor for spore germination (Beyer and Verreet 2005).

In favourable conditions, the fungus forms thin and unbranched germ tubes and a dense mycelia network in stomatal cavities 6 to 24 hours post inoculation (hpi) (Pritsch et al. 2000; Wanjiru, Zhensheng, and Buchenauer 2002). At 24-36 hpi, the fungus forms infection hyphae, which invade the ovary and inner surface of the lemma and palea. Once the fungus enters the anthers, the palea is heavily colonized. Those cells having direct contact with the fungus show physical damage and alterations in the cells of ovary, lemma and rachis (Wanjiru et al. 2002, Trail 2009). At this stage, symptoms such as water soaking can be observed. The fungus spreads to neighbouring spikelets through the xylem and pith (Brown et al. 2010) (Figure 2). At three days post inoculation (dpi), the mycelia starts to spread into neighbouring spikelets (Trail 2009). Heavy colonization causes visible bleached to blight symptoms on the spikelets. Secondary infection may result from macroconidia produced from asexual hyphae within the infected spikes (Pasquali and Kistler 2006).

Fusarium graminearum causes not only significant yield losses but also contaminates the grain with mycotoxins. The fungus secretes Zearalenone (ZEA) and trichothecene of type B such as Deoxynivalenol (DON) and Nivalenol (NIV), which are toxic to humans and livestock. The Joint Expert Committee on Food Additives has set a maximum consumption level of 1 µg of DON per kilogram of body weight in the daily diet (Nakajima 2010). Based on a typical trichothecene produced, *F. graminearum* has been classified into three chemotypes, 3-ADON (3-*O* acetyl DON), 15-ADON (15-*O* acetyl DON) and NIV. DON has been shown to be a virulence factor in the infection of wheat since it is required to assist the fungus to invade the neighbouring spikelets (Jansen et al. 2005). A *TR15* deletion mutant impaired in the production of DON remained restricted to the initially infected spikelet. On the other hand, NIV seems important for the infection of maize. A deletion mutant generated from a NIV producing strain showed significant lower virulence levels in the maize ear when compared to the WT (Maier et al. 2006).

The transcription profiles of genes related to mycotoxin production and other proteins of *F. graminearum* during infection in different host plants had been studied. The transcriptome of *F. graminearum* in wheat heads revealed 355 differentially expressed genes. Most of them (72.6%) encoded putative proteins with unknown functions. These proteins were predicted to be involved in allantoin and allantoate transport, detoxification processes, nitrogen, sulphur and selenium metabolisms, secondary metabolisms, carbohydrate

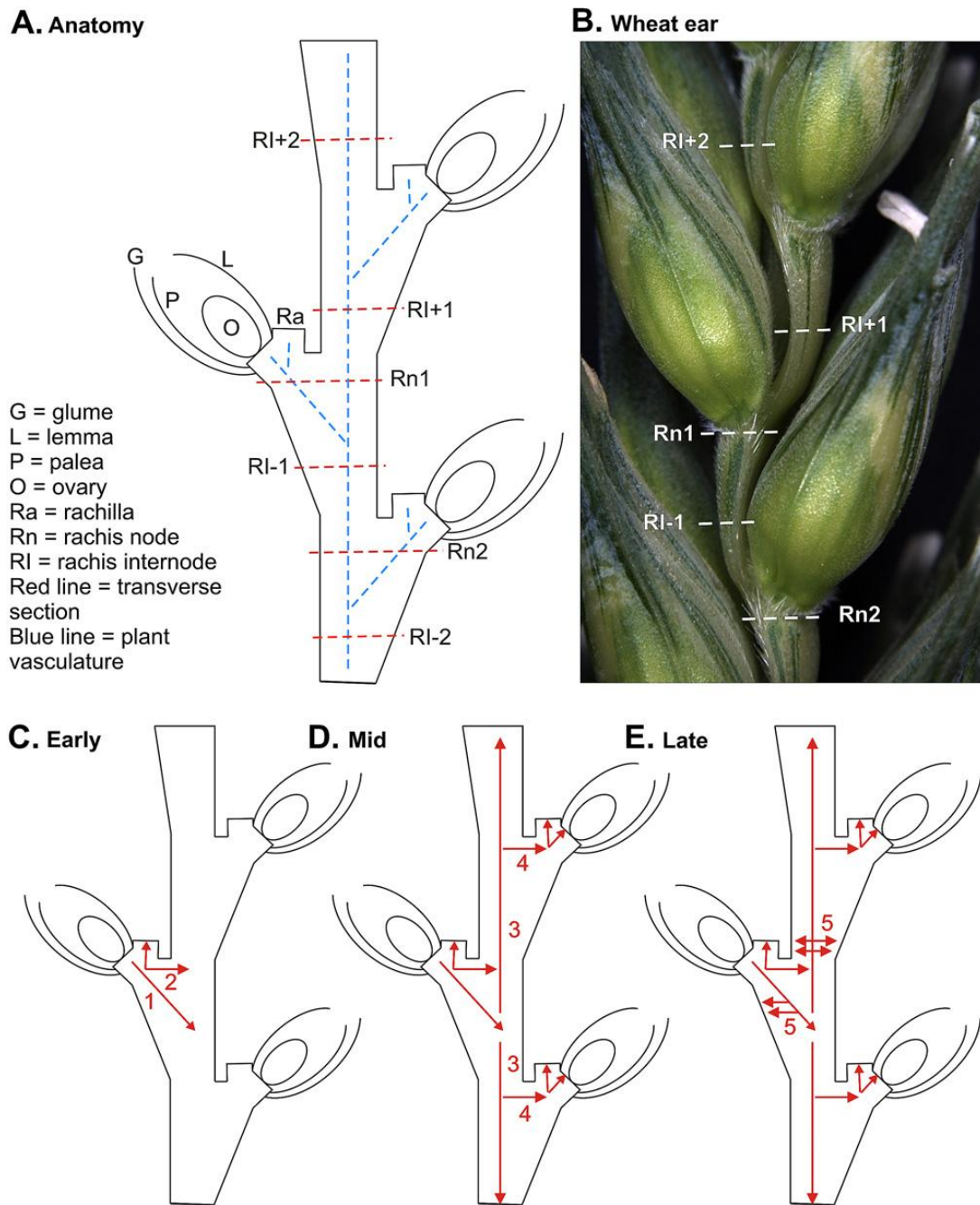


Figure 2. The infection pattern of *F. graminearum* in wheat adopted from (Brown et al. 2010). A) Schematic diagram of a longitudinal section of a partial wheat spike illustrating the individual parts. B) Photograph of a partial wheat spike. C - E) Progression of hyphal growth within an infected wheat spike during early, middle and late stages, respectively.

metabolisms, degradation of polysaccharides and ester compounds (Lysøe, Seong, and Kistler 2011).

From the plant side, a cDNA microarray consisting of 5739 expressed sequence tags (EST) was derived from Suppression Subtraction Hybridization (SSH) analysis of wheat spikes infected with *F. graminearum* (Golkari et al. 2007). One hundred eighty five ESTs (3.2%) were up-regulated and 16 ESTs (0.28%) were down-regulated. About half of the up-regulated ESTs (46.67%) had homologues in other plants with sequences of unknown function. The remaining ESTs showed homology with genes involved in plant defence responses, oxidative-burst, regulatory functions, protein synthesis, and the phenylpropanoid pathway (Golkari et al. 2007). In another study, genes related to jasmonate and ethylene signalling, lipid-transfer protein, thionin, defensin and GDSL-like lipase genes were also up-regulated (Gottwald et al. 2012).

In barley spikes, 467 genes were differentially expressed during infection of *F. graminearum* as determined with an Affymetrix GeneChip probe array (Boddu et al. 2006). These genes encoded defence response proteins, oxidative burst-associated enzymes and enzymes of the phenylpropanoid pathway. Most of the transcripts were detected at 72 hpi, suggesting an important time point in barley-*F. graminearum* infection. In spite of that, a control strategy such as fungicide application that prevents early infection of *F. graminearum* on the host plant might be an effective strategy in reducing the potential risk of higher disease severity and toxin contamination of the grains.

I.2. Control of *F. graminearum* using azole fungicides

Wheat management practices provide several approaches for the control of *F. graminearum*. Cultivation practices, cultivar resistance, biological and chemical control approaches have been applied to control FHB (Pirgozliev et al. 2003). Cultivation practices involve crop rotation, fertilizer application and weed control to reduce fungal inoculum in the field. A resistant cultivar may possess morphological characters that confer improved survival during FHB attack. In wheat, type I resistance describes a physical or chemical block preventing the initial infection, while type II resistance inhibits the spreading of *F. graminearum* from the initially infected to the neighbouring spikelets (Beyer et al. 2006; Langevin, Eudes, and Comeau 2004; Foroud 2011). Biological control employs antagonistic fungi, bacteria and viruses. *Microsphaerosis* sp., *Phoma betae*, *Bacillus* spp., *Cryptococcus* sp. (Pirgozliev et al. 2003) and double stranded RNA viruses from the family Hypoviridae are examples of antagonists that control *F. graminearum* in laboratory and glass house conditions

(Wang et al. 2013). However, up to now disappointing results were achieved when these agents were up-scaled for field application. In contrast, chemical control provides a fast and effective measure to prevent early infection by *F. graminearum* and subsequent mycotoxin accumulation in the grains.

Several groups of fungicides with different modes of action have been used to control *F. graminearum*. Captan from the phthalimides group (FRAC Nr. M4) and oxin-copper from the polyoxin group (FRAC Nr. 19) were shown to be as effective as tebuconazole from the triazole group (FRAC Nr. 3) in suppressing DON accumulation (Nakajima 2010). Even though it is mostly the sterol biosynthesis inhibitors (SBI), mainly triazoles (FRAC Nr. 3; a subclass of azole) that have consistently produced good results, and have thus been recommended for commercial application in the field (McMullen et al. 2008; Osborne and Stein 2007).

Azoles have been widely used to control many human and plant fungal pathogens (Troesken 2005; Faro 2010). An azole compound, benzimidazole, was first described by Woolley (1944). Afterward, the first commercial product, chlormidazole, was introduced into the market in 1958, but other azole products such as miconazole started to become popular and dominated the fungicide market after the 1970s (Sheehan, Hitchcock, and Carol 1999). According to the chemical structure, azole contains a five-member atom heterocyclic ring (azole ring) in which at least one of the atoms must be nitrogen (Fera and Sarro 2009; Sharma and Bhatia 2011). The most widely-used subgroup of azole, the triazole, contains three nitrogen atoms in the azole ring (Saag and Dismukes 1988). Other subgroups of azole i.e. imidazole, pyrimidine, pyridine and piperazine contain two nitrogen atoms (Figure 3) (Saag and Dismukes 1988). Principally, azole inhibits ergosterol biosynthesis, the major sterol component of the fungal cell membrane. The number 4 nitrogen atom of the triazole ring binds to a ferric heme iron of the cytochrome P450-dependent enzyme lanosterol 14- α -demethylase which inhibits its activity (Nowaczyk and Modzelewska-Banachiewicz 2008; Musiol and Kowalczyk 2012). Therefore, the demethylation step required to convert 14 α -methylsterols is inhibited. Consequently, ergosterol is depleted and alternate toxic 14 α -methylergosta-8,24-dien-3,6-diol accumulates, as shown in *C. albicans* (Lo et al. 2005). This concomitant effect interferes with ergosterol production, membrane fluidity and other membrane-bound enzyme activities such as chitin synthase (Maertens 2004). Growth inhibition and fungal death may come as the final result.

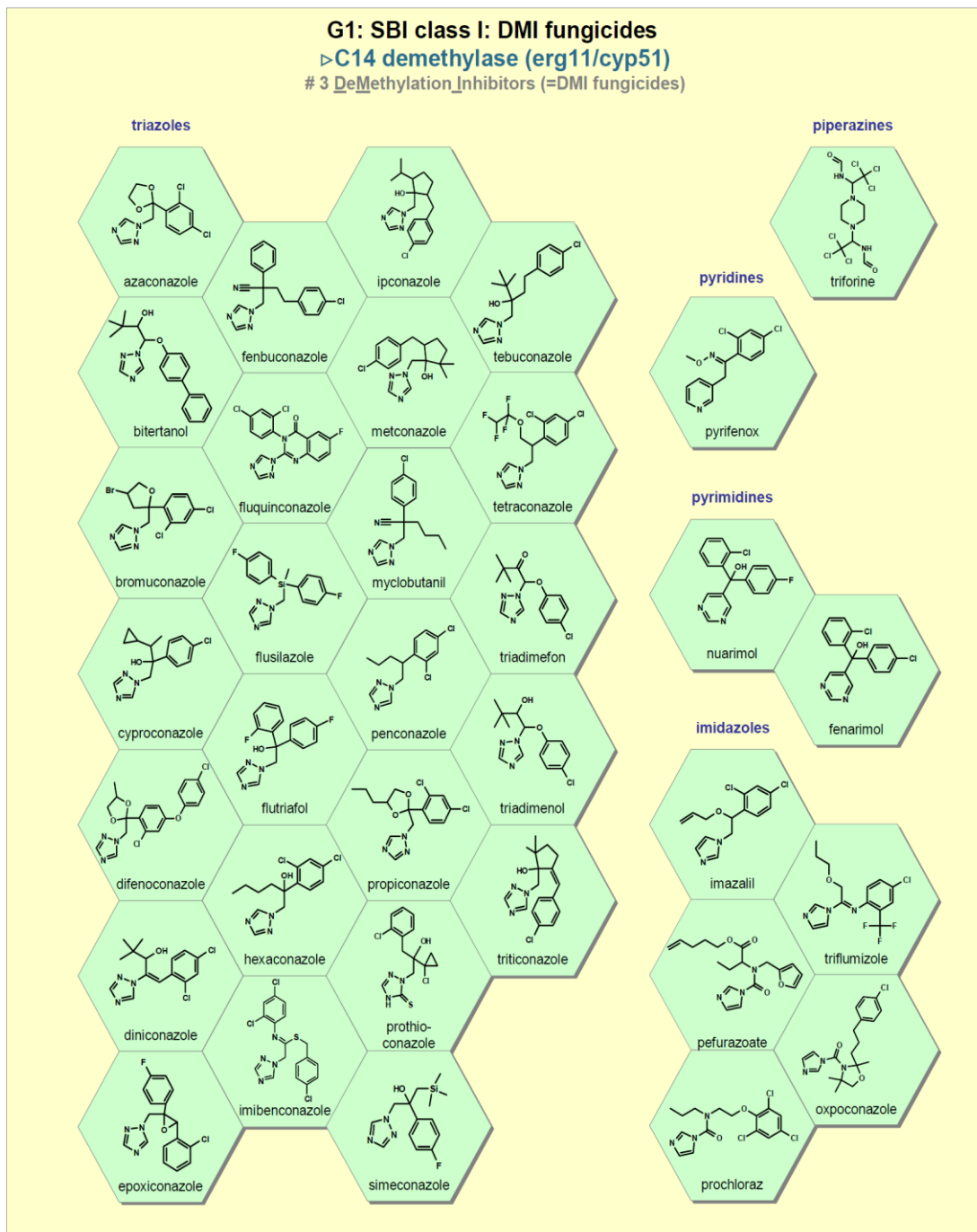


Figure 3. Classification of azole fungicides into five sub-classes and chemical structures of representative compounds (Fungicide Resistance Action Committee 2007).

I.2.1. Field application of azoles to control *F. graminearum*

Fungicide application during wheat cultivation is a common practice among farmers to control FHB. Chemical treatment is important for wheat production in the USA and

elsewhere because of the fast and devastating effect FHB may have on yield. In addition, the legal threshold values for mycotoxins must be met. In Europe, it has been estimated that 1,071 million Euro per annum has been spent on azole fungicides in the last decade by Denmark, UK and France (Blake, Wynn, and Jørgensen 2011). Thus, attempts are now focused on optimizing the dosage and timing of azole applications in the field.

The efficacy of azoles in controlling *F. graminearum* and *F. culmorum* in field scales was evaluated in Italy from 2001 until 2003 in two winter wheat varieties, i.e. the susceptible cv. Serio and the moderately resistant cv. Guadalupe. The treatment with azoles (tebuconazole or prochloraz) at the middle of the anthesis stage resulted in a 52% reduction in disease incidence, a 48% reduction of DON concentration and a 20% yield increase (Blandino, Minelli, and Reyneri 2006). Furthermore, application of metconazole alone and a mixture of prochloraz plus epoxyconazole successfully reduced FHB severity 12 and 13% respectively (Blandino et al. 2011). Similar research was conducted using different azoles. Mixtures of cyproconazole plus prochloraz and tebuconazole plus azoxystrobin significantly reduced FHB severity by 25% and 77% and DON content by 32% and 89%, respectively (Haidukowski et al. 2005). In addition, prothioconazole application at the beginning of wheat anthesis significantly reduced FHB severity from 39% to 93%, reduced DON level from 40% to 91%, and increased yield from 0.4 to 5.6 t/ha (Haidukowski et al. 2012).

Anthesis has become the recommended time for azole application since this is the crucial period when infection of wheat by *F. graminearum* occurs. Triazole application at anthesis reduced DON content up to 53% \pm 4% in wheat compared to the untreated control (Beyer et al. 2006). Application of each 60 g/ha triadimefon and 120 g/ha propiconazole at anthesis and four days post anthesis (dpa) was observed whereas *F. graminearum* was inoculated at two dpa. At all stages of application, both fungicide significantly reduced DON levels by 39-61% and 34-79%, respectively (Boyacioglu, Hettiarachchy, and Stacks 1992). (Yoshida et al. 2012) reported that anthesis is a critical time for controlling FHB incidence while the late milk stage around 20 dpa is crucial only for controlling mycotoxin contamination significantly. Thus, the period starting from anthesis until the late milk stage is the critical period for controlling both FHB incidence and mycotoxin contamination.

1.2.2. Emergence of azole-resistant strains

An intensive application of azoles in the field increases the risk of developing fungal strains with resistance. As an example, epoxiconazole showed the highest inhibition against *F. graminearum* strains that were isolated in 1987 better than those isolated in 1994, 1999, and 2004 (Klix, Verreet, and Beyer 2007). The efficacy of epoxiconazole has been decreasing on average by 0.22% per year. While this might not seem to be very critical when considering the long period of time that this fungicide has been applied it does highlight the need for continued research (Klix, Verreet, and Beyer 2007). Other triazole fungicides, for instance metconazole and tebuconazole exhibited an increasing EC₅₀ value by a factor of 1.39 for each, during 10 years (Klix, Verreet, and Beyer 2007). Overall, the effective triazole concentration required to control *F. graminearum* has increased by a factor of 2.95 during 10 years in Germany (Klix, Verreet, and Beyer 2007). A similar study was conducted in the state of New York, USA, where one out of 50 field isolates of *F. graminearum* exhibited higher resistance levels to tebuconazole (Spolti et al. 2014). The EC₅₀ value of this resistant isolate was 8.09 mg/L compared to 0.28 mg/L for the most susceptible isolate (Spolti et al. 2014). In addition, in tebuconazole-treated spikes the DON level of 123.35 mg/kg of samples found in infections with resistant isolates was significantly higher, compared to 23.73 mg/kg for the sensitive isolate (Spolti et al. 2014). This may result from the intensive use of tebuconazole that is commonly applied in North American wheat production to control FHB.

The azole concentration required to control *F. graminearum* is increasing, potentially as an indication of slowly developing quantitative resistance in field populations. A survey was conducted in Serbia from 2005 to 2006 to test the resistance levels of eight *F. graminearum* field isolates against difenoconazole, prothioconazole and thiophanate-methyl (Rekanović, Mihajlović, and Potočnik 2011). The highest resistance factors (RF) observed in this study were 11.34 for difenoconazole, 5.38 for prothioconazole and 5.29 for thiophanate-methyl with EC₅₀ values of 19.16, 9.69 and 64.03 mg/L, respectively (Rekanović, Mihajlović, and Potočnik 2011). Those concentrations are much higher than the metconazole concentrations tested against 101 field isolates collected from Japan, which found a minimum inhibitory concentration range from 0.20-1.56 mg/L and an EC₅₀ value of <0.1 mg/L (Tateishi et al. 2010).

From 2007 to 2008, 118 *F. asiaticum* and 41 *F. graminearum* isolates were collected from infected wheat heads in different regions in China where tebuconazole and prochloraz

have never been used before. Among those isolates, *F. graminearum* HN8 and *F. asiaticum* JS3 and JS6 were the most resistant isolates against tebuconazole with EC₅₀ values of 6.24, 4.15 and 4.52 mg/L. Similarly, these three isolates also showed also high resistance levels to the imidazol prochloraz with EC₅₀ values of 4.58, 1.47 and 2.89 mg/L (Yin et al. 2009). The reason for this may be an intensive use of the triazole triadimefon for controlling powdery mildew by farmers in China. Thus, these strains might have developed a resistance against other azole fungicide such as tebuconazole and prochloraz.

Since these studies have indicated that quantitative azole resistance is developing in *F. graminearum* field populations, further studies have established an in vitro model for analysing this phenomenon. *F. graminearum* NRRL 13383 was grown submerged in a liquid medium with a high, but sublethal dose of tebuconazole (10 mg/L) for 33 days. From such cultures, isolates were recovered by single spore purification and then inoculated on PDA medium amended with 10 mg/L tebuconazole. Surprisingly, among the arising colonies two distinct phenotypes, called P1 and P2, were observed. The P1 strains had a higher resistance to triazoles, whereas the P2 strains had acquired cross-resistance to amine fungicides (Becher et al. 2009). The mechanism on how *F. graminearum* could adapt to such high fungicide concentration is being investigated.

I.3. Azole resistance mechanisms known in other fungi

Resistance mechanism against azoles has been studied especially in human fungal pathogens, for instance *Candida albicans*. In this species, four possible mechanisms were described (Figure 4) (Cowen and Steinbach 2008). First, mutation and or up-regulation of *CYP51* syn. *ERG11* that encodes for lanosterol 14 α -demethylase, the molecular target of azoles. Mutation in *CYP51* at a certain position alters the protein structure and lowers the binding affinity to azole (Lupetti et al. 2002; H. J. Cools et al. 2006; Becher and Wirsal 2012). Up-regulation of *CYP51* ensures sufficient ergosterol biosynthesis production in the presence of azole (Hans J. Cools et al. 2007; Becher et al. 2011; Hans J Cools et al. 2012). Second, a mutation and or up-regulation of transporter genes encoding drug efflux pump proteins may also increase tolerance to azoles (Coleman and Mylonakis 2009; Cannon et al. 2009; Guo et al. 2012). Third, when *ERG11* is blocked by an azole, the biosynthesis of ergosta-5,7,22-trien-3 β -ol (ergosterol) is diverted to the production of 14 α -methylergosta-8,24-dien-3,6-diol, which leads to a failure of respiration (Prasad, Sethumadhavan, and

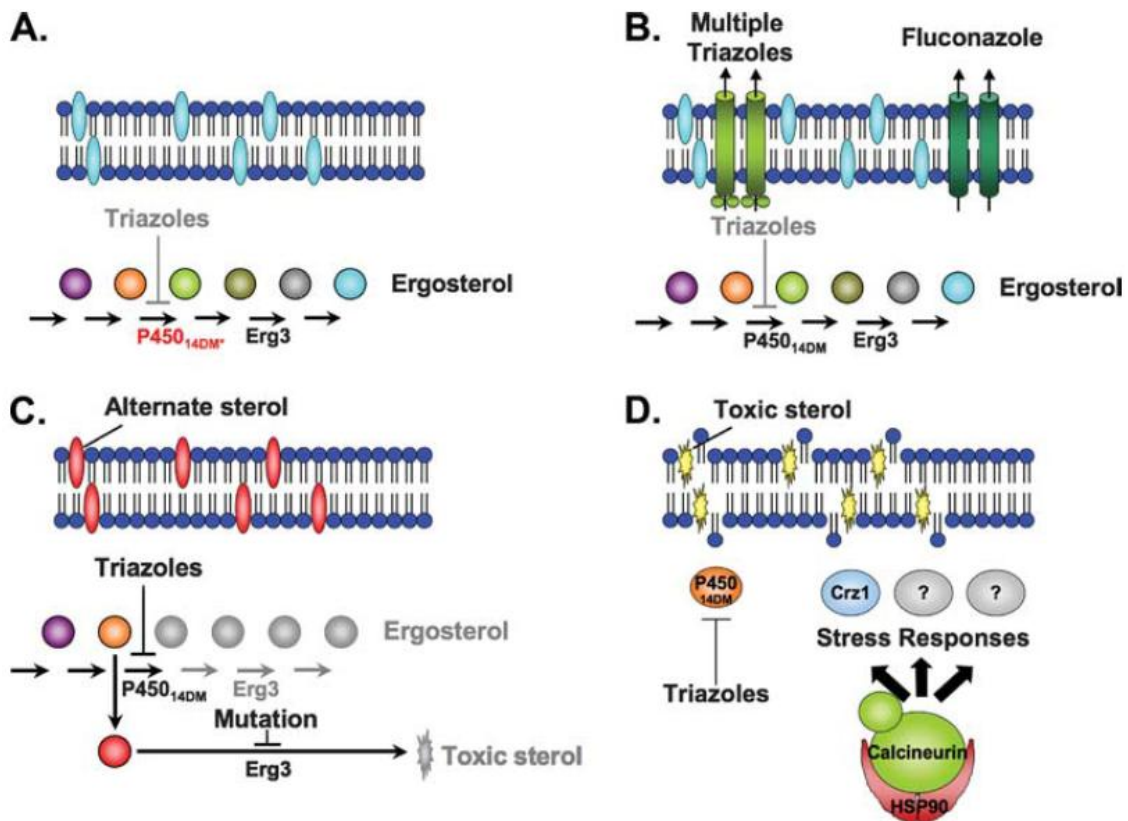


Figure 4. Mechanisms of azole resistance shown in *Candida albicans* adopted from (Cowen and Steinbach 2008). A) A mutation and/or an up-regulation of ERG11 or CYP51. B) A mutation and/or an up-regulation of a fungal transporter in the cell membrane. C) A mutation of ERG3 may prevent the accumulation of a toxic sterol intermediate. D) The general stress response activation by a molecular complex of calcineurin and HSP90.

Fatima 2011; Musiol and Kowalczyk 2012). This is caused by activity of delta 5,6-desaturase encoded by *ERG3*, which is responsible for the *cis* removal of hydrogen from the alpha positions of carbon 5 and 6 in the 14 α -methylfecosterol (Smith and Parks 1993). When *ERG3* is deleted or mutations in it occur, episterol is formed instead and the fungus still can grow. Fourth, HSP90 binds the catalytic subunit of calcineurin to assist this client protein's folding. This chaperone activates a key effector of the calcineurin-dependent response to azole i.e. the transcription factor CRZ1. Calcineurin is a protein phosphatase that dephosphorylates CRZ1. Upon this, CRZ1 is translocated to the nucleus to regulate gene transcription to counter azole stress (Cowen et al. 2006; Cowen 2009).

In fungal phytopathogens, azole resistance has been observed in *Mycosphaerella graminicola* (Mullins et al. 2011; Hans J. Cools and Fraaije 2013), *Pyrenophora tritici-*

repentis (Reimann and Deising 2005), *Nectria haematococca* (Akallal et al. 1998), *Botrytis cinerea* (Hayashi et al. 2001; Hayashi, Schoonbeek, and De Waard 2002) and *F. graminearum* (Yin et al. 2009; Spolti et al. 2014). In all of these species either CYP51 and/or drug transporter proteins were found to be involved in resistance. This indicates how important both proteins are in azole resistance.

I.3.1. CYP51 based mechanisms

Lanosterol 14 α -demethylase, a member of the cytochrome P450 family (CYP51) protein, catalyses a methyl removal reaction at position C14 of lanosterol at an intermediate stage of ergosterol biosynthesis (Figure 5). In the presence of a triazole, the nitrogen atom No. 4 displaces the water molecule as the sixth ligand in the heme iron of lanosterol 14 α -demethylase (Musiol and Kowalczyk 2012). Consequently, lanosterol stays methylated and thus inactive for ergosterol biosynthesis, leading to a depletion of that essential sterol in membranes. These effects result in direct membrane damage and inhibition of fungal growth (Saag and Dismukes 1988; Maertens 2004). Azole resistant strains have been found in several fungal species with mutations in CYP51, which lowers the affinity of azoles to the enzyme.

An up-regulation of CYP51 expression, caused by mutations in its promoter or in a gene for a transcription factor regulating *Cyp51*, could provide a more active enzyme, which would counteract the inhibition by azole. In resistant strains of *C. albicans*, it is known that *CYP51* alleles may have two nucleotide substitutions that lead to amino acid changes, i.e. Y132H and F145L (Bellamine, Lepsheva, and Waterman 2004). The strain having both mutations has a 10-fold increased resistance to fluconazole (Bellamine, Lepsheva, and Waterman 2004). Nevertheless, it was discovered that F145L was responsible for the resistance and not the Y132H mutation. F145 is part of the active binding site of fluconazole (Bellamine, Lepsheva, and Waterman 2004). CYP51 mutations are also involved in azole resistance in *M. graminicola*. The Y137F mutation confers resistance to triadimenol, I381V confers resistance to tebuconazole and V136A confers resistance to prochloraz (Mullins et al. 2011). The mutation Y459/G460 is commonly found in populations that show a high resistance to azoles (Mullins et al. 2011).

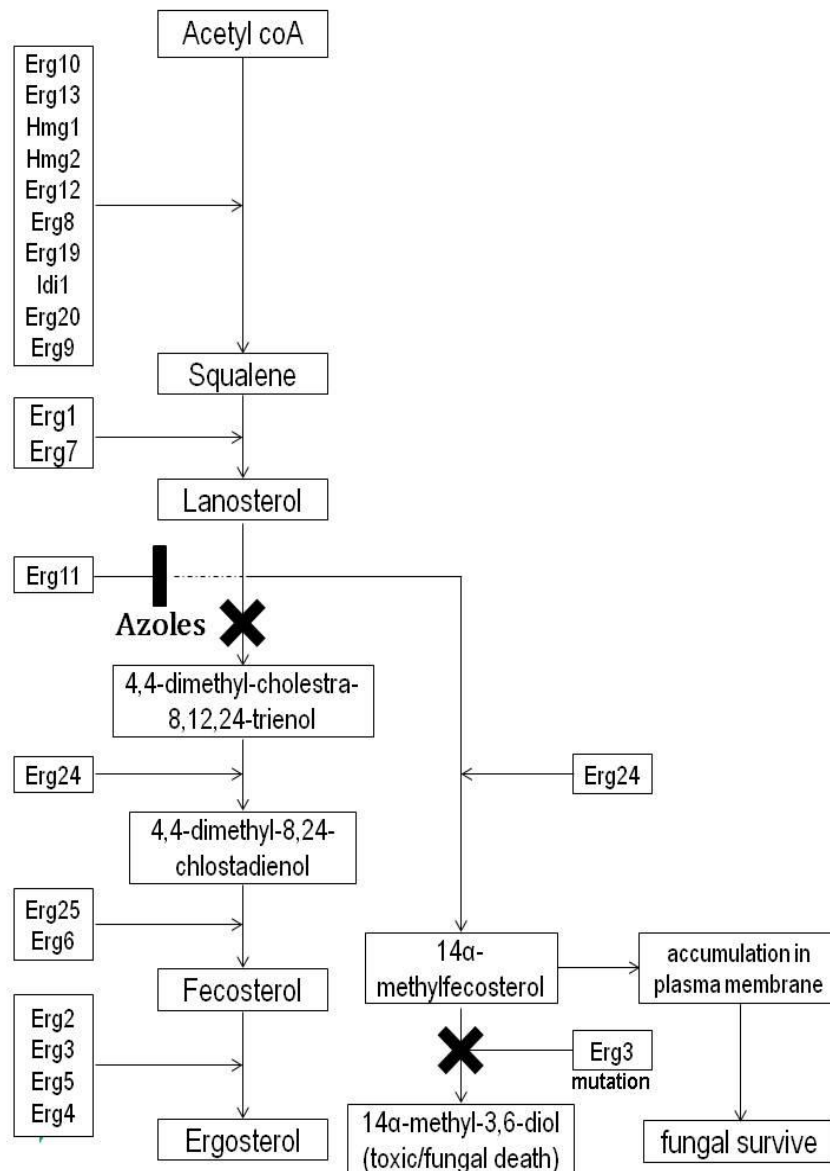


Figure 5. Scheme of ergosterol biosynthesis in *S. cerevisiae* modified from (Lupetti et al. 2002; Onyewu et al. 2003). In the presence of azole, C14 α -demethylase encoded by *ERG11* (= *CYP51*) is blocked. When *ERG3* is lost because of deletion or mutation, 14 α -methylfecosterol will accumulate in the plasma membrane and the fungus may survive.

Nevertheless, *CYP51* mutations are not always involved in the emergence of azole resistance. This was shown in field isolates of *F. graminearum* collected in China where azole resistance was not correlated with sequence variation in *CYP51* (Yin et al. 2009). Similarly, no mutation of three *CYP51* encoding genes was found in six strains of *F. graminearum* that were selected *in vitro* as azole resistant (Becher et al. 2009; this study). These strains exhibited an up-regulation of all *CYP51* encoding genes in the presence of 5

mg/L tebuconazole based on microarray and RT-qPCR analysis (Becher et al. 2011). Interestingly, some ABC transporter encoding genes were also up-regulated as well, suggesting a putative contribution of ABC transporters in azole resistance.

I.3.2. ABC transporter based mechanisms

As mentioned above, the contribution by ABC transporters is also important for fungal azole resistance. These transporters are required to move a range of substances including cytotoxic drugs across membranes. Increased tolerance to azoles may result from a mutation in a gene encoding an ABC transporter that changes protein structure. Beyond, a mutation in the promoter region of such genes may affect the efficiency of their transcription. However, it is also possible that a mutation may occur in a gene encoding a transcription factor that regulates ABC transporter expression. In consequence, all these mutations will enhance the capability of the fungus to extrude azoles from the cell resulting in increased tolerance.

Mutations in ABC transporters that contribute to azole resistance have been identified amongst others in *S. cerevisiae*. The multidrug resistance protein Pdr5 confers azole resistance through active efflux of the drugs. It is known that the amino acid at position 1352 located in the short intracellular loop No. 4 is important for drug efflux function. A change from alanine to methionine at that position decreases the mutants ability to grow in a medium amended with 3 µg/mL fluconazole and 75 ng/mL cycloheximide (Guo et al. 2012).

Another azole resistance mechanism involving ABC transporters is the up-regulation of their expression to increase cellular pump activities. Microarray analysis revealed that seven ABC transporters of *F. graminearum* were significantly up-regulated in response to a treatment with 5 ppm tebuconazole for 12 hours with at least four fold changes compared to the untreated cultures (Becher et al. 2011). Another study, using Deep Serial Analysis of Gene Expression (DeepSAGE), found that 15 of the *F. graminearum* ABC transporters were significantly up-regulated in response to a treatment with 2.5 mg/L tebuconazole for 6 hours. Transcript levels of these genes increased from 0.3 to 11.51-fold compared to an untreated control (Liu et al. 2010), underlining the roles of ABC transporters in mediating azole tolerance.

I.4. Fungal ABC transporters

The ATP – binding cassette (ABC) transporter is one of the largest protein families and found in all biological species (Higgins 2001), although different species have different numbers of ABC transporter proteins. Based on *in silico* analysis, 49 ABC transporters were found in *Homo sapiens*, 28 in *Saccharomyces cerevisiae*, 56 in *Drosophila melanogaster*, 56 in *Caenorhabditis elegans*, 129 in *Arabidopsis thaliana*, 70 in *Neurospora crassa*, 58 in *Fusarium graminearum*, 35 in *Magnaporthe oryzae* and 49 in *Aspergillus nidulans* (De Waard et al. 2006).

ABC transporters use energy from adenosine triphosphates (ATP) hydrolysis to transport various substrates across cell membranes (Del Sorbo, Schoonbeek, and De Waard 2000). The proteins are inserted in the plasma membrane or in organelle membranes such as vacuoles, mitochondria and peroxisomes (Kang et al. 2011). ABC transporters comprise trans-membrane domains (TMD) and nucleotide-binding domains (NBD) located in the cytoplasm. Each TMD consists of six transmembrane segments (TMS). ABC transporters comprising two TMDs and two NBDs are called full length, while those composed of one TMD and one NBD are called half-length ABC transporters (Kovalchuk and Driessen 2010). NBDs are characterised by conserved motifs called walker A (G-(X)4-G-K-(T)-(X)6-I/V), ABC (L-S-G-G-(X)3-R-hydrophobic- X-hydrophobic-A), and walker B motifs (R/K-(X)3-G-(X)3-L-(hydrophobic)4-D) (De Waard et al. 2006). However, the topology of TMDs and NBDs structure varies among ABC transporters, which has implications for function and nomenclature.

I.4.1. Nomenclature

ABC transporter classification is based on protein structure. In general ABC transporters consist of two TMDs embedded in the membrane bilayer, and two NBDs located in the cytoplasm (Rees, Johnson, and Lewinson 2009). The two TMDs or two NBDs might be encoded from the same or different genes that translate one to four polypeptide chains (Procko et al. 2009). The TMDs motifs are variable indicating diverse substrates to be translocated by these proteins. In contrast, the NBDs are highly conserved. However, all ABC transporter proteins must have at least one NBD with the characteristic of Walker A and Walker B motifs (Kovalchuk and Driessen 2010).

Implementing the Human Genome Organization (HUGO) classification scheme for ABC transporters, Kovalchuk & Driessen (2010) used the genome sequences of 27 fungal species representing five phyla and 18 orders to classify all 1109 predicted ABC transporters. There are eight subfamilies of ABC transporter proteins, A to H (Figure 6). The subfamily A comprises full-length ABC transporters with two TMDs and two NBDs. There are additional multiple phosphorylation sites behind each NBD, which differentiate it from subfamily B that lacks them. Subfamily B comprises two structures, one representing full length and the other half-length ABC transporters, as mentioned above. The subfamily C comprises only full-length ABC transporters that have, however, an additional N-terminal extension before the TMDs and NBDs. Subfamily C corresponds to MRP of the yeast scheme. The subfamily D is a group of ABC transporter proteins with a half size structure. The subfamilies E and F consist of two NBDs in each structure without any TMD. The subfamily G comprises full-length ABC transporters, however, with a reversed order of domains, i.e. the NBD is followed by the TMD. The members of this subfamily are also known as Pleiotropic Drug Resistance (PDR) proteins according to the yeast classification. The last subfamily H has only one NBD and no TMD (Figure 6). An alternative classification scheme of ABC transporters exists based on the proteins in *S. cerevisiae*. According to the yeast scheme, there are three main subfamilies i.e. the multidrug resistance (MDR), multidrug resistance-associated protein (MRP) and pleiotropic drug resistance (PDR) (De Waard 1997). MDR, MRP and PDR correspond to subfamily A, C and G of the HUGO scheme respectively.

Fusarium graminearum has 62 predicted ABC transporter proteins distributed in all subfamilies from A to H with the following numbers: 1, 16, 16, 2, 1, 5, 19 and 2, respectively (Kovalchuk and Driessen 2010). They occupy 1.7 Mb out of the 36.45 Mb total genome of the fungus (Kovalchuk and Driessen 2010). ABC transporter genes represent 0.46% of all 13,332 genes in *F. graminearum* (Ma et al. 2013). Among the ABC transporter subfamilies, subfamily C (=MRP) is especially interesting because of its unique structure with an additional N-terminal extensions in front of the domains typically found in full length ABC transporter proteins. Currently, it is not known whether this extension may contribute to the function of these proteins.

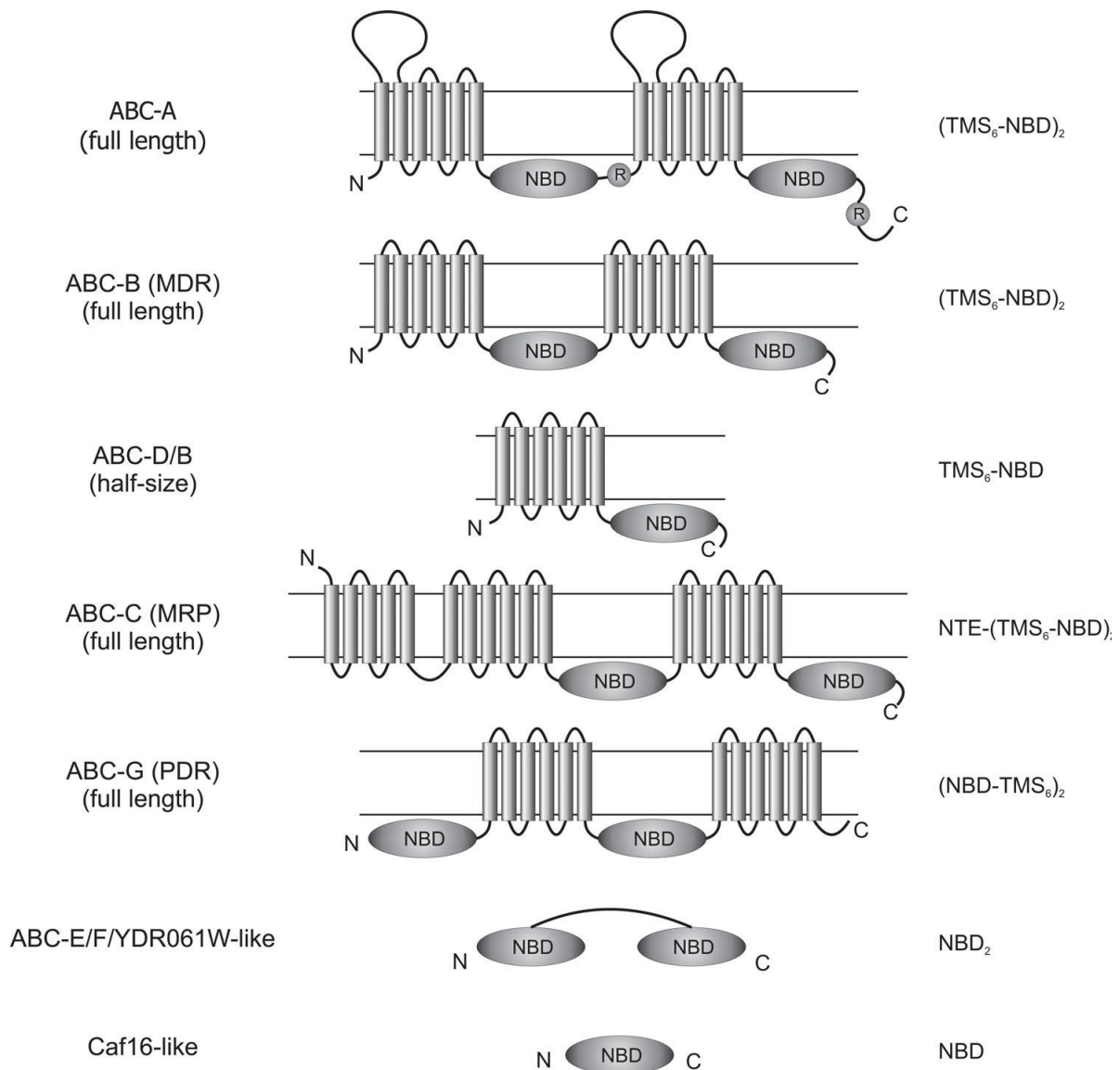


Figure 6. Differentiation of fungal ABC transporter subfamilies based on the HUGO scheme adopted from (Kovalchuk and Driessen 2010). TMS, trans-membrane segment; NBD, nucleotide binding domain; NTE, N-terminal extension; R, ~120 amino acid residues.

I.4.2. Biological functions of MRP transporters (ABC subfamily C)

ABC transporters have diverse biological functions. The proteins can act as importers or exporters in prokaryotes, but exclusively as exporters in eukaryotes (Rees, Johnson, and Lewinson 2009). A broad range of substrates including sugars, amino acids, drugs, antibiotics, toxins, lipids, sterols, salts, peptides, nucleotides, endogenous metabolites and ions are transported across cell membranes (Sharom 2008). Synthetic compounds such as

fungicides, drugs and other bio-control agents are also known as substrates being transported (De Waard et al. 2006). In addition, in plant pathogenic fungi ABC transporters play an important role in exporting fungal metabolites that may contribute to virulence. Furthermore, they may export plant-defence compounds that may have seeped into fungal cells (Waard 1997, Stergiopoulos et al. 2002).

Most often the subfamily C proteins (=MRP) found in fungi seem to export fungal metabolites (Kovalchuk and Driessen 2010). These transporters are also known to contribute to drug resistance. The first MRP protein to be characterised was YCF1 from *S. cerevisiae* (De Waard 1997). This gene encodes a protein with a domain structure characterised as TMD4-[TMD6-NBD]2. This transporter protein has been identified as a vacuolar glutathione S-conjugate pump, involved in the protection of cells against cadmium, drugs and other stress-metabolites (De Waard 1997). Other MRP proteins have been characterised in *C. albicans*, for example MLT1. This protein showed highest similarity (42%) to the yeast cadmium factor 1, YCF1 (accession no. p39109) and 41% to the yeast bile pigment transporter, BPT1 (accession no. p14772) in *S. cerevisiae* (Theiss et al. 2002). Even though, this protein is not involved in the primary cadmium detoxification in *C. albicans* as shown for YCF1 in *S. cerevisiae* (Paumi et al. 2009; Li et al. 1996). The expression of MLT1 in the presence of cadmium chloride (CdCl₂) and 1-chloro-2,4-dinitrobenzene (CDNB) is high, but apparently only as a general stress response. MLT1 plays a more important role in the virulence of *C. albicans* in mice liver as evidenced by decreased levels of alanine aminotransferase (ALT) in blood compared to the wild type. ALT is a liver specific enzyme whose appearance in the blood is an indication of damaged liver cells (Theiss et al. 2002).

In humans, an MRP1 protein encoded by *ABCC1* is involved in tissue protection against toxic xenobiotics and endogenous metabolites. This transporter is highly expressed in tumour cells to confer resistance during chemotherapy treatments. Single Nucleotide Polymorphisms (SNP) in that transporter are believed to contribute to the ineffectiveness of such clinical cancer treatments (Sharom 2008).

Only a few MRP proteins have been characterised in fungal plant pathogens. One exception is *Magnaporthe oryzae* that was predicted to have 50 ABC transporters scattered throughout the nine subfamilies. The MDR (=subfamily A), MRP (=subfamily C) and PDR (=subfamily G) proteins belong to the largest subfamilies with 19 genes (38%), 11 genes (22%) and 8 genes (16%), respectively. Interestingly, transcript levels of most genes in the

MRP subfamily increased during infection and under various abiotic stress conditions. Three genes of the MRP subfamily i.e. *MoABC5*, *MoABC6*, *MoABC7* were deleted. Deletion mutants of *MoABC5* exhibited reduced virulence on rice leaves, those of *MoABC6* reduced mycelial growth on minimal medium amended with 1 M sorbitol, 1 M KCl and 1 M NaCl, and those of *MoABC7* reduced conidia formation rate (Kim et al. 2013).

I.4.3. Objectives of this study

Microarray experiments have indicated that several ABC transporter genes were transcriptionally up-regulated after treatment with tebuconazole (Becher et al. 2011). Among those were also members of MRP transporters (subfamily C). Because this subfamily has not been as intensively analysed as for example the PDR transporters, I functionally characterised two MRP transporter genes of *F. graminearum* in this study. For this purpose, I created deletion mutants that were analysed first for several parameters assessing vegetative vitality. Furthermore, the mutants were tested on a range of fungicides to determine whether the deletion has increased their sensitivity to azoles and other fungicide classes. The mutants were inoculated onto three host plants of *F. graminearum*, i.e. winter wheat, barley and maize to assess whether the deletion has changed their virulence. Finally, it was analysed whether they still could secrete trichothecene and zearalenone into the medium. This study analyses the contribution of two similar ABC transporter proteins of *F. graminearum* grouped in the MRP subfamily to azole resistance and virulence in host plants.

II. Materials and methods

II.1. Fungal strains

Two wild type strains of *F. graminearum* were used in this study, PH-1 (NRRL 31084) and NRRL 13383. These strains were kindly provided by Dr. Kerry O'Donnell (USDA). These strains differ by their trichothecene chemotype and geographical origin. PH-1 has a 15-ADON chemotype and was isolated from an infected wheat spike in Michigan, USA. NRRL 13383 has a NIV chemotype that was isolated from infected maize ear in Iran. They were used as the genetic backgrounds for the deletion study of *FgABC1* (FGSG_10995) and *FgABC4* (FGSG_17058).

After PCR and Southern blot analyses, two deletion mutants for each gene in each background were used for further experiments. In the PH-1 background, the mutants were $\Delta FgABC1$ -PH.2, $\Delta FgABC1$ -PH.3, $\Delta FgABC4$ -PH.4, and $\Delta FgABC4$ -PH.15. In the NRRL 13383 background, the mutants were $\Delta FgABC1$ -NRRL.4, $\Delta FgABC1$ -NRRL.7, $\Delta FgABC4$ -NRRL.2, and $\Delta FgABC4$ -NRRL.3. The $\Delta FgABC1$ -NRRL.4 and $\Delta FgABC4$ -NRRL.2 mutants were chosen for another round of transformation using another selection marker plus the WT alleles of *FgABC1* and *FgABC4*, to generate complementation strains. After validation by PCR and Southern blot analyses, for each gene two transformants were chosen for further experiments. The complementation strains of $\Delta FgABC1$ were cFgABC1-NRRL.4.7 and cFgABC1-NRRL.4.18. The complementation strains of $\Delta FgABC4$ were cFgABC4-NRRL.2.3 and cFgABC4-NRRL.2.8.

The strain NRRL 13383 was used previously as the wild reference in a tebuconazole adaptation study (Becher et al. 2010) that generated six adapted strains called P1-1, P1-9, P1-11, P2-1, P2-4 and P2-8. These strains were included in the sequencing of *FgCYP51A* (FGSG_04092), *FgCYP51B* (FGSG_01000), *FgCYP51C* (FGSG_11024), and *FgABC4*. I used the strain P1-11 as another genetic background for studying the effects of a deletion of *FgABC4*. Here, three deletion mutants and two ectopic mutants were analyzed further. The three deletion mutants were $\Delta FgABC4$ -P1-11.1, $\Delta FgABC4$ -P1-11.4, $\Delta FgABC4$ -P1-11.7, and the two ectopic transformants were $\Delta FgABC4$ -P1-11.5, $\Delta FgABC4$ -P1-11.8, NRRL 13383.

II.2. Storage of fungal isolates

All fungal strains were stored as -80°C cultures. The cultures were prepared by inoculating 10^6 conidia per mL into 5 mL potato dextrose broth medium (PD) in a 15 mL Falcon tube that was incubated at 25°C for 24 hours with 100 rpm agitation. The mycelia

were precipitated by centrifugation at 3,000x g for five minutes. The pellet was re-suspended with 1.2 mL of 30% (v/v) glycerol and mixed by pipetting up- and downwards five times to distribute evenly the glycerol at the mycelial surfaces. Aliquots of 300 μ L were dispensed into 1.5 mL tubes and placed on ice for one hour before storage in a -80⁰C freezer. The strains were revived by inoculating a PDA plate with an aliquot of frozen suspension using a sterilized inoculation needle. The plate was incubated at 23⁰C for five days.

II.3. Culture media and buffers

II.3.1. Media

PD and Potato Dextrose Agar (PDA) were prepared by dissolving 24 g potato dextrose (Becton, Dickinson and Company, Heidelberg, Germany) in one liter of deionized water. In the case of PDA, 15 g agar per liter was added. The medium was autoclaved at 121⁰C with 1 bar pressure for 20 min. For selection medium, after autoclaving the medium was allowed to cool down to about 50⁰C. It was then amended with either nourseothricin or hygromycin at a final concentration of 100 μ g/mL.

Spezieller Nährstoffarmer Agar (SNA) (Leslie and Summerell 2006) was prepared by weighing 1 g KH₂PO₄, 1 g KNO₃, 0.5 g MgSO₄x7H₂O, 0.5 g KCl, 0.2 g glucose, 0.2 g sucrose and 15 g agar. All compounds were dissolved in one liter of deionized water and autoclaved as stated before. For selection medium, the respective antibiotic was amended as described above.

Mung Bean Broth (MBB) was adopted from Bai and Shaner (1996). The medium was prepared by adding 40 g of mung beans to one liter boiling deionized water and cooking for 15 min. After cooling, the filtrate was sieved using cheesecloth and autoclaved as above.

Yeast Extract Potato Dextrose (YEPD) was prepared as two solutions to avoid the Maillard reaction which is a browning reaction between amino acids and sugars at elevated temperatures. The first solution consisted of 3 g yeast extract, 10 g trypto-peptone and 950 mL deionized water. The second solution consisted of 20 g glucose and 50 mL deionized water. Both solutions were autoclaved as above and mixed in a laminar flow cabinet prior to use.

Luria Bertani (LB) and Luria Bertani Agar (LBA) were prepared by dissolving 10 g tryptone, 5 g yeast extract and 10 g sodium chloride in one liter deionized water. In the case of LBA, 15 g agar per liter was added to the medium and autoclaved as above. For selection medium, the respective antibiotic was amended as described above.

Regeneration Medium (RM) was prepared using two solutions. Solution A consisted of 0.5 g yeast extract, 0.5 g casein hydrolysate, 5 g agar, and 500 mL deionized water. Solution B consisted of 275 g saccharose and 500 mL deionized water. Both solutions were autoclaved and mixed in the laminar flow cabinet prior to use. The selection medium was amended with the respective antibiotic as described above.

Complete Medium (CM) was composed of 1 liter autoclaved basal medium, 30 g sucrose, 2 g NaNO₃, 2.5 g casein hydrolysate, 1 g yeast extract and 10 mL vitamin stock solution. The basal medium consisted of 1 g KH₂PO₄, 0.5 g MgSO₄·7H₂O, 0.5 g KCl, 0.2 mL trace element solution in one liter of deionized water. The trace element solution was filter-sterilized using a 0.45 micron syringe filter (Sartorius AG, Göttingen, Germany) and added to autoclaved basal medium. The trace element solution itself consisted of 5 g citric acid, 5 g ZnSO₄·6H₂O, 1 g Fe(NH₄)₂(SO₄)₂·6H₂O, 250 mg CuSO₄·5H₂O, 50 mg MnSO₄, 50 mg H₃BO₃, 50 mg Na₂MoO₄·2H₂O in 100 mL of deionized water. The citric acid was added first to prevent precipitation with other salts. The vitamin stock solution consisted of 4 g inositol, 200 mg Ca-pantothenate, 200 mg choline, 100 mg thiamine, 75 mg pyridoxine, 75 mg nicotinamide, 50 mg ascorbic acid, 30 mg riboflavin, 5 mg *p*-aminobenzoic acid, 5 mg folic acid, 5 mg biotin in one liter ethanol:deionized water (50:50).

II.3.2. Buffers

The following buffers were used for gel electrophoresis. TAE buffer was used for DNA electrophoresis and consisted of 40 mM Tris-Cl, 20 mM sodium acetate, 2 mM EDTA, pH 8.0. RNA running buffer was used in RNA electrophoresis and consisted of 50 mM sodium acetate, 10 mM EDTA, 20% (v/v) formaldehyde, 200 mM 3-(N-morpholino) propanesulfonic acid (MOPS), pH 7.0.

The following buffers were used in DNA isolation experiments. The breaking buffer consisted of 1% (w/v) SDS, 2% (v/v) Triton X 100, 100 mM NaCl, 10 mM Tris-Cl, 1 mM EDTA, pH 8.0. The extraction buffer I consisted of 7 M urea, 2% (w/v) SDS, 50 mM Tris-Cl, 5 mM EDTA, pH 8.0. Extraction buffer II consisted of 150 mM NaCl, 50 mM Tris-Cl, 5 mM EDTA, pH 8.0.

The following buffers were used in Southern blot experiments. The transfer buffer was 20x SSC, which consisted of 3 M NaCl and 0.3 M sodium citrate, pH 7.5. The hybridization buffer consisted of 25% (v/v) 20x SSC buffer, 10% (v/v) 1% N-lauryl sarcosine, 0.1% (v/v) 20% SDS, 1% (v/v) 10x blocking solution. The 2x wash buffer consisted of 10% (v/v) 20x SSC buffer and 0.1% (v/v) 20% SDS solution. The 0.5x and 0.25x wash buffers were made

by diluting the 2x wash buffer with water. The wash buffer M consisted of 0.1 M maleic acid, 0.15 M NaCl, 0.3% (w/v) Tween 20, pH 7.5. The maleic buffer consisted of 100 mM maleic acid, 150 mM NaCl, pH 7.5. The 10x blocking solution consisted of 1% (w/v) blocking reagent (Roche Diagnostics, Mannheim) in maleic buffer, which was autoclaved at 121⁰C for 20 minutes and stored at -20⁰C. The 1x blocking solution was a dilution of the 10x blocking solution using maleic buffer. The detection buffer consisted of 100 mM NaCl and 100 mM Tris-HCl, pH 9.5.

The following buffers were used in the transformation experiments. The protoplasting solution was made by dissolving 500 mg driselase, 1 mg chitinase, 100 mg lysing enzyme of *Trichoderma harzianum* (all from Sigma-Aldrich, Schnellendorf, Germany) in 20 mL 1.2 M KCl. The solution was stirred gently at RT for 30 minutes. This solution was sterilized using a 0.45 micron syringe filter (Sartorius AG, Göttingen, Germany). The STC buffer consisted of 1.2 M sorbitol, 50 mM CaCl₂, 10 mM Tris-HCl, pH 7.5. It was autoclaved as above.

II.4. Nucleic acid isolation

II.4.1. Small scale DNA preparation

This procedure was designed to yield sufficient DNA that was pure enough for PCR screening tests. One mycelial plug (Ø 5 mm) was transferred into a 2 mL Eppendorf tube containing one mL PD medium and incubated at 23⁰C for three days with 50 rpm agitation. The mycelia were centrifuged at 3,000x g for 5 minutes. The supernatant was discarded and replaced with 800 µL breaking buffer. Two steel balls (Ø 2 mm) were added to the tube. Mycelia were disrupted in the TissueLyser device (Qiagen GmbH, Hilden, Germany) with 30 Hertz for 2 x 30 seconds. Both steel balls were removed and 800 µL phenol:chloroform:isoamylalcohol (25:24:1) were added. The tube was vortexed vigorously for ten seconds and centrifuged at 4⁰C and 13,000x g for 20 minutes. The upper aqueous phase was transferred into a new tube containing 750 µL of 2-propanol and incubated at 4⁰C for one hour. The DNA was precipitated through centrifugation at 4⁰C and 13,000x g for 20 minutes. The DNA pellet was washed with 500 µL of 70% ethanol and centrifuged again at 4⁰C and 13,000x g for 10 minutes. The supernatant was discarded and the pellet was dried in a SpeedVac vacuum concentrator (Savant Instruments Inc., USA) for 10 minutes to remove remaining ethanol. The pellet was re-suspended with 50 µL sterile deionized water and incubated at 4⁰C for one hour prior to DNA quantification. The DNA was stored at -20⁰C.

II.4.2. Large scale DNA preparation

This method was applied to isolate higher amounts of DNA at higher purity than the one described in Section II.5.1 above. Five mycelia plugs (\varnothing 5 mm) were transferred into 100 mL PD in a 250 mL Erlenmeyer flask. The flask was incubated at 23⁰C with 100 rpm agitation for five days. Mycelia were sieved through one layer of No.1 Whatman filter paper and air dried for five minutes in the laminar flow cabinet. The mycelia were frozen in liquid nitrogen and ground to a fine powder using a mortar and pestle. One gram of mycelia powder was added into 800 μ L Extraction buffer I and 800 μ L phenol:chloroform:isoamylalcohol (25:24:1). The suspension was homogenized by vortexing at the highest speed for ten seconds and then centrifuged at 4⁰C 13,000x g for 20 minutes. The supernatant was added to 800 μ L of 2-propanol and incubated at 4⁰C for one hour. The suspension was centrifuged again at 4⁰C and 6,800x g for 15 minutes and the supernatant was discarded. The pellet was re-suspended with 700 μ L Extraction Buffer II, amended with 3.5 μ L RNase A (10 mg/mL) and incubated at 37⁰C for 30 minutes. Afterwards, 17.5 μ L of 20% SDS was added and the tube inverted five times. Subsequently, Proteinase K was added, the tube was inverted five times, and incubated at 60⁰C for one hour. Additionally, 800 μ L phenol:chloroform:isoamylalcohol (25:24:1) was added and vortexed at the highest speed for ten seconds. The suspension was centrifuged at 4⁰C and 13,000x g for 20 minutes. The supernatant was transferred into 800 μ L of 2-propanol and centrifuged at 4⁰C and 6,800x g for 15 minutes. The supernatant was discarded and the pellet washed with 500 μ L 70% ethanol then agitated at 50 rpm at RT for five minutes on a Polymax 1040 shaker (Heidolph Instruments GmbH und Co.KG, Schwabach) and centrifuged at 4⁰C and 6,800x g for 10 minutes. The supernatant was discarded and the pellet was dried in a SpeedVac vacuum concentrator (Savant Instruments Inc., USA) for 10 minutes to remove remaining ethanol. The pellet was re-suspended with 50 μ L sterile deionized water and incubated at 4⁰C for one hour before DNA quantification. The DNA was stored at -20⁰C.

II.4.3. Total RNA preparation

Total RNA was used in the RT-qPCR assay to determine the transcriptional responses of the deletion mutants to 5 ppm tebuconazole. For each strain tested, two 300 mL Erlenmeyer bottles containing 100 mL CM medium were inoculated with one million conidia and then incubated at 23⁰C for 24 hours with 150 rpm agitation. One culture was amended with 5 ppm tebuconazole, the other not, since it served as a control. The incubation continued for an additional 12 hours. For each variant tested, four cultures were grown that served as

biological repeats. The fungal tissues were harvested by filtration using filter paper (Karl Roth GmbH Co. KG, Karlsruhe, Germany), frozen in liquid nitrogen and ground to a fine powder using a mortar and pestle. One hundred mg of mycelium powder were added to 450 μ L RNA Lysis buffer T (RLT, Qiagen, Hilden, Germany). The subsequent procedure followed the instructions of the PeqGold Plant RNA Kit (PEQLAB Biotechnologie GmbH, Erlangen, Germany). The RNA was re-suspended in 50 μ L of DNase/RNase free water (Bioline GmbH, Luckenwalde, Germany). The RNA was stored at -20°C .

II.4.4. DNA/RNA quantification

The DNA concentration was quantified using the NanoDrop ND-1000 (Thermo Scientific, Wilmington, USA) in accordance with the manufacturer's instructions. The quality of DNA was checked by electrophoresis in a 0.7% (w/v) agarose gel (Biozym Scientific, Hessisch Oldendorf, Germany) run at 100 V for one hour in 1xTAE buffer. GeneRuler DNA ladder mix (Fisher Scientific, Schwerte, Germany) was included in the electrophoresis as the marker. The gel was soaked in 1 $\mu\text{g}/\text{mL}$ of ethidium bromide solution for 20 minutes, washed in water and documented digitally using UV light illumination (320 nm) in a UV Solo TS2 gel imaging system (Biometra, Göttingen, Germany).

The RNA concentration was quantified using the technique described for DNA quantification. An additional analysis used the RNA 6000 pico assay for the 2100 Bioanalyzer instrument (Agilent, Waldbronn, Germany) to assess the quality and quantity of total RNA. RNA samples showing two bands that represented the 28S and 18S rRNA were considered as good RNAs. The quality of RNA was also confirmed by electrophoresis on a 1% (w/v) agarose gel (Biozym Scientific, Hessisch Oldendorf, Germany) run at 100 V for one hour in RNA running buffer. The result was documented using the same method as described above for DNA.

II.5. Nucleic acid analyses

II.5.1. Polymerase Chain Reaction (PCR)

II.5.1.1. Standard PCR

The standard PCR was performed in 20 μ L volume (Table 1). The enzyme and reaction buffer were obtained from Thermo Scientific (Fisher Scientific, Schwerte, Germany). The reactions were run in a Tpersonal thermal cycler (Biometra, Göttingen, Germany) using the

Table 1. Components of standard PCR reaction.

Components	Stock conc.	Final conc.	Volume (μL)
HF buffer	5 x	1 x	4
dNTP mix	10 mM	0.2 mM	0.4
forward primer	10 μM	0.3 μM	0.6
reverse primer	10 μM	0.3 μM	0.6
Phusion polymerase	2 U/μL	0.02 U/μL	0.2
DNA template	variable	20 ng/20 μL	variable
water	-	-	add to 20

Table 2. Standard PCR program.

Steps	Temperature (°C)	Duration (min:sec)	Cycle(s)
1	98	Pause	1x
2	98	00:30	1x
3	98	00:15	1x
4	T _m -5	00:15	1x
5	72	15-30 sec/kb	back to 3: 34x
6	72	10:00	1x
7	4	pause	1x

program described in table 2. Steps 4 and 5 were adjusted according to the melting temperature (T_m) of the primers and the target length. The T_m calculation was based on the method described by Howley et al. 1979 that also considered salt concentration in the reaction.

$$T_m = 81,5 + 16,6 \times \log[\text{Na}^+] + 41 \times (G + C)/n - 500/n$$

$\log[\text{Na}^+]$ = logarithm of salt concentration (PCR need of 0.01 – 1.00 M monovalent cations)

G = number of Guanine

C = number of Cytosine

n = number of nucleotides

II.5.1.2. Double-Joint PCR

DJ PCR was performed in 50 μL volume (Table 3). The reaction was run in a Tpersonal thermal cycler (Biometra, Göttingen, Germany) using the program described in table 4. The Phusion high-fidelity DNA polymerase and the reaction buffer were obtained from Thermo Scientific (Fisher Scientific, Schwerte, Germany). The DJ PCR was applied to fuse the two flanks of the target gene with a resistance cassette used for selection of transformants. The method is based on a procedure described by (Yu et al. 2004). The PCR product was purified using the GeneJET PCR purification kit (Fisher Scientific, Schwerte, Germany) in accordance with the manufacturer's instructions.

Table 3. Components of DJ-PCR reaction.

Components	Stock conc.	Final conc.	Volume (μL)
HF buffer	5 x	1 x	10
dNTP mix	10 mM	0.2 mM	1
left flank	variable	10 ng/ μL	variable
resistance cassette	variable	30 ng/ μL	variable
right flank	variable	10 ng/ μL	variable
Phusion polymerase	2 U/ μL	0.02 U/ μL	0.5
water	-	-	add to 50

Table 4. DJ-PCR program.

Steps	Temperature ($^{\circ}\text{C}$)	Duration (min:sec)	Cycle(s)
1	98	pause	1x
2	98	00:30	1x
3	98	00:15	1x
4	60	00:15	1x
5	72	02:00	back to 3: 10 x
6	98	00:15	1x
7	72	02:00	back to 6: 20 x
8	72	10:00	1x
9	4	Pause	1x

II.5.1.3. Generation of Digoxigenin-labelled PCR fragments

Probes used for hybridization with filter-bound DNA, were generated by a modification of the standard PCR using the DIG (digoxigenin)-labeling Kit (2 mM dATP; dCTP; dGTP; 0.19 mM dTTP and 0.1 mM DIG-11-dUTP, alkali labile). In a control reaction, the DIG-11-dUTP was replaced by the corresponding concentration of dTTP. Aliquots of the labelling and the control reactions were analyzed by electrophoresis on an agarose gel. Incorporation of DIG into DNA diminishes its migration rate thus allowing visualizing the success of the labelling reaction. The probe was purified using the GeneJET PCR purification kit.

II.5.2. Reverse transcription – quantitative PCR (RT-qPCR)

The RT-qPCR was performed in 20 μL volume (Table 5). The reaction was run in a MyiQ-Single Color Real-Time PCR Detection System equipped with the iQ5 version 2.1 optical system software (Bio-Rad Laboratories GmbH, Munich, Germany) with the program described in table 6. The Power SYBR[®] Green RNA-to-CT[™] 1-Step Kit (Life Technologies GmbH, Darmstadt, Germany) was used to amplify three reference genes and *FgABC1* and *FgABC4*. The reference genes were cofilin (FGSG_06425), pre-mRNA splicing factor (FGSG_01244) and RNA helicase (FGSG_10791). These reference genes were chosen because they were shown to be appropriate for studying transcriptional responses of *F. graminearum* to a tebuconazole treatment (Becher et al. 2011). Eight data points were used to

Table 5. Components of RT-qPCR reaction.

Components	Stock conc.	Final conc.	Volume (μL)
<i>Power SYBR® Green RT-PCR Mix</i>	2 x	1 x	10
forward primer	10 μM	0.1 μM	0.2
reverse primer	10 μM	0.1 μM	0.2
RT enzyme Mix	125 x	1 x	0.16
RNA template	variable	20 ng / 20 μL	1
water			add to 20

Table 6. RT-qPCR program.

Steps	Temperature ($^{\circ}\text{C}$)	Duration (min:sec)	Cycle(s)
1	48	30:00	1x
2	95	10:00	1x
3	95	00:15	1x
4	60	01:00	back to 3: 40 x
5	72	5:00	1x
6	4	pause	1x

average the transcription data that represented two technical repeats of the RT-qPCR performed on each of the four biological repeats of RNA preparation.

The transcript abundance was determined by measuring the initial fluorescence (R_0) that was calculated by application of sigmoidal curve-fitting method (Liu and Saint 2002) using the software Sigmaplot version 11 (Systat Software, Erkrath, Germany). The raw transcript data of *FgABC1* and *FgABC4* were normalized with a factor obtained from the averaged transcript data of three reference genes. Two statistical comparisons were made for each *FgABC1* and *FgABC4* transcript levels. First, within the same strain for each gene data were compared between the control and the tebuconazole treatment. Second, for a given treatment for each gene data were compared among strains.

II.5.3. DNA digestion using restriction enzyme

For Southern hybridization experiments, genomic DNA was digested using a restriction enzyme that did not cut within the transformed construct. DNA samples of 10 μg were digested using the appropriate restriction enzyme and buffer in a total volume of 25 μL . This reaction was incubated at 37°C for 16 hours. Five- μL -aliquots of digested DNA were separated by electrophoresis on a 0.7% (w/v) agarose minigel. In cases where only partial digestion occurred, the volume of the reaction was increased and more buffer and enzyme were added accordingly. Completely digested DNA was run on a preparative 0.7% (w/v) agarose gel at 80 V for 4 hours. The gel was soaked for 10 minutes in ethidium bromide

solution, briefly rinsed with water and visualized using UV light as described above (see II.4.4).

II.5.4. Southern blot

Southern blot analysis used two probes to detect the candidate gene and the resistance marker cassette on two separate filters. Southern blot analysis employed digestion of genomic DNA, electrophoresis, DNA blotting onto a nylon membrane, probe preparation, probe hybridization, and X-ray film detection.

Genomic DNA preparation and digestion were performed as described above (see II.4.2 and (see II.5.3 respectively). The gel was depurinated with 0.25 M HCl at RT for 30 minutes with gentle shaking on a Polymax 1040 shaker (Heidolph Instruments GmbH und Co.KG, Schwabach). The gel was briefly rinsed with deionized water and the DNA was denatured with 0.4 M NaOH at RT for 30 minutes with gently shaking. Again, the gel was briefly rinsed with deionized water. The DNA was transferred from the gel onto a nylon membrane Amersham Hybond-N+ (GE Healthcare Europe, Freiburg, Germany) via downward capillary transfer using a high-salt transfer buffer (20 x SSC buffer). A 10 cm stack of paper towels was laid at the bottom. On top of this, three layers of buffer-wetted blotting filter papers (Karl Roth GmbH Co. KG, Karlsruhe, Germany) were placed. The nylon membrane was laid above them. The gel was carefully placed on the nylon membrane ensuring no bubbles were present. Three layers of buffer-wetted blotting filter paper were placed on top of the gel. Another longer strip of filter paper was placed over the top. It was long enough so that both ends of the paper reached into two containers, which were filled with transfer buffer. A glass plate was placed above the paper strip and a 250 mL Pyrex bottle filled with water was added as a weight. After 4-5 hours at RT the blot was disassembled, the gel was stained again in ethidium bromide solution and visualized under UV light as described above to control for successful transfer of the DNA to the membrane (see II.5.4).

The membrane was incubated at 80°C for two hours, then placed into a glass tube and covered with 40 mL hybridization buffer. Pre-hybridization was performed at 68°C for two hours in a hybridization oven (Biozym Scientific GmbH, Hess. Oldendorf, Germany).

The probe was denatured prior to hybridization by incubation at 98°C for five minutes, followed by an immediate chilling on ice for two minutes. The denatured probe was added to the hybridization buffer and hybridized at 68°C overnight. The next morning, the hybridization buffer was discarded and replaced with 20 mL of 2x SSC buffer. Incubation continued in the hybridization oven and the same glass tube at RT for five minutes. This

washing step was repeated once more. The next steps were a wash in 0.5x SSC and then 0.25x SSC at 68⁰C, each for 15 minutes. The membrane was equilibrated with maleic acid buffer for one minute and incubated with 20 mL of 1x blocking solution for two hours. Subsequently, 4 µL of anti-DIG antibody-coupled alkaline phosphatase (Roche Diagnostics, Mannheim, Germany) was added. The incubation continued for 30 min. The membrane was washed three times with 20 mL of maleic acid buffer at RT for 10 minutes each. Afterwards, the membrane was washed with 20 mL of detection buffer for two minutes. Next, the membrane was taken from the glass tube and laid on a plastic sheet (Carl Roth GmbH, Karlsruhe, Germany). A 980 µL detection buffer and 20 µL CSPD solution were mixed by pipetting in a 1.5 mL Eppendorf tube and spread evenly over the membrane, which was wrapped in the plastic sheet and incubated at R.T. in a film cassette for five minutes. Afterwards, the membrane was exposed to an X-ray film (Hyperfilm ECL, Amersham Pharmacia Biotech, Freiburg, Germany) in darkness for 3 hours. Finally, the film was developed using an Optimax TR (MS Laborgeräte, Heidelberg, Germany) to visualize the captured chemiluminescence. Typically, a second exposure was performed to adjust the signal to an appropriate intensity.

II.5.5. DNA sequencing

The BigDye Terminator version 1.1 Cycle Sequencing Kit (Life Technologies, Darmstadt, Germany) was used for DNA sequence reactions. Sequencing reactions consisted of 2 µL of 5x sequencing buffer, 1 µL BigDye reaction mix, 1 µL 2 µM primer, 10 - 20 ng of purified PCR fragment that was used as template and deionized water to give a final volume of 10 µL. The sequencing reaction was performed in a thermal cycler machine (Biometra, Göttingen, Germany) with the sequencing program (Table 7). At the end of the reaction, 60 µL of absolute ethanol, 5 µL 0.125 M EDTA and 10 µL deionized water were added. After incubation at room temperature for 15 min, the DNA was precipitated by centrifugation for 20 min at 20,000x g and 4⁰C. The pellet was washed with 60 µL 70% ethanol and precipitated for 10 min by centrifugation at 20,000x g and 4⁰C. The pellet was air dried in a SpeedVac device for 10 min to remove the remaining ethanol. The readout of the sequences was obtained using an ABI PRISM 3100 genetic analyzer (Applied Biosystems Inc., Foster City, California, USA) in the Biology Department of the Martin-Luther-University.

Table 7. PCR sequencing program.

Steps	Temperature (°C)	Duration	Cycle(s)
1	96	pause	1x
2	96	2:00	1x
3	96	0:10	
	50	0:05	
	60	1:15	back to 3: 15x
4	96	0:10	
	50	0:05	
	60	1:30	back to 4: 5x
5	96	0:10	
	50	0:05	
	60	2:00	back to 5: 5x
6	4	pause	1x

II.6. Transformation

II.6.1. *E. coli* transformation

Escherichia coli strain XL-1 blue was used for bacterial transformation. Competent *E. coli* cells were made by inoculating 25 mL LB with 200 µL of an overnight culture in LB, which was started from a fresh LB agar plate. The cells were grown at 37°C with 200 rpm agitation for three hours and then harvested by centrifugation at 1,000x g and 4°C for 10 min. The cells were washed with 5 mL TSS buffer and centrifuged as above. The cells were resuspended in 2.5 mL TSS buffer and dispensed in 100 µL aliquots in sterile 1.5 mL Eppendorf tubes. Approximately, each tube contained 2.5×10^8 cells. The cells were incubated on ice for 15 min and either were used directly for transformation or stored at -80°C.

All deletion constructs were ligated into the plasmid vector pJET1.2 (Fisher Sci., Schwerte, Germany) for a transformation into in *E. coli*. Ligation was performed using the CloneJET PCR Cloning Kit (Fisher Sci., Schwerte, Germany) in accordance with the manufacturer's instructions for Blunt-End cloning. For transformation of competent *E. coli* cells, 10 µL of the ligation reaction was added to the cell suspension, which was previously thawed on ice. After mixing by gentle pipetting, the suspension was incubated on ice for one hour. A heat shock was applied at 42°C for 90 seconds, then 900 µL of LB was added and the reaction was incubated for one hour at 37°C. The cells were dispensed in 100 µL aliquots onto LBA containing 100 µg/mL of ampicillin and the plates were incubated overnight at 37°C. Single colonies were selected and inoculated in 1 mL LB. The cultures were incubated

overnight at 37°C. Plasmids were isolated from the cells using the GeneJET plasmid miniprep Kit (Fisher Sci., Schwerte, Germany) and analyzed by restriction enzymes (see II.5.3) and DNA sequencing to confirm the correctness of the recombinant clones.

II.6.2. *F. graminearum* transformation

Protoplasts were used to transform *F. graminearum*. To obtain protoplast, 100 mL YEPD were inoculated with 5×10^6 conidia and then incubated for 12 hours at 23°C with 175 rpm agitation. The young mycelium was harvested on a filter paper (Whatman 3MM, Whatman GmbH, Dassel, Germany) and suspended in 20 mL protoplast solution (500 mg driselase, 1 mg chitinase, 100 mg lysing enzyme of *Trichoderma harzianum* (all from Sigma-Aldrich, Schnellendorf, Germany) in 1.2 M KCl for 3-4 hours with 90 rpm agitation. Afterwards, the protoplasts were harvested by filtration on miracloth tissue (Merck, Darmstadt, Germany). The eluate was subjected to centrifugation at 1000x g for five minutes. Protoplasts were resuspended in 1 mL STC buffer and directly used for transformation.

A transformation reaction consisted of 10^7 protoplasts in 100 µL STC buffer, 50 µL 30% PEG 8000 and 8 µg DNA of the construct in 50 µL water. The ingredients were mixed by gentle pipetting. In case of co-transformation, which was used to complement a previous deletion, 6 µg DNA of the native gene of interest and 3 µg DNA of the resistance cassette were added to a transformation reaction. This was incubated at RT for 20 min with 50 rpm agitation. 2 mL of 30% PEG 8000 were added and incubation continued for five minutes. 4 mL STC buffer were added to the suspension and mixed by gently inverting the tube three times. 600 µL of suspension was mixed with 15 mL molten regeneration medium (see II.3.1) and poured into a 90 mm Petri dish. The plates were incubated at 23°C for 12 hours. Another 15 mL of molten regeneration medium containing 200 µg/mL of an antibiotic corresponding to the selection marker was overlaid on the agar surface. The transformants were able to grow and reach the agar surface over the next four to five days. Single colonies were transferred to new PDA plates with the corresponding antibiotic and incubated at 23°C for five days. The mutants were then transferred to SNA plates that were incubated at 23°C for 10 days to induce conidiation. Single spore isolation was conducted by rinsing an SNA plate with 1 mL of water and by plating 100 µL of the conidial suspension onto PDA plates containing the appropriate antibiotic. The plate was incubated at 23°C for 48 hours. Emerging colonies that were well separated from their neighbors were transferred individually to a new PDA plate amended with 100 µg/mL of either nourseothricin or hygromycin depending on the resistance marker employed. Such plates were taken for further experiments as PCR and Southern blot

analysis (see II.5.4). Finally, strains confirmed to represent the anticipated genotypes were permanently stored as described above (see II.2).

II.7. Fungal fitness assays

II.7.1. Vegetative growth

The vegetative growth assay was performed on PDA plates (Ø 90 mm) at three different temperatures i.e. 15⁰C, 23⁰C and 30⁰C. The strains were revived from -80⁰C on PDA plates at 23⁰C for 5 days. The strains were then transferred to fresh PDA plates that were amended with nourseothricin or hygromycin as selective antibiotic in the case of transgenic strains. Incubation was again at 23⁰C for 5 days. From these plates, mycelia plugs (Ø 5 mm) were taken from the edge of each colony and transferred to four PDA plates for each temperature tested. The growth data were recorded by measuring two perpendiculars directions of colony diameters for seven days. Student´s T-test (P<0.05) in the Microsoft Excel 2010 software was used to determine significant differences between WT and the mutants.

II.7.2. Conidia germination

Germination rates were determined on glass slides carrying 20 µL of a conidial suspension containing approximately 200 conidia that were overlaid with a cover glass. Incubation was on three layers of moistened paper towels inside a 120x120x17 mm plastic dish (Greiner Bio-One, Solingen, Germany) at 23⁰C for 24 h under illumination with near-UV light (L18W/73, Osram, Munich, Germany). The germinated and ungerminated conidia were recorded from eight conidial suspension drops as technical repetitions. Statistical analysis was performed as stated above (see II.7.1).

II.8. Fungicide and plant metabolite sensitivity assay

Sensitivity assays were performed in dark conditions by incubating inoculated PDA plates (12x12 cm, Greiner-BioOne) at 23⁰C for strains of the NRRL 13383 and at 30⁰C for strains of the PH-1 background. Pre-experiments were performed for the WT and mutants to narrow down on the inhibitory concentration for each substance. Formulated and pure substance fungicides were tested in this assay. The formulated fungicides were azoxystrobin (Amistra, BASF), fenpropimorph (Corbel, BASF), metconazole (Caramba, BASF), prochloraz (Sportak, BASF) and tebuconazole (Folicur, Bayer). The pure substance fungicides were epoxyconazole, fenarimol, spiroxamine, boscalid, dithianon obtained from

Sigma-Aldrich (Schnelldorf, Germany) and prothioconazole from Bayer. Tolnaftate (Sigma-Aldrich) was included as a xenobiotic compound that has never been used in agricultural practice. Five plant secondary metabolites were also tested, i.e. 2-Benzoxazolinone (= BOA), 3-(Dimethylaminomethyl)indole (= Gramine), 2,3-Dihydro-5,7-dihydroxy-2-(4-hydroxyphenyl)-4H-1-benzopyran-4-one, 4',5,7-Trihydroxyflavanone (= Naringenin) and 3,3',4',5,7-Pentahydroxyflavone dihydrate (= Quercetin) (Sigma-Aldrich). Dimethylsulfoxide (DMSO) was used as a solvent to make stock solution of all substances. The stock solutions were amended into autoclaved PDA that was equilibrated at 50°C in a water bath. The medium was stirred well before aliquots of 50 mL were dispensed into the plates. For testing sensitivity, two types of fungal inoculation were used. First, 2 µL of $1 \times 10^5 \text{ mL}^{-1}$ conidia was pipetted onto the medium. The second inoculated mycelia plug (Ø 5 mm) onto the plates. Controls employed unamended PDA. A minimum of three plates were used as biological repeats. Fungal colonies were documented by digital photography at the third, fifth, and seventh day. The colony area was quantified in mm^2 using ImageJ software version 1.46 (<http://rsbweb.nih.gov/ij/index.html>). Statistical analysis was applied as described previously (see II.7.1).

II.9. Analysis of mycotoxins produced *in vitro*

The extraction of mycotoxins and all following steps were performed in the laboratory of Professor Karlovsky at Georg-August-Universität Göttingen as reported (Abou Ammar et al. 2013). For each isolate, five independent fungal cultures were analyzed. Statistical analysis was performed as outlined above.

II.10. Virulence assays

II.10.1. *Triticum aestivum* (Wheat)

Virulence on wheat plant was tested using spring wheat cv. Kadrlj (SW Seed Hadmersleben, Hadmersleben, Germany). This variety has been chosen because it showed medium susceptibility to FHB and had been used in a previous study (Becher et al. 2010). The plants were grown under the same conditions as described (Becher et al. 2010). A point inoculation method was used for the assay. One thousand conidia were inoculated into the 11th spikelets of mature wheat heads when the anthers began to extrude. The palea was slightly lifted from the lemma by hand to create a small opening in which 10 µL of spore suspension in Tween20 was carefully pipetted by taking care not to injure the surrounding

tissues. All spikes, at least nine, growing in a single pot were used as repetitions. The symptomatic spikelets were counted every other day up to 14 dpi. The disease severity was scored as the percentage of symptomatic spikelets per head.

II.10.2. *Zea mays* (Maize)

The maize cv. Golden Jubilee (Territorial Seed Company, Cottage Grove, OR, USA) was used for the stem infection assay based on the results of pre-experiments, which showed that the cv Golden Jubilee allowed for the strongest necrotic symptoms compared to cv. Mikado and cv. Farmtop (KWS Saat AG, Einbeck, Germany). Each pot contained one plant and four pots were used as repetitions. The plants were cultivated for six weeks in a greenhouse at 24°C with 50% RH and 14 hours photoperiod using Planstar 600 Watt E40 lamps (Osram, Munich, Germany). The first internode of a maize stem was punched with a sterile toothpick. One thousand conidia suspended in 10 µL of Tween20 were injected into the hole. Parafilm was wrapped around the stem to protect the hole from secondary infections and to maintain a high humidity. The parafilm was removed after seven days and the incubation allowed to continue for another seven days. The stem was then split longitudinally and the lesion area documented by digital photography. Image J software version 1.46 was used to calculate the necrotic area (mm²) for both halves of the split stem. Thus, each stem was represented by two data points. Four stems were used as replications, thus rendering eight data points. These data were averaged and each treatment was compared to the WT data. Student's T-test (P<0.05) was used for statistical analysis.

II.10.3. *Hordeum vulgare* (barley)

Barley plants cv. Barke (SW Seed Hadmersleben, Hadmersleben, Germany) were cultivated applying the same conditions as described for maize. Ten week old plants were used for inoculation. For each strain, a minimum of nine spikelets growing in one pot were used as repetitions. Initially, two methods were used for inoculation. In the first, the entire barley ear was dipped for 10 sec into a 15 mL falcon tube containing 12 mL of 1000 conidia/mL suspended in 0.02% Tween 20. In the second method, 1 mL of 1000 conidia/mL suspended in 0.02% Tween 20 were sprayed with a 20 mL a glass falcon onto each barley spike. The inoculated spikes were covered for 48 hours with a plastic bag, which had been sprayed before with water on the inside, to raise the humidity. After an additional incubation period of 14 dpi, scoring and statistical analysis was performed as described above for wheat.

Table 8. Vectors used in this study.

Names	Description
pAN7-1	Plasmid containing the hygromycin B phosphotransferase (<i>hph</i>) gene to confer resistance to hygromycin B (Punt et al. 1987).
pNR1	Plasmid containing the nourseothricin acetyltransferase 1 (<i>nat1</i>) gene to confer resistance to nourseothricin (Malonek et al. 2004)
pJET1.2	Plasmid containing the β -lactamase gene (<i>bla</i>) to confer resistance to ampicillin (ThermoScientific 2013)
pJET1.2/ Δ FgABC1	Plasmid pJET1.2 plus the <i>FgABC1</i> deletion construct which confers resistance to hygromycin B
pJET1.2/ Δ FgABC4	Plasmid pJET1.2 plus the <i>FgABC4</i> deletion construct which confers resistance to nourseothricin

II.11. Accession numbers

The sequences of genes analyzed in this study are available in the Fusarium Genome Database http://mips.helmholtz-muenchen.de/gbrowse2/cgi-bin/gbrowse/p3_p13839_Fus_grami_v32/?name=supercontig_3.1:1097796..1109796. The accession numbers of the genes encoding reductase and translation elongation factor 1-alpha are FGSG_03224 and FGSG_08811, respectively. The accession number of *FgTRI3* is FGSG_03534 and that of *FgTRI2* is FGSG_03541. The accession numbers of ABC transporter genes *FgABC1* and *FgABC4* are FGSG_10995 and FGSG_17058, respectively. The three genes encoding CYP51 (eburicol 14 alpha-demethylase) in *F. graminearum* are accessible under the accession numbers FGSG_04092 (*FgCYP51A*), FGSG_01000 (*FgCYP51B*), and FGSG_11024 (*FgCYP51C*). The three reference genes used to normalize the data from RT-qPCR experiments are FGSG_06425, FGSG_01244 and FGSG_10791 that encode cofilin, pre-mRNA splicing factor and RNA helicase, respectively.

II.12. Vectors

All vectors used in this study are listed below (Table 8).

II.13. Oligonucleotide sequences

All oligonucleotides used in this study are provided below (Table 9).

Table 9. Oligonucleotides used in this study.

No	Name	Sequences 5' to 3'	Purposes
1	RED1	TCTCAGAAAGACGCATATATG	sequencing of reductase
2	RED2	CGTAACTGCGTCATTCCGGC	sequencing of reductase
3	EF1	ATGGGTAAGGARGACAAGAC	sequencing of <i>tef1-α</i>
4	EF2	GGARGTACCAGTSATCATGTT	sequencing of <i>tef1-α</i>
5	3NA	GTGCACAGAATATACGAGC	PCR test of chemotype
6	3D15A	ACTGACCCAAGCTGCCATC	PCR test of chemotype
7	3D3A	CGCATTGGCTAACACATG	PCR test of chemotype
8	3CON	TGGCAAAGACTGGTTCAC	PCR test of chemotype
9	12NF	TCTCCTCGTTGTATCTGG	PCR test of chemotype
10	12-15F	TACAGCGGTCGCAACTTC	PCR test of chemotype
11	12-3F	CTTTGGCAAGCCCCTGCA	PCR test of chemotype
12	12CON	CATGAGCATGGTGATGTC	PCR test of chemotype
13	Fg1.Fw1	GGCGATGTCATTGGTGAACAG	Deletion of <i>FgABC1</i>
14	Fg1.Hyg.Rv	GTGCAACTGACAGTCGTACA TCTCGAGGCCAAGAGTCCC	Deletion of <i>FgABC1</i>
15	Fg1.Hyg.Fw	GTCTGGAGTCTCACTAGCTT CGCCATGTCATCCACCTTGC	Deletion of <i>FgABC1</i>
16	Fg1.Rv1	GAGCATGAGACTCCTGGTTAC	Deletion of <i>FgABC1</i>
17	Fg1.Fw2	CTGTGCCACGTTTGTAGACT	Deletion of <i>FgABC1</i>
18	Fg1.Rv2	CGAACTGGGTGCAATGCAAAC	Deletion of <i>FgABC1</i>
19	Fg1.probe.Fw	CAGCGGATTGGTGAGCAGTG	Deletion of <i>FgABC1</i>
20	Fg1.probe.Rv	ATGCAGCCGTCTTGACCCTC	Deletion of <i>FgABC1</i>
21	Fg4.Fw1	TGTTGGCGATGTGGTTCAGG	Deletion of <i>FgABC4</i>
22	Fg4.Nours.Rv	GTGCAACTGACAGTCGTACA GGTGTGCTGACATGTCGAGC	Deletion of <i>FgABC4</i>
23	Fg4.Nours.Fw	GTCTGGAGTCTCACTAGCTT TCTGTAGTTTGAAGTAGAAG	Deletion of <i>FgABC4</i>
24	Fg4.Rv1	TTCGTCTTGGAGGCCGAAGGAG	Deletion of <i>FgABC4</i>
25	Fg4.Fw2	CTTTGCGGAACTCGTGTAGG	Deletion of <i>FgABC4</i>
26	Fg4.Rv2	GTGTCGATCCCGCGTTGAAACC	Deletion of <i>FgABC4</i>
27	Fg4.probe.Fw	TGTCAGGATCGTGTCTCTTC	Deletion of <i>FgABC4</i>
28	Fg4.probe.Rv	ATCCAACGGCGAGATACGGAG	Deletion of <i>FgABC4</i>
29	uni-hyg.F1	TGTACGACTGTCAGTTGCACTG ACCGGTGCCTGGATCTTC	Deletion of <i>FgABC1</i> and complementation of <i>FgABC4</i>
30	uni-hyg.R1	AAGCTAGTGAGACTCCAGACG GTCGGCATCTACTCTATTCC	Deletion of <i>FgABC1</i> and complementation of <i>FgABC4</i>
31	uni-nours.F1	TGTACGACTGTCAGTTGCACA TTCGGGCCGGATTG	Deletion of <i>FgABC4</i> and complementation of <i>FgABC1</i>
32	uni-nours.R1	AAGCTAGTGAGACTCCAGACA CCGATGAAACGATTCTCAAC	Deletion of <i>FgABC4</i> and complementation of <i>FgABC1</i>
33	hyg.Fw2	GACATCACCATGCCTGAACTC	<i>hph</i> probe and complementation of <i>FgABC4</i>
34	hyg.Rv2	GGTCGGCATCTACTCTATTCC	<i>hph</i> probe and complementation of <i>FgABC4</i>
35	nours.Fw2	CTCTTGACGACACGGCTTAC	<i>nat1</i> probe and complementation of <i>FgABC1</i>
36	nours.Rv2	GGCAGGGCATGCTCATGTAG	<i>nat1</i> probe and complementation of <i>FgABC1</i>
37	RSF.FG01244.F1	ATGGAGACAACCCATGACCCACAC	RT-qPCR of FGSG_01244
38	RSF.FG01244.R1	ATGATGCGTGCGTGAATGGCA	RT-qPCR of FGSG_01244

continued

39	Cof.FG06245.F1	TGTCATTGGCCTGCAACTCGGT	RT-qPCR of FGSG_06245
40	Cof.FG06245.R1	ACGACTTCGAGTACAACCTGGCCT	RT-qPCR of FGSG_06245
41	Hel.FG10791.F1	TCGAACTCCAGGCCCTTTGTG	RT-qPCR of FGSG_10791
42	Hel.FG10791.R1	GCGGATCAGCTAGCAGACAAG	RT-qPCR of FGSG_10791
43	FG1.FG10995.F1	ATTTATGACCACGCAGTCTGG	RT-qPCR of <i>FgABC1</i>
44	FG1.FG10995.R1	CTGCGAAAAGAGGTTTCGTTAC	RT-qPCR of <i>FgABC1</i>
45	FG4.FG17058.F1	ACAGGCTCGTCTATTCACAG	RT-qPCR of <i>FgABC4</i>
46	FG4.FG17058.R1	GACCCCTTGATAACCTCTAAC	RT-qPCR of <i>FgABC4</i>
47	CYP51A.F1	CTGGCCACGCAAAGGTATAG	Sequencing of <i>Cyp51A</i>
48	CYP51A.R1	CTCTGGCCAATGATAACAACC	Sequencing of <i>Cyp51A</i>
49	CYP51A.F2	TACGTTTCCTCAGGAGCTCAGTAG	Sequencing of <i>Cyp51A</i>
50	CYP51A.R2	ACAAGGGTCCAGGCCGTAAG	Sequencing of <i>Cyp51A</i>
51	CYP51A.F3	GGGAAACCCTGCTTGAGTAG	Sequencing of <i>Cyp51A</i>
52	CYP51A.R3	GTTATCTCAGCCATTGCCTTG	Sequencing of <i>Cyp51A</i>
53	CYP51A.F4	CTACGTCGAAACTGATCCATC	Sequencing of <i>Cyp51A</i>
54	CYP51A.R4	GATTGAGTGGATGGAAGAGTG	Sequencing of <i>Cyp51A</i>
55	CYP51A.F5	AGCTCCCTCTTCTCCAGAAC	Sequencing of <i>Cyp51A</i>
56	CYP51A.R5	GATGTCGGATCTTCATGCAAG	Sequencing of <i>Cyp51A</i>
57	CYP51A.F6	ACTGTTGCGAACCACCCTGTC	Sequencing of <i>Cyp51A</i>
58	CYP51A.R6	CTCGGTGATGCTCGTGGTGCTATG	Sequencing of <i>Cyp51A</i>
59	CYP51B.F1	GACCATGTCATAGCCCTGAAG	Sequencing of <i>Cyp51B</i>
60	CYP51B.R1	GAAAGCAGATGGCGAAGGAG	Sequencing of <i>Cyp51B</i>
61	CYP51B.F2	TCGAAAGAGTGCAGGCGGTGTG	Sequencing of <i>Cyp51B</i>
62	CYP51B.R2	GAACCAGTGGAAGACCATAG	Sequencing of <i>Cyp51B</i>
63	CYP51B.F3	ACTACGGCGACGATTCTCTC	Sequencing of <i>Cyp51B</i>
64	CYP51B.R3	AGCATATGTCAGTATACAGGTC	Sequencing of <i>Cyp51B</i>
65	CYP51B.F4	CAACGCCAAGCTCATGGAAC	Sequencing of <i>Cyp51B</i>
66	CYP51B.R4	TTGGCAAGGTCTTCGTAAG	Sequencing of <i>Cyp51B</i>
67	CYP51B.F5	CACATCATGGAAGAGCTCTAC	Sequencing of <i>Cyp51B</i>
68	CYP51B.R5	CATTCAACTCCGCAGCATGC	Sequencing of <i>Cyp51B</i>
69	CYP51B.F6	CTCTGGAGCCCGCCAACATTCAC	Sequencing of <i>Cyp51B</i>
70	CYP51B.R6	TCGCTCATGATGTCTTGCTGTG	Sequencing of <i>Cyp51B</i>
71	CYP51C.F1	TGAGGTGACCTGGCCAAGCTATC	Sequencing of <i>Cyp51C</i>
72	CYP51C.R1	CCATCGTGCTCTAACTCAGG	Sequencing of <i>Cyp51C</i>
73	CYP51C.F2	CTAACCTCGAGACGAACGATG	Sequencing of <i>Cyp51C</i>
74	CYP51C.R2	TGTGTCACCCTTGAAGTATGG	Sequencing of <i>Cyp51C</i>
75	CYP51C.F3	GCTCGTTTCATGGACAAAAG	Sequencing of <i>Cyp51C</i>
76	CYP51C.R3	GCATGGGTGATTTGACTTGTC	Sequencing of <i>Cyp51C</i>
77	CYP51C.F4	CTGACATGGGAGAACTTACAG	Sequencing of <i>Cyp51C</i>
78	CYP51C.R4	GCTGGGTATCATTAGCATCTA	Sequencing of <i>Cyp51C</i>
79	CYP51C.F5	CATGAACCCTGCCGAGATCC	Sequencing of <i>Cyp51C</i>
80	CYP51C.R5	GGATGTGGCGGAGGCTAATTTG	Sequencing of <i>Cyp51C</i>
81	FG17058.F5	CGACTTGTTGGCGTTAACTTG	Sequencing of <i>FgABC4</i>
82	FG17058.F6	CCGAGGCGACTTTGACTTTAC	Sequencing of <i>FgABC4</i>
83	FG17058.F7	CAAGAACGCGCACGATCTCTG	Sequencing of <i>FgABC4</i>
84	FG17058.F8	CCGCCATAAACTCACCATTG	Sequencing of <i>FgABC4</i>
85	FG17058.F9	CCTTACAACGCAGCTACTGAC	Sequencing of <i>FgABC4</i>
86	FG17058.F10	TACCCACTGTCTGGAGTCTAC	Sequencing of <i>FgABC4</i>
87	pJET1.2-seq.F	CGACTCACTATAGGGAGAGCGGC	Sequencing of pJET vector
88	pJET1.2-seq.R	AAGAACATCGATTTTCCATGGCAG	Sequencing of pJET vector

III. Results

III.1. Verification of strains used in this study

III.1.1. Determination of the phylogenetic lineage within the *F. graminearum* species complex

O'Donnell et al. (2000) used six single-copy protein-encoding nuclear genes to classify *F. graminearum* within the species complex (FGSC). The genes used were ammonia ligase, 3-*O*-acetyltransferase, phosphate permease, reductase, β -tubulin, and translation elongation factor 1-alpha. Except for phosphate permease, every gene consistently differentiated seven lineages within the FGSC that comprised *F. austroamericanum* (lineage 1), *F. meridionale* (lineage 2), *F. boothii* (lineage 3), *F. mesoamericanum* (lineage 4), *F. acacia-mearnsii* (lineage 5), *F. asiaticum* (lineage 6), *F. graminearum* (lineage 7). Since the phylogenetic trees were congruent these lineages were proposed to represent distinct species. Later on, genes encoding histone H3 and four mating types (*MAT1-1-1*, *MAT1-1-2*, *MAT1-1-3*, *MAT1-2-1*) revealed two additional species in a larger set of strains, *F. cortaderiae* (lineage 8) and *F. brasiliicum* (lineage 9) (O'Donnell et al. 2004). Using the extended set of genes for analysis, a total of 16 species has been identified up to now (Aoki et al. 2012). The additional species are *Fusarium* sp. NRRL 34461, *F. gerlachii* and *F. vorosii* (Starkey et al. 2007), *F. aethiopicum* (O'Donnell et al. 2008), *F. ussurianum* (Yli-Mattila et al. 2009), *F. nepalense* (Desjardins and Proctor 2011) and *F. louisianense* (Sarver et al. 2011). Based on this finding, the reductase (*RED*) and translation elongation factor 1-alpha (*TEFI- α*) genes were employed to determine the lineage of the isolates of PH-1 and NRRL 13383 used in this study.

The sequences of *FgRED* were obtained from a PCR product generated using the primer pair Red1-Red2 (Table 9) that amplified 930 bp fragments. The sequences obtained were truncated at their ends to give a 838 bp fragment of high sequence quality that comprised 307 bp of the upstream region and 531 bp of the ORF of *FgRED* (Figure 7, top). For the PH-1 isolate used in the laboratory a BlastN search of the NCBI database yielded an exact match with the database annotation AY452925.1, which is described as “*Gibberella zeae* strain NRRL 31084 (PH-1) reductase gene, partial cds”. The *FgRED* sequence of the strain labelled as NRRL 13383 matched perfectly with database annotation AF212568.1, which described a “*Gibberella zeae* strain NRRL 13383 reductase-like gene, partial sequences” (Figure 7, bottom). The alignment analysis between PH-1 and NRRL 13383 revealed one SNP in position 227 of the ORF that resulted in an amino acid change. In PH-1,

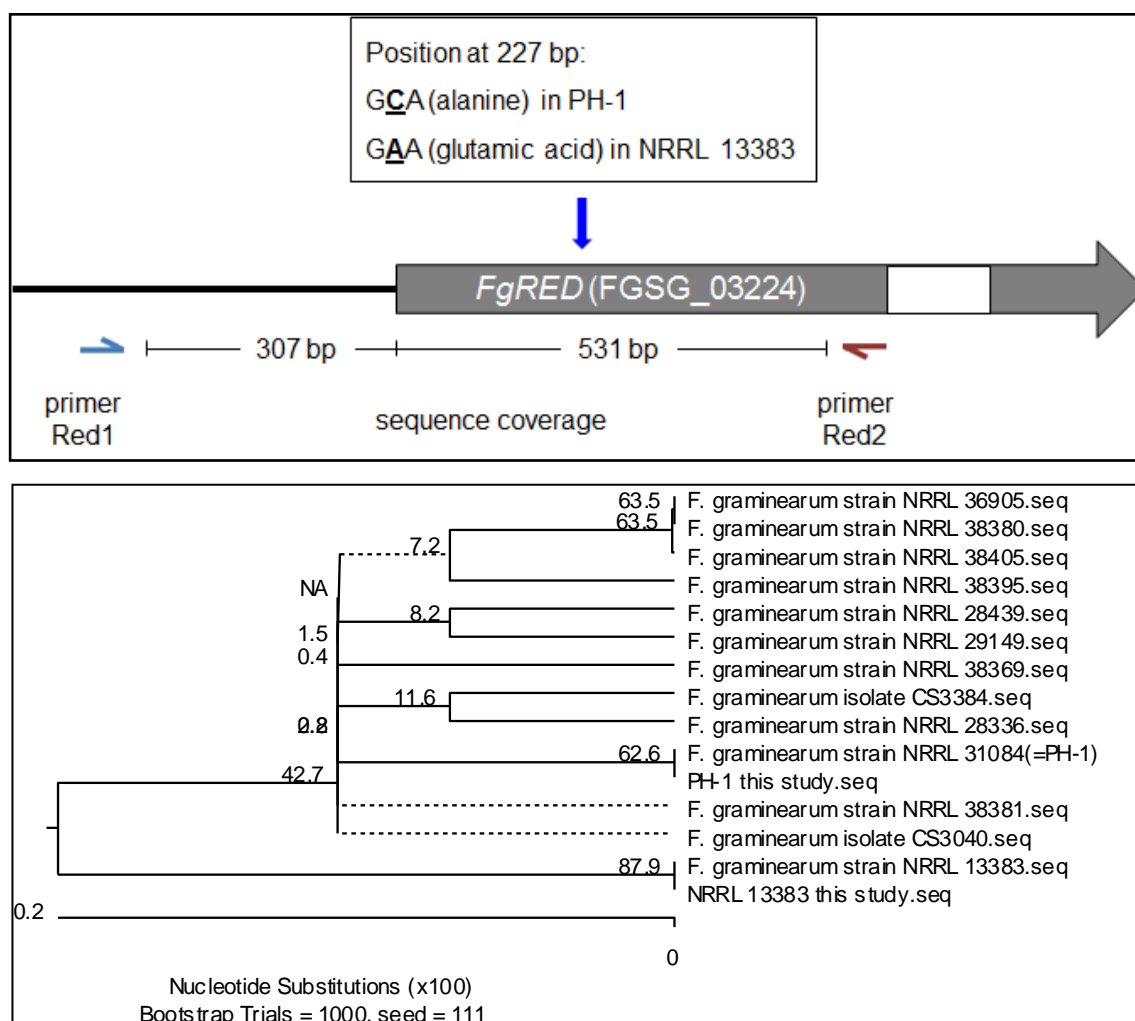


Figure 7. Sequence analysis of *FgRED*. Top) an illustration of sequence reading. Gray boxes indicate exons, a white box an intron. Blue arrow points to the position of a SNP in NRRL 13383 differing from the PH-1 reference sequence. Bottom) phylogenetic tree of *RED* nucleotide sequences. The tree was obtained by the neighbor joining algorithm implemented in the software DNASTAR Lasergene MegAlign Version 7.0.0.

at this position codon GCA encodes for alanine, whereas in NRRL 13383, codon GAA encodes for glutamic acid.

The sequencing of a PCR product of *FgTEF1- α* supported the *FgRED* sequencing result. Primer pair Ef1-Ef2 (Table 9) amplified a PCR product of 706 bp that was truncated at the end to give a fragment of 655 bp within the ORF (Figure 8, top). This sequence was used for a BlastN search in the NCBI database. For the PH-1 isolate used in our laboratory, the best match was found with annotation HM744693.1 that described a “*Gibberella zeae* strain NRRL 31084 transcription elongation factor 1 alpha (*TEF*) gene, partial cds”. For our isolate of NRRL 13383, the *FgTEF1- α* sequence matched best with annotation AF212457.1 that

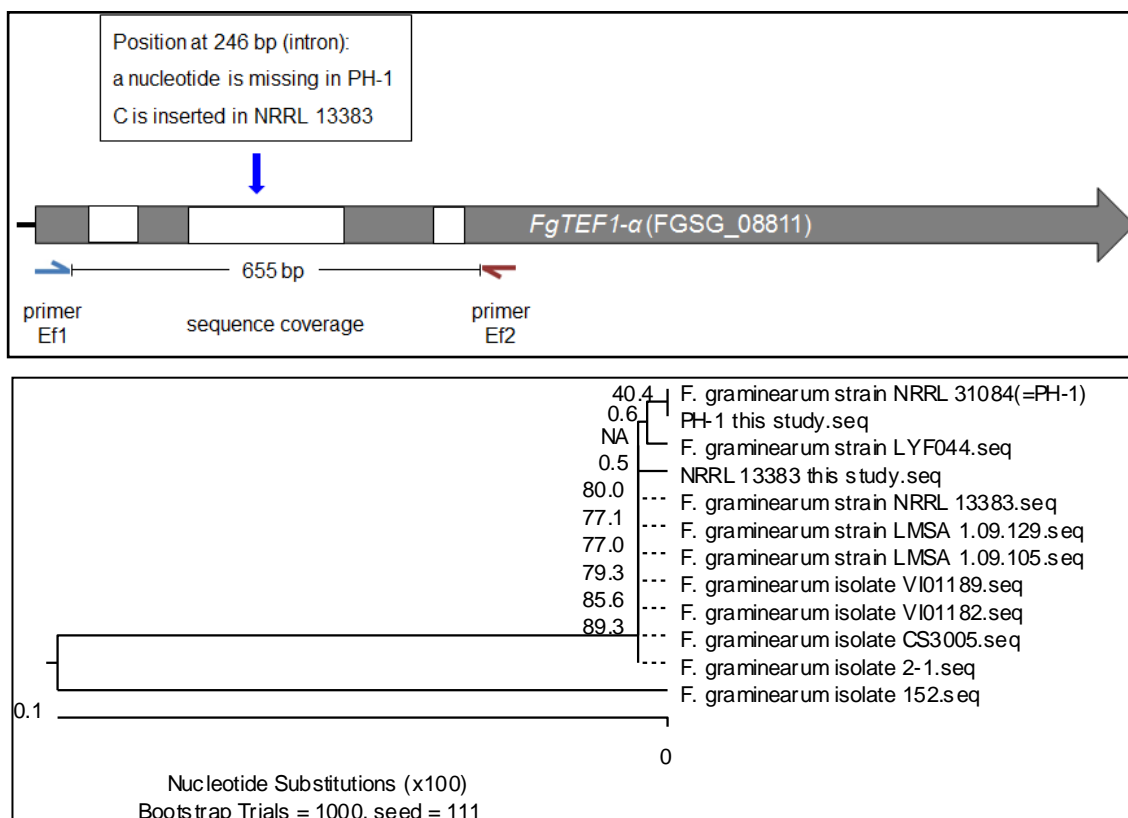


Figure 8. Sequence analysis of *FgTEF1-α*. Top) an illustration of sequence reading. Gray boxes indicate exons, white boxes introns. Blue arrow points to the position of a SNP in NRRL 13383 differing from the PH-1 reference sequence. Bottom) phylogenetic tree of *FgTEF1-α* nucleotide sequences. The tree was obtained by the neighbor joining algorithm implemented in the software DNASTAR Lasergene MegAlign Version 7.0.0.

described a “*Gibberella zeae* strain NRRL 13383 translation elongation factor-1 alpha gene, partial CDS” (Figure 8, bottom). Alignment analysis of NRRL 13383 uncovered an insertion of a cytosine at position 246 bp of the ORF within an intron. In PH-1, this nucleotide is missing. This insertion did not change the amino acid sequence of TEF1alpha in NRRL 13383. The sequences of *FgRED* and *FgTEF1-α* in the laboratory strains were exactly the same as those deposited in the NCBI database for PH-1 and NRRL 13383, thus supporting their use in this study.

III.1.2. Determination of the chemotype

PH-1 and NRRL 13383 are strains of *F. graminearum*. that differ in colony morphology *in vitro*, geographical origin and the host plants where these fungi had been isolated from. As a consequence, the spectra of the mycotoxins formed by them could be different. *Fusarium graminearum* isolates belong to one out of three known trichothecene B chemotypes, i.e. the

3-ADON, 15-ADON and NIV chemotypes (Kimura et al. 2003). The chemotypes were named according to that molecule that is most distinct for them, which does not mean that other trichothecenes will not be formed.

The chemotypes of PH-1, NRRL 13383 and six adapted strains were determined using two multiplex PCRs that targeted genes encoding trichothecene 15-*O*-acetyltransferase (*FgTRI3*) and trichothecene efflux pump (*FgTRI2*) according to the techniques described by (Starkey et al. 2007). The multiplex PCR for *FgTRI3* employed as forward primer 3CON (Table 9) and as reverse primers 3NA, 3D15A and 3D3A (Table 9) that distinguished nivalenol (NIV), 3-acetyldeoxynivalenol (3-ADON), or 15-acetyldeoxynivalenol (15-ADON) chemotypes through PCR product sizes of 840, 610, or 243 bp, respectively. Similarly, the multiplex PCR targeting gene *FgTRI2* used as forward primer 12CON (Table 9) and three reverse primers, 12NF, 12-15NF and 12-3F (Table 9) that differentiated NIV, 3-ADON or 15-ADON chemotypes with PCR product sizes of 840, 670, or 410 bp, respectively.

In the PCR targeting *FgTRI3*, the PH-1 isolate showed a 610 bp band indicating that of the three reverse primers only 3D15A had annealed to the DNA template. In the PCR targeting *FgTRI2*, the same PH-1 isolate showed a 670 bp band indicating that of the three reverse primers, only 12CON/12-15NF had annealed to the DNA template. Both PCRs thus indicated that the PH-1 isolate had the 15-ADON chemotype. On the other hand, isolate NRRL 13383 and six azole-resistant strains derived from it yielded in both PCR assays, products of 840 bp that differed from those of PH-1. This implied that reverse primers 3NA and 12NF, respectively, had specifically annealed to the template DNA (Figure 9). This result proved that NRRL 13383 had the nivalenol chemotype. Also the six azole resistant strains analyzed exhibited the nivalenol chemotype, which was expected because they were descendants of strain NRRL 13383 (Becher et al. 2010). The PCR assays targeting *FgTRI3* and *FgTRI2* thus demonstrated that the PH-1 isolate had the 15-ADON chemotype, whereas the NRRL 13383 isolate had the NIV chemotypes.

III.2. Sequence analyses of *FgCYP51A*, *FgCYP51B*, *FgCYP51C* and *FgABC4* in azole resistant P1 and P2 mutants

In a previous study NRRL 13383 had been treated *in vitro* with 10 mg/L tebuconazole for 33 days (Becher et al. 2010). This resulted in the selection of azole resistant strains that were discerned by colony morphology in two phenotypes, P1 and P2 (Becher et al. 2010). However, the mutations leading to resistance remained unknown. *FgCYP51A*, *FgCYP51B*, *FgCYP51C* were sequenced in this study because they encode the molecular target of azoles

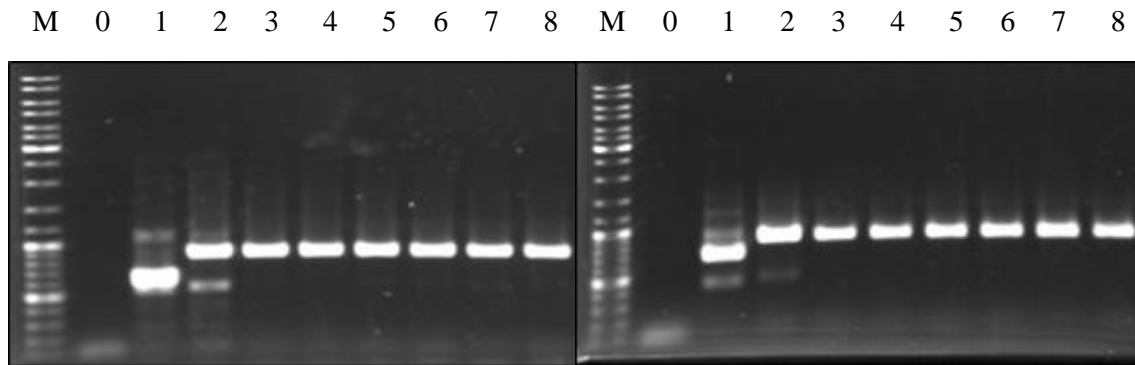


Figure 9. Multiplex PCR of *Tri3* (left) and *Tri12* (right) to determine the chemotypes of PH-1, NRRL 13383 and six adapted strains. Lane M: GeneRuler DNA ladder Mix; Lane 0: no-template control; Lane 1: PH-1; Lane 2: NRRL 13383; Lane 3: P1-1; Lane 4: P1-9; Lane 5: P1-11; Lane 6: P2-1; Lane 7: P2-4; Lane 8: P2-8.

and because they exhibited altered transcript levels after a treatment of strain PH-1 with tebuconazole (Becher et al. 2011). Another group of genes responding in that treatment were ABC transporters. Two of them were the focus of this study and thus their gene sequences were analysed in three P1 and three P2 strains for mutations, as well.

The sequencing of *FgCyp51A*, *-B* and *-C* covered the complete ORFs of the genes and furthermore 878 bp, 868 bp and 644 bp of the upstream, and 848 bp, 541 bp and 685 bp of the downstream regions, respectively. The entire sequences of all three *FgCyp51* genes in the six adapted strains were identical to those of their progenitor strain NRRL 13383. These data showed that tebuconazole resistance in the six adapted strains did not emerge by a *CYP51* mutation. However, some SNPs existed between PH-1 and NRRL 13383. The *FgCYP51A* sequence had four substitutions in the downstream region and one silent substitution in the ORF at nucleotide position 305, where GTC in PH-1 is changed to GTT in NRRL 13383 (Table 10). Both codons encode valine. In contrast, the *FgCYP51B* sequences were found identical in both strains. Sequencing of the *FgCYP51C* genes revealed the presence of three substitutions in the upstream region, six substitutions in the ORF and four substitutions in the downstream region when comparing NRRL 13383 to the reference PH-1 strain. All SNPs in the coding region resulted in amino acid changes except for the one located at position 727 (Table 10).

Since no mutation existed in any of the *CYP51* genes for the six adapted strains, azole resistance must have other causes. One of the other known possibilities might be a mutation in an ABC transporter gene (Cowen and Steinbach 2008). One such gene, *FgABC4* identified in this work was found to contribute to azole tolerance in *F. graminearum*. Thus, I sequenced

Table 10. SNPs between PH-1 and NRRL 13383 in *FgCYP51A*, *FgCYP51B*, *FgCYP51C* and *FgABC4*.

genes	position of the SNP	PH-1			NRRL 13383			
		SNP	codon	amino acid	SNP	codon	amino acid	
<i>FgCYP51A</i>	-465	thymine	-	-	cytosine	-	-	
	305	cytosine	<u>GUC</u>	valine	uracyl	<u>GUU</u>	valine	
	+192	cytosine	-	-	adenine	-	-	
	+233	adenine	-	-	guanine	-	-	
	+249	cytosine	-	-	thymine	-	-	
	+271	thymine	-	-	cytosine	-	-	
<i>FgCYP51B</i>	n.a.	none			none			
<i>FgCYP51C</i>	-489	guanine	-	-	adenine	-	-	
	-391	guanine	-	-	adenine	-	-	
	-31	adenine	-	-	guanine	-	-	
	32	uracyl	<u>CUA</u>	leucine	cytosine	<u>CCA</u>	proline	
	727	cytosine	<u>CCC</u>	proline	adenine	<u>CCA</u>	proline	
	815	adenine	<u>AUU</u>	isoleucine	guanine	<u>GUU</u>	valine	
	821	uracyl	<u>UCC</u>	serine	guanine	<u>GCC</u>	alanine	
	975	uracyl	<u>GUU</u>	valine	cytosine	<u>GCU</u>	alanine	
	1326	uracyl	<u>GUG</u>	valine	adenine	<u>GAG</u>	glutamic acid	
	+65	thymine	-	-	cytosine	-	-	
	+157	thymine	-	-	cytosine	-	-	
	+388	adenine	-	-	guanine	-	-	
	+562	guanine	-	-	thymine	-	-	
	<i>FgABC4</i>	-777	cytosine	-	-	thymine	-	-
		-242	thymine	-	-	cytosine	-	-
304		uracyl	-	intron	guanine	-	intron	
386		uracyl	<u>UAU</u>	tyrosine	cytosine	<u>UAC</u>	tyrosine	
636		guanine	<u>GCU</u>	alanine	adenine	<u>ACU</u>	threonine	
1103		uracyl	<u>GUU</u>	valine	cytosine	<u>GUC</u>	valine	
1118		cytosine	<u>CUC</u>	leucine	guanine	<u>CUG</u>	leucine	
1995		adenine	<u>AUC</u>	ileucine	guanine	<u>GUC</u>	valine	
2036		cytosine	<u>GCC</u>	alanine	uracyl	<u>GCU</u>	alanine	
2394		cytosine	<u>CUG</u>	leucine	uracyl	<u>UUG</u>	leucine	
2414		uracyl	<u>UCU</u>	serine	cytosine	<u>UCC</u>	serine	
3297		cytosine	<u>CUG</u>	leucine	uracyl	<u>UUG</u>	leucine	
3485		adenine	<u>CAA</u>	glutamine	guanine	<u>CAG</u>	glutamine	
+105		guanine	-	-	adenine	-	-	
+147		cytosine	-	-	thymine	-	-	
+623		cytosine	-	-	thymine	-	-	

n.a. (not available). Negative number indicates SNP position in the upstream region. In contrast, positive numbers indicates SNP position in the downstream region.

this gene in the six adapted strains to determine whether it carried mutations. The *FgABC4* sequences obtained covered 800 bp upstream region, 4562 bp comprising the ORF, and 650 bp downstream regions. No mutations were observed in the adapted strains when compared with the WT progenitor NRRL 13383. However, there existed SNPs between PH-1 and NRRL 13383. Two SNPs existed in the upstream region, 10 in the ORF, and one in the downstream region. One SNP in the ORF was located in an intron, and nine in exons. Two

SNPs in exons led to amino acid changes, at positions 636 and 1,995 of the ORF (Table 10). Taken together, sequence analysis of the three *FgCyp51* genes and *FgABC4* did not reveal any mutation in any of the six adapted strains. This suggests that mutations in other genes may exist in these strains that confer resistance.

III.3. Generation and characterization of deletion mutants for *FgABC1* and *FgABC4* in PH-1 and NRRL 13383

III.3.1. Generation and validation of deletion mutants

Sequence analysis reveals neither a mutation in any of the genes encoding the azole target (*FgCYP51A*, *-B*, *-C*) nor in the ABC transporter *FgABC4*. This suggests thus there must be another mechanism responsible for the increased azole resistance in the P1 and P2 strains. An up-regulation of these genes in response to azole treatment (Becher et al. 2011) is an important clue towards identifying their role. This upregulation is unlikely to result from mutations in the cis-regulatory regions upstream of their start codons and is thus an indirect outcome of another, unknown mutation. Nevertheless, it is important to determine whether their upregulation is occurring by coincidence or whether the encoded proteins are indeed involved in mediating azole tolerance. For the three *FgCyp51* genes this has been published (Liu et al. 2011; Fan et al. 2013). However, for ABC transporters of *F. graminearum* this is not known. Therefore, this study analysed the functional role of *FgABC4* in azole resistance. Interestingly, the *FgABC4* amino acid sequence shares high similarity to FGSG_10995 (*FgABC1*) which groups in the same MRP subfamily (Becher et al. 2011; Kovalchuk and Driessen 2010). Therefore, the role of both ABC transporters was characterized through a gene deletion study.

Deletion mutants were created through homologous integration that replaced *FgABC1* with a *hph* cassette at the same locus. For this purpose, a deletion construct was designed that had two flanking regions homologous to the corresponding target and a *hph* cassette in the middle of it (Figure 10-A). This construct was created in three consecutive PCR steps. The first step amplified separately the left flank, the *hph* cassette and the right flank by standard PCR (chapter II.7.1.1). Left and right flank fragments were amplified from PH-1 gDNA producing 1,225 bp and 1,253 bp products, respectively, using primer pairs Fg1.Fw1-Fg1.Hyg.Rv and Fg1.Hyg.Fw-Fg1.Rv1 (Table 9). The *hph* cassette was amplified from pAN7-1 that produced a 2,095 bp product using uni-hyg.F1 and uni-hyg.R1 primers (Table 9). The second PCR step used DJ-PCR (chapter II.7.1.2) to fuse the three fragments into one

PCR product. This resulted in a 4,573 bp product. The third step was a nested PCR, a standard PCR using Fg1.Fw2 and Fg1.Rv2 primers (Table 9) designed to amplify a somewhat smaller (4,490 bp) fragment from the DJ PCR product.

Since the amounts resulting from the nested PCR were too small to use them directly for fungal transformation, the construct was ligated into pJET1.2 that was then transformed into *E. coli*, which could conveniently be propagated and stored at -80°C. The transformation of an aliquot of the ligation reaction (see II.6.1) resulted in more than thirty *E. coli* colonies growing on LBA amended with 100 µg ampicillin. Twenty colonies were chosen to extract their plasmid DNA. These plasmids were digested with *Bgl*III which should result in bands of 3,796 bp, 2,928 bp and 740 bp for one orientation. In case of the opposite orientation, restriction should result in bands of 3,778 bp, 2,928 bp and 758 bp. Plasmids showing the anticipated bands were sequenced using pJET-seq.F and pJET-seq.R primers (Table 9) to confirm the correctness of their insert by another approach. This resulted in three validated plasmids that were used to amplify the deletion construct via PCR for fungal transformation.

The construct was transformed into strains PH-1 and NRRL 13383 which resulted in 19 and 18 transformants, respectively. After generating single spore isolates, all transformants were analyzed by PCR and Southern hybridisation for the type of integration events. The primer pair Fg1.probe.Fw and Fg1.probe.Rv (Table 9) produced a 515 bp PCR fragment of *FgABC1* in the WT strains. In case of a homologous integration of the transformed construct, this PCR should not result in any band since the binding sites of the primers were missing as a result of the deletion. In case of an ectopic integration, this PCR resulted a band at the predicted size. Thereby, ten transformants in the PH-1 and 12 in the NRRL 13383 backgrounds probably had lost *FgABC1* and were thus considered candidate deletion mutants (Figure 10-B).

The same primer pair was used to generate a DIG-labelled *FgABC1* probe from genomic DNA of PH-1 and NRRL 13383 for Southern blot analysis. *Ase*I was used to digest genomic DNA from each strain analysed. After capillary transfer of the DNA to a Nylon membrane, hybridisation with the *FgABC1* probe produced the anticipated 7,437 bp band in PH-1 and NRRL 13383. This serves as positive control to show that the probe is functional and working. However, this band was not found in transformants no. 2 and 3 of PH-1 and no. 1, 4, 7, 8 and 12 of NRRL backgrounds (Figure 10-C) indicating that *FgABC1* is no longer present in their genomes.

The probe for the *hph* resistance cassette was generated using pAN7-1 as template and primers hyg.Fw2 and hyg.Rv2 (Table 9), which amplified a 1,043 bp product. *Ase*I was also

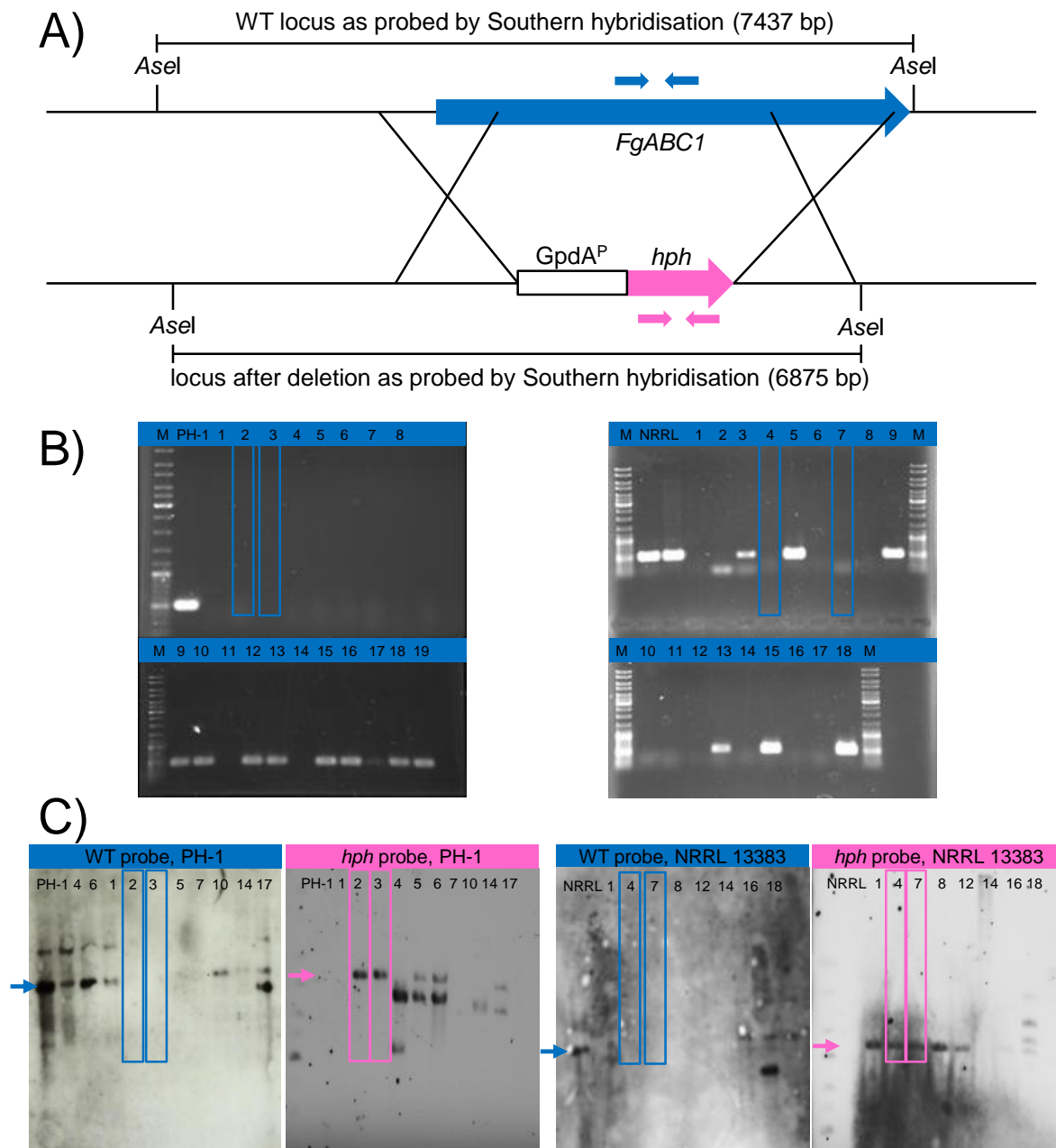


Figure 10. A) Strategy to delete *FgABC1*. Blue arrows show the positions of primers used to detect the wild type locus by PCR and to generate a DIG-labelled hybridisation probe for the detection of the gene. Pink arrows indicate the respective primers to detect the hygromycin resistance cassette (*hph*) and to generate a *hph* probe. B) Results of PCR targeting the wild type locus in the PH-1 (left) and NRRL 13383 backgrounds (right). C) Results of Southern hybridisation detecting the wild type locus (blue) and the *hph* marker (pink) in the PH-1 (left) and NRRL 13383 backgrounds (right). Arrows indicate the expected band. Boxed lanes indicate clones used for subsequent analyses.

used to digest genomic DNA of the strains analysed that was blotted to another Nylon membrane. The latter was hybridized with the *hph* probe, which produced a 6,875 bp band in

case of a deletion mutant. As been expected, transformant no. 2 and 3 in PH-1 and no. 1, 4, 7, 8, 12 in NRRL 13383 backgrounds showed a single band at this size. This means that these transformants had a single copy of the *hph* cassette integrated in their genome. PH-1 and NRRL 13383 did not show this band, thus acting as negative controls. Both Southern analyses confirmed two deletion mutants from PH-1 and five from NRRL 13383 that had lost *FgABC1*, and carried a single integration of the transformed construct at the predicted genomic locus (Figure 10-C). Two mutants from each WT background were selected for further characterization. These mutants were designated $\Delta FgABC1$ -PH.2, $\Delta FgABC1$ -PH.3, $\Delta FgABC1$ -NRRL.4 and $\Delta FgABC1$ -NRRL.7.

Deletion mutants were also generated for *FgABC4* in both backgrounds, PH-1 and NRRL 13383, by employing the same strategy as for *FgABC1*. The deletion construct for *FgABC4* comprised two homologous flanking regions and a *nat1* resistance cassette in between (Figure 11-A). Left and right flank fragments were amplified from gDNA of PH-1 using primer pairs Fg4.Fw1-Fg4.Nours.Rv and Fg4.Nours.Fw-Fg4.Rv1, which resulted in 1,151 bp and 1,320 bp products (Table 9), respectively. The *nat1* cassette was amplified from pNR1 using primers uni-nours.F1 and uni-nours.R1 which resulted in a 1,473 bp product (Table 9). The second PCR step fused the three products of the first round of PCR to one product (3,864 bp) by the DJ-PCR method (chapter II.7.1.2). The third PCR was a nested PCR using Fg4.Fw2 and Fg4.Rv2 as primers (Table 9) and the DJ PCR product as template, which yielded the 3,569 bp deletion construct.

This construct was ligated into the pJET1.2 cloning vector (chapter II.8.1) whose transformation resulted in more than thirty ampicillin resistant *E. coli* colonies. Twenty colonies were chosen to extract their plasmid DNA. These plasmids were digested with *NotI* which should produce a single band of 6,543 bp for the correct insertion. Five clones showed this size that was then sequenced using pJET-seq.F and pJET-seq.R primers (Table 9) to confirm the correctness of the insert. All five clones showed the expected fusion of the *FgABC4* deletion construct to the vector backbone. The plasmids were mixed and used as template in a PCR primers Fg4.Fw2 and Fg4.Rv2 (Table 9) to produce sufficient amounts of deletion construct for fungal transformation.

The transformation resulted in 32 and 17 transformants in the PH-1 and NRRL 13383 backgrounds, respectively. PCR tests verified the absence of *FgABC4* in some transformants using primer pair Fg4.probe.Fw and Fg4.probe.Rv (Table 9) that amplified 533 bp of the ORF in the WT. As result, five transformants from PH-1 and 11 from NRRL 13383 backgrounds were considered as candidate deletion strains (Figure 11-B).

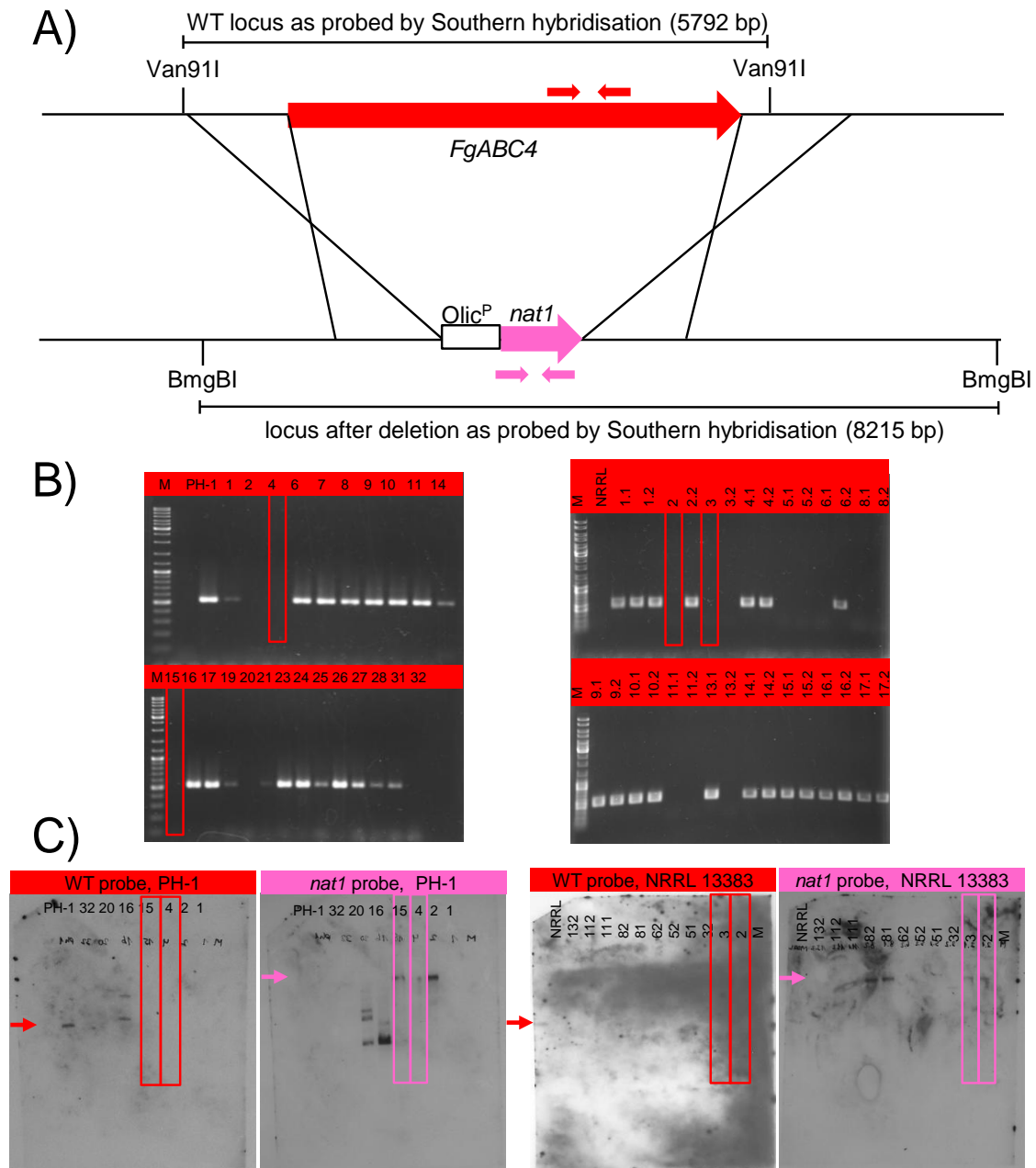


Figure 11. A) Strategy to delete *FgABC4*. Red arrows show the positions of primers used to detect the WT type locus by PCR and to generate a DIG-labelled hybridisation probe for the detection of the gene. Pink arrows indicate the respective primers to detect the nourseothricin resistance cassette (*nat1*) and to generate a *nat1* probe. B) Results of PCR targeting the wild type locus in the PH-1 (left) and NRRL 13383 backgrounds (right). C) Results of Southern hybridisation detecting the wild type locus (blue) and the *nat1* marker (pink) in the PH-1 (left) and NRRL 13383 backgrounds (right). Arrows indicate the expected band. Boxed lanes indicate clones used for subsequent analyses.

The same primer pair was used to generate a DIG-labelled *FgABC4* probe from genomic DNA of strains PH-1 and NRRL 13383 for Southern blot analysis. *Van91I* was used

to digest genomic DNA of each tested clone that was transferred from an agarose gel to a Nylon membrane. Hybridisation of the filter with a DIG-labelled *FgABC4* probe resulted in a 5,792 bp band for the WT PH-1 and NRRL 13383 as the positive controls. In contrast, transformants No. 1, 2, 4, 15, 20 and 32 in the PH-1 and transformants no. 2, 3, 8.1 and 8.2 in the NRRL backgrounds did not produce this band (Figure 11-C), which indicated that *FgABC4* had been lost in their genomes.

The *nat1* probe was generated from pNR1 as a template using primer pair *nours.Fw2* and *nours.Rv2* (Table 9) that amplified a 558 bp product. For Southern blot analysis, *BmgBI* was used to digest genomic DNA of each tested clone that was transferred from an agarose gel to a Nylon membrane. Hybridisation with the DIG-labelled *nat1* probe resulted in a band of 8,215 bp size in the case of the anticipated deletion mutants. Transformants no. 4 and 15 in PH-1 and no. 2, 3, 81 and 82 in NRRL 13383 backgrounds showed this band. This indicated that these strains have a single copy of the *nat1* cassette integrated into their genome (Figure 11-C). Strains PH-1 and NRRL 13383 were as negative control and thus did not showed any band with the *nat1* probe. Both Southern blots confirmed that two deletion mutants in the PH-1 and four in the NRRL 13383 backgrounds had lost *FgABC4* and instead carried a single integration of the *nat1* cassette at that locus (Figure 11-C). Two mutants from each WT background were selected for further characterization. These mutants were designated as $\Delta FgABC4$ -PH.4, $\Delta FgABC4$ -PH.15, $\Delta FgABC4$ -NRRL.2 and $\Delta FgABC4$ -NRRL.3.

III.3.2. Vegetative fitness

The vegetative fitness of the deletion mutants was determined by assessing the kinetics of *in vitro* growth on PDA plates. In addition, the percentage of conidial germination was determined on an object glass placed in a humid plastic dish for 24 hpi. These assays were performed to check whether the deletion of *FgABC1* and *FgABC4* may have affected the viability of the transformants.

For transformants in both genetic backgrounds, i.e. PH-1 and NRRL 13383, the kinetics of *in vitro* growth did not differ significantly from those of the respective WT strains (Figure 12-A). In the PH-1 background, all mutants grew at a similar rate as shown by the WT. In the NRRL 13383 background, the mutants grew even a bit faster than the WT from the second day on. These results showed that the deletion did not negatively influenced vegetative growth irrespective of background.

Similarly, deletion of *FgABC1* and *FgABC4* did not affect conidial germination of the mutants. Irrespective of their background, germination of all mutants and the WT strains was

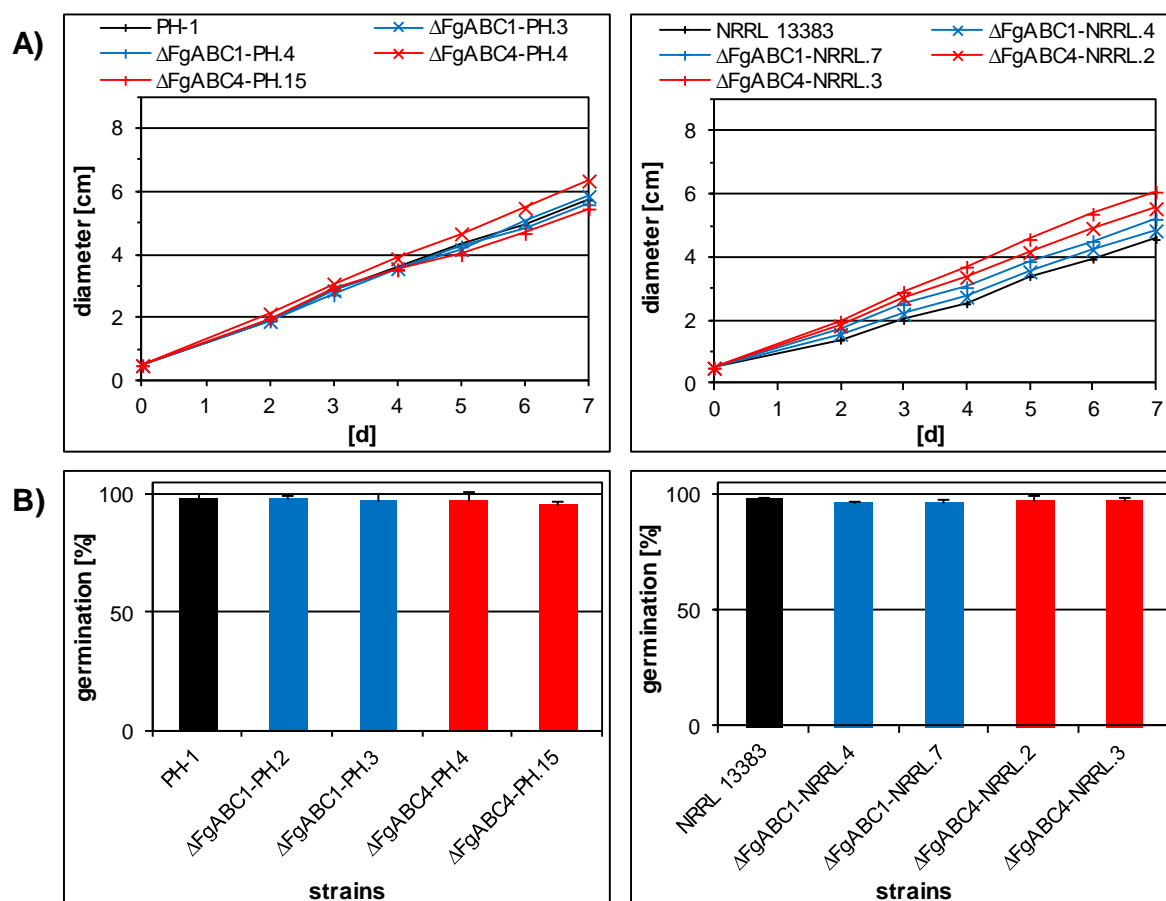


Figure 12. A) Kinetics of *in vitro* growth on PDA at 23°C during seven day. B) Percentages of conidial germination. Left and right panels provide data for strains having the PH-1 and NRRL 13383 backgrounds, respectively.

> 90% (Figure 12-B). This provided evidence that deletion of both ABC transporters did not cause defects in conidial germination of the mutants.

III.3.3. Sensitivities against fungicides and plant metabolites

Twelve fungicides from different chemical groups and five plant secondary metabolites were used to determine the sensitivity levels of the deletion mutants (Table 11). The different fungicide groups were triazoles, imidazoles, pyrimidines, morpholines, spiroketal-amines, methoxy-acrylates, anthraquinones, pyridine-carboxamides, and thiocarbamate. These fungicides were obtained as formulations or pure substances. Those that did not have a trademark name were obtained as pure substances. In cases of formulations, concentrations applied were calculated on the basis of the effective compound. Tolnaftate has never been used in agricultural practice and was used as a control.

Table 11. List of xenobiotics used in the sensitivity assay of PH-1, NRRL 13383 and the deletion mutants.

No	Active ingredient	Chemical group	FRAC code*	Provider
Fungicides				
1	metconazole	triazole	3	(Caramba, BASF)
2	tebuconazole	triazole	3	(Folicur, BASF)
3	epoxiconazole	triazole	3	Sigma-Aldrich
4	prothioconazole	triazole	3	Bayer Inc.
5	prochloraz	imidazole	3	(Sportak, BASF)
6	fenarimol	pyrimidines	3	Sigma-Aldrich
7	fenpropimorph	morpholines	5	(Corbel, BASF)
8	spiroxamine	spiroketal-amines	5	Sigma-Aldrich
9	boscalid	pyridine-carboxamides	7	Sigma-Aldrich
10	azoxystrobin	methoxy-acrylates	11	(Amistra, BASF)
11	tolnaftat	thiocarbamate	18	Sigma-Aldrich
12	dithianon	anthraquinones	M9	Sigma-Aldrich
Plant secondary metabolites				
1	BOA	2-benzoxazolinone	n.a	Sigma-Aldrich
2	gramine	3-(dimethylaminomethyl)indole	n.a	Sigma-Aldrich
3	benzopyran	2,3-dihydro-5,7-dihydroxy-2-(4-hydroxyphenyl)-4H-1-benzopyran-4-one	n.a	Sigma-Aldrich
4	naringenin	4',5,7-trihydroxyflavanone	n.a	Sigma-Aldrich
5	quercetin	3,3',4',5,7-pentahydroxyflavone dihydrate	n.a	Sigma-Aldrich

* (Fungicide Resistance Action Committee 2012); n.a: not available; provider with bracket indicates the respective active ingredient was derived as formulated substance, while the others were derived as pure

The growth of the $\Delta FgABC1$ mutants in both backgrounds was not affected significantly by any of the tested fungicide groups. In contrast, the mutants of $\Delta FgABC4$ in the PH-1 background exhibited a significant growth reduction when exposed to prothioconazole, and fenarimol. The corresponding mutants in the NRRL 13383 background were also inhibited significantly by these substances and by epoxyconazole. Results obtained were not affected by the type of inoculum, conidia or mycelia, used in this experiment, except for fenarimol where inhibition occurred only when using mycelia, irrespective of the background. None of the plant secondary metabolites was effective in differentiating the growth of the WT strains and any of the corresponding mutants (Figure 13).

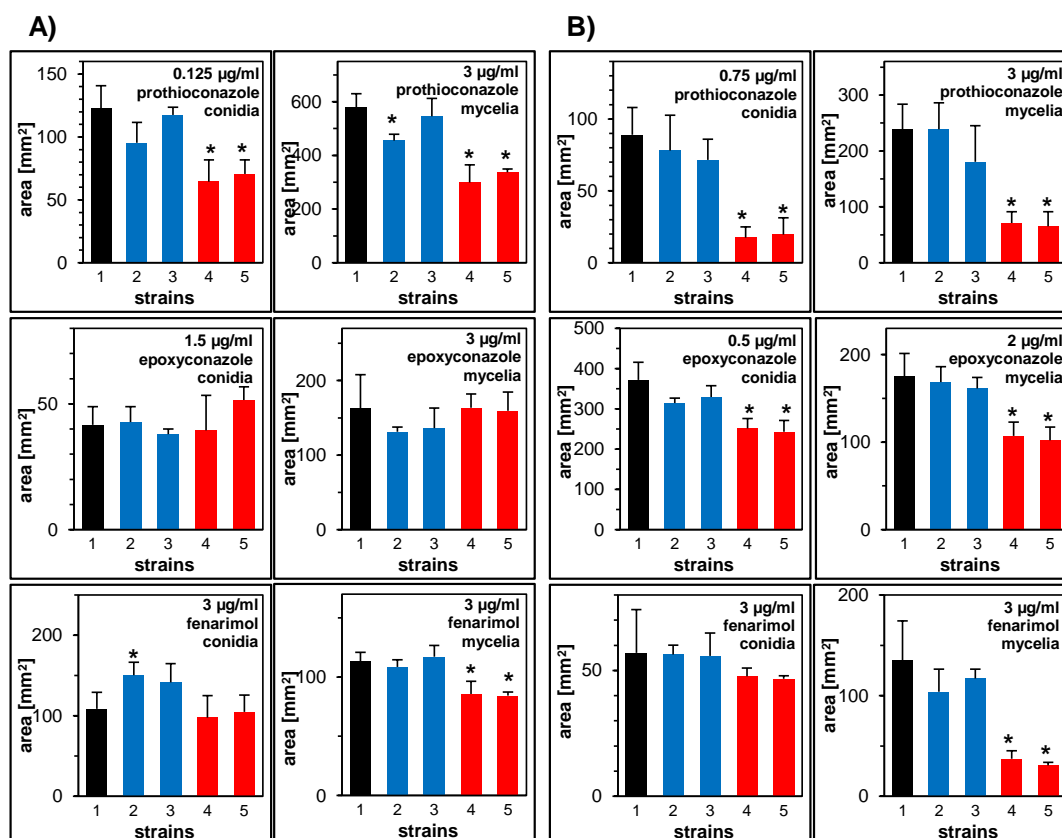


Figure 13. Azole sensitivity assay. A) PH-1 background, strains tested: 1: PH-1, 2: $\Delta FgABC1.PH.2$, 3: $\Delta FgABC1.PH.3$, 4: $\Delta FgABC4.PH.4$, 5: $\Delta FgABC4.PH.15$. B) NRRL 13383 background, strains tested: 1: NRRL 13383, 2: $\Delta FgABC1.NRRL.4$, 3: $\Delta FgABC1.NRRL.7$, 4: $\Delta FgABC4.NRRL.2$, 5: $\Delta FgABC4.NRRL.3$. Error bars represent SD. An asterisk indicates a significant difference between the wild type and a mutant. Significance level was determined using Student's T-Test ($P \leq 0.05$).

III.3.4. Transcript levels

It has been shown above that *FgABC4* mediates certain levels of azole tolerance in the wild type strains. Transcript levels of *FgABC1* and *FgABC4* in the deletion mutants and the wild type strains were determined to assess whether the deletion of a given ABC transporter gene may affect transcription of the other gene. For this analysis, a deletion mutant from each gene in the NRRL 13383 background was exposed to 5 mg/L tebuconazole for 12 hours. RNA was prepared from the mycelia and analysed by RT-qPCR for the abundances of *FgABC1* and *FgABC4* transcripts (see II.5.2). Both were significantly up-regulated, whereas the initial fluorescence value increased 2.98 and 3.87 fold, respectively, by the fungicide treatment, when compared to the appropriate controls (Figure 14). As expected, *FgABC1* and *FgABC4* mRNA were not detected in corresponding deletion mutants.

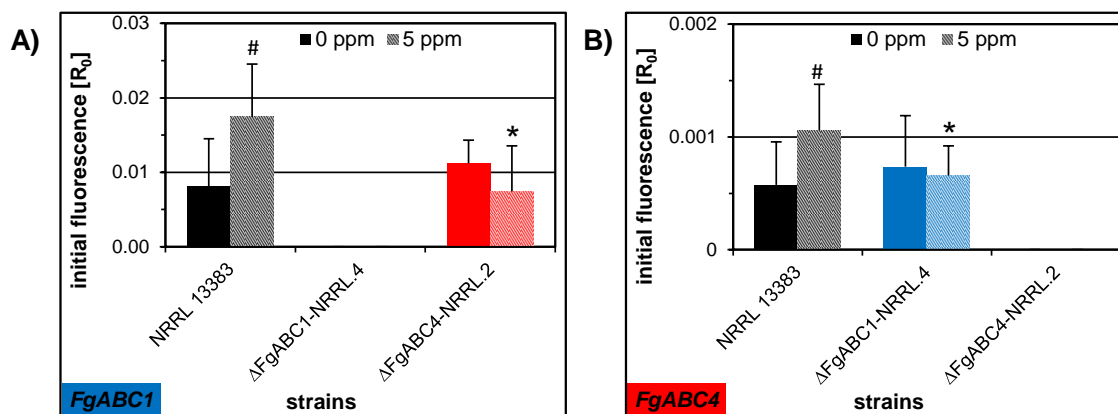


Figure 14. Transcript levels of *FgABC1* (A) and *FgABC4* (B) as determined by RT-qPCR in NRRL 13383, $\Delta FgABC1$ -NRRL.4 and $\Delta FgABC4$ -NRRL.2. Strains were treated for 12 h with 5 mg/L tebuconazole, control cultures remained untreated. Error bars represent SD. A hashtag (#) indicates significant differences between 0 and 5 mg/L in the same strain. An asterisk (*) indicates a significant difference between wild type and a mutant for the same culture condition. Significance level was determined using Student's T-Test ($P \leq 0.05$).

Interestingly, the significantly increased transcript levels of *FgABC1* and *FgABC4* observed after treating NRRL 13383 with 5 mg/L tebuconazole were not observed in the deletion mutants. In cultures of the $\Delta FgABC4$ mutant that were not treated with tebuconazole, the mRNA abundance of *FgABC1* was at similar levels to those of the WT. However, in contrast to NRRL 13383, treatment with tebuconazole did not significantly increase the transcript levels of *FgABC1* in strain $\Delta FgABC4$ -NRRL.2. This initial fluorescence difference between the two strains was 2.34-fold and was statistically significant (Figure 14-A).

In untreated cultures, the transcript levels of *FgABC4* did not differ significantly between the $\Delta FgABC1$ mutant and the WT. In contrast to NRRL 13383, treatment with tebuconazole did not significantly increase the mRNA abundance of *FgABC4* in strain $\Delta FgABC1$ -NRRL.4. This initial fluorescence difference between the two strains was 1.61-fold and was statistically significant (Figure 14-B).

III.3.5. Virulence levels on three host plants

F. graminearum is a pathogen of several cereals including wheat, maize and barley. The two wild type strains used in this study have different chemotypes, i.e. PH-1 has the 15-ADON and NRRL 13383 the NIV chemotype. Although it is poorly understood why different chemotypes exist in natural populations of the fungus, it is known that B trichothecenes may

differentially affect virulence in different host plants. Whereas DON is a virulence factor in wheat (Jansen et al. 2005), NIV is important for the infection of maize (Maier et al. 2006). Although the transporter for trichothecenes is known (*FgTRI12*), I wanted to rule out that some side activity of the ones analysed here may contribute as well. On the other hand, it was also known that phytoalexins made by the host may serve as substrates for ABCs, although it was not known which host is making which phytoalexin. For that reason, all deletion mutants in each WT background were tested on wheat heads, maize stems and barley heads to analyze the role of ABC transporter in virulence.

In wheat, both WT strains caused clear FHB symptoms on inoculated heads starting from 2 dpi. Nevertheless, PH-1 was more virulent than NRRL 13383. PH-1 inoculation resulted on average in 72% symptomatic spikelets while NRRL 13383 resulted in 20%. Deletion of *FgABC1* from the PH-1 genome, caused a significant reduction in virulence in mutants $\Delta FgABC1$ -PH.2 and $\Delta FgABC1$ -PH.3. These produced only 22% and 19% symptomatic spikelets, respectively. A similar phenotypic effect was observed in mutants $\Delta FgABC1$ -NRRL.4 and $\Delta FgABC1$ -NRRL.7, which caused only 6% and 10% symptomatic spikelets, respectively. Deletion of *FgABC4* did not influence significantly virulence in any of the deletion mutants irrespective of their genetic background (Figure 15-A).

In maize stems, PH-1 and NRRL 13383 produced on average 72.59 and 68.41 mm², respectively, of necrotic tissue at 14 dpi. Irrespective of their genetic background, all deletion mutants of *FgABC1* showed a significant virulence reduction when compared to their appropriate WT strain. $\Delta FgABC1$ -PH.2, $\Delta FgABC1$ -PH.3, $\Delta FgABC1$ -NRRL.4 and $\Delta FgABC1$ -NRRL.7 mutants produced 10.72, 13.18, 18.04 and 15.87 mm² of necrotic tissue, respectively. These levels were significantly lower than the corresponding WT. All deletion mutants of *FgABC4* produced areas of necrotic tissue that did not differ significantly from the respective WT strain (Figure 15-B).

On barley ears, PH-1 and NRRL 13383 showed FHB symptoms in 74% and 58% of the spikelets at 14 dpi. As has been observed in the two other host plants tested, all deletion mutants of *FgABC1* in both WT backgrounds showed a significant reduction in virulence. Mutants $\Delta FgABC1$ -PH.2, $\Delta FgABC1$ -PH.3, $\Delta FgABC1$ -NRRL.4 and $\Delta FgABC1$ -NRRL.7 caused FHB symptoms in 51.26, 36.90, 16.47 and 11.18%, respectively, of the spikelets per ear. All deletion mutants of *FgABC4* exhibited virulence levels that were similar to their respective WT strain (Figure 15-C).

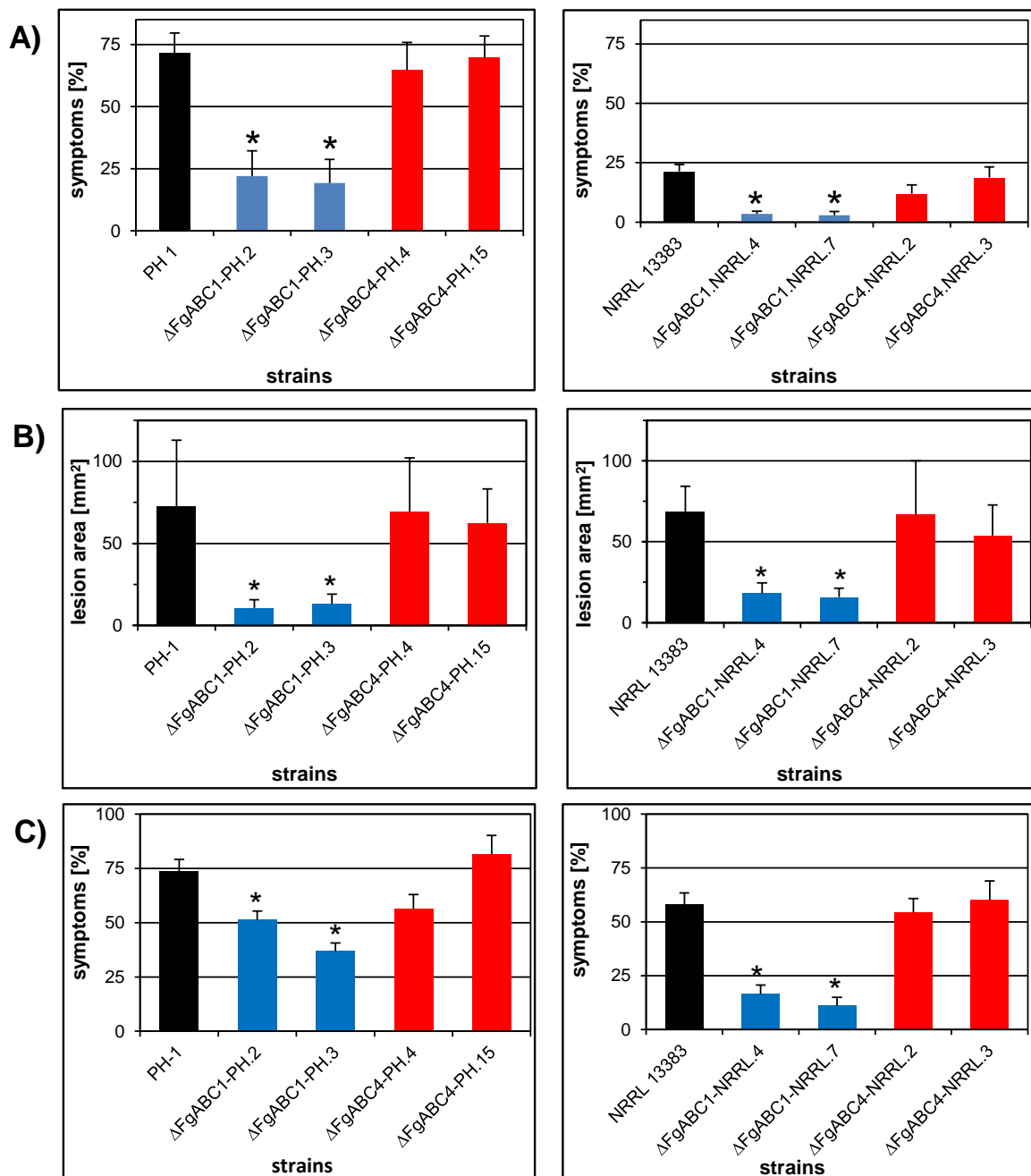


Figure 15. Virulence assays on three host plants. Left and right panels: strains of PH-1 and NRRL 13383 backgrounds, respectively. A) Wheat heads. B) Maize stems. C) Barley heads. An asterisk indicates a significant difference between wild type and a mutant. Significance level was determined using Student's T-Test ($P \leq 0.05$).

The $\Delta FgABC1$ and $\Delta FgABC4$ mutants behaved differently in wheat, maize and barley. In both genetic backgrounds, the $\Delta FgABC1$ mutants showed reduced virulence compared to their respective WT strain. In contrast, $\Delta FgABC4$ mutants showed virulence levels that were similar to the corresponding WT strains.

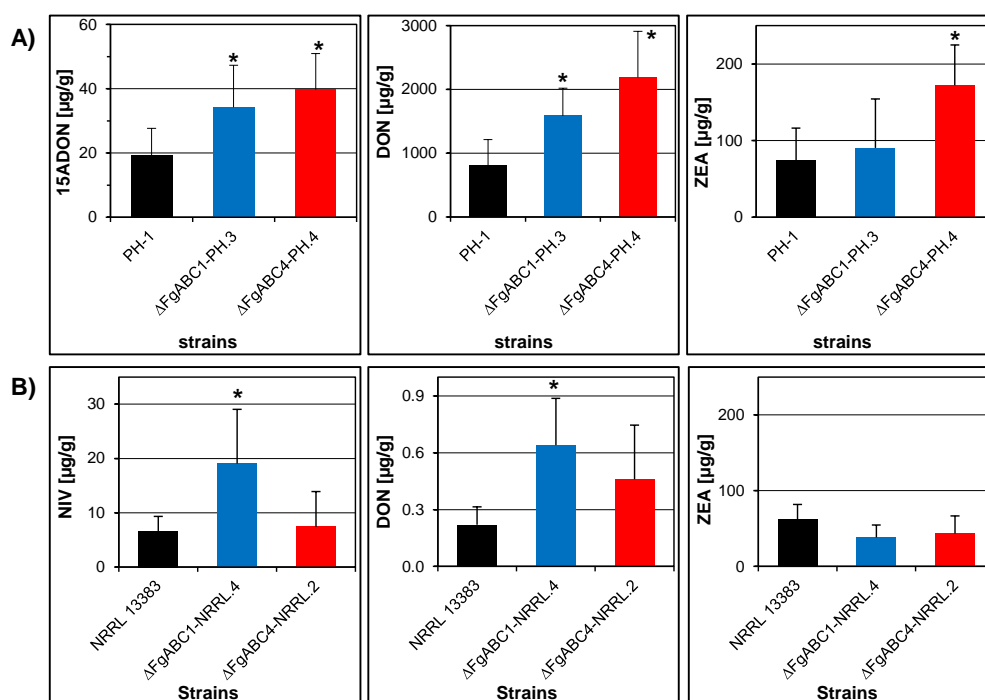


Figure 16. Mycotoxin production of WT strains and the deletion mutants in PH-1 (A) and NRRL 13383 backgrounds (B). An asterisk (*) indicates a significant difference between wild type and a mutant. Significance level was determined using Student's T-Test ($P \leq 0.05$).

III.3.6. Mycotoxin production

FgABC1 and *FgABC4* are similar ABC transporters that both belong to the MRP subfamily. Notable, above experiments exhibited that deletion of these genes resulted in remarkable phenotypical differences in virulence. Whereas *FgABC1* is important for virulence, *FgABC4* plays a role in azole tolerance. Since trichothecenes such as DON are important virulence factors in *F. graminearum*, mycotoxin production of the deletion mutants was analysed *in vitro* to determine whether these genes may play a role in their secretion from the cell.

Deletion of *FgABC1* and *FgABC4* did not reduce the levels of B-trichothecenes and ZEA measured in rice grain cultures of the corresponding mutants, irrespective of their genetic background. In contrast, the majority of the mutants showed significantly higher levels of mycotoxins. The production of DON, 15-ADON and ZEA by the deletion mutants in the PH-1 background were significantly higher than PH-1, except for ZEA levels of ΔFgABC1-PH.1. Similarly, the production of NIV, DON and ZEA by the deletion mutants in the NRRL 13383 background were similar or higher than NRRL 13383 (Figure 16). This result indicated that *FgABC1* and *FgABC4* has no role in mycotoxin extrusion in *F. graminearum*.

III.3.7. Complementation of deletion mutants with wild alleles

The contribution of *FgABC1* in virulence and of *FgABC4* in azole resistance was shown indirectly by analyzing the corresponding deletion mutants. To ascertain that the observed effects were indeed only caused by the integration of the transformed DNA at the targeted loci, complementation strains were generated by a co-transformation approach. The co-transformation restored the WT allele at its original locus in parallel with the integration of a new resistance marker at an ectopic locus. This resistance marker was needed to select for transformants. One deletion strain per gene in the NRRL 13383 background was used as the recipient strain in the transformation. The chosen deletion strains were $\Delta FgABC1.NRRL.4$ and $\Delta FgABC4.NRRL.2$. These strains were chosen because they were also used for the RT-qPCR assays.

The hygromycin cassette in the $\Delta FgABC1.NRRL.4$ mutant was replaced with the native *FgABC1* allele that was amplified from genomic DNA of NRRL 13383 yielding a product of 5,005 bp using primers Fg1.Fw2 and Fg1.Rv2 (Table 9). The new resistance marker providing nourseothricin resistance was amplified from pNR1 yielding a product of 1,473 bp using primers uni-nours.F1 and uni-nours.R1 (Table 9). The *FgABC1* DNA and nourseothricin cassette were transformed simultaneously into $\Delta FgABC1.NRRL.4$ protoplasts. Twenty one transformants grew on regeneration medium (RM) supplemented with 100 $\mu\text{g}/\mu\text{L}$ nourseothricin. Five of them did not grow when transferred to PDA supplemented with 100 $\mu\text{g}/\mu\text{L}$ hygromycin and were thus considered candidates that might had replaced the HygR-marker with the transformed WT allele. These five clones were analyzed by three PCR assays for the presence of the nourseothricin marker using primers nours.Fw2 and nours.Rv2 (Table 9), the hygromycin marker using primers hyg.Fw2 and hygRv3 (Table 9), and for the size of the targeted locus using nested primers for *FgABC1*. All five clones showed a band of 558 bp in the PCR for the nourseothricin resistance cassette (Figure 17-A), but showed no band in the PCR for the hygromycin resistance cassette (Figure 17-B), which confirmed the observed phenotypes on the corresponding selective media. In addition, the third PCR using primers binding in the flanks of the *FgABC1* locus amplified a product of 4,573 bp. This band had the same size as that of NRRL 13383, but differed from that of the deletion strain, which was 5,088 bp (Figure 17-C). The three PCRs thus confirmed that all five clones had the anticipated genotype. These strains were cFgABC1.NRRL.4.5, cFgABC1.NRRL.4.7, cFgABC1.NRRL.4.8, cFgABC1.NRRL.4.15 and cFgABC1.NRRL.4.18.

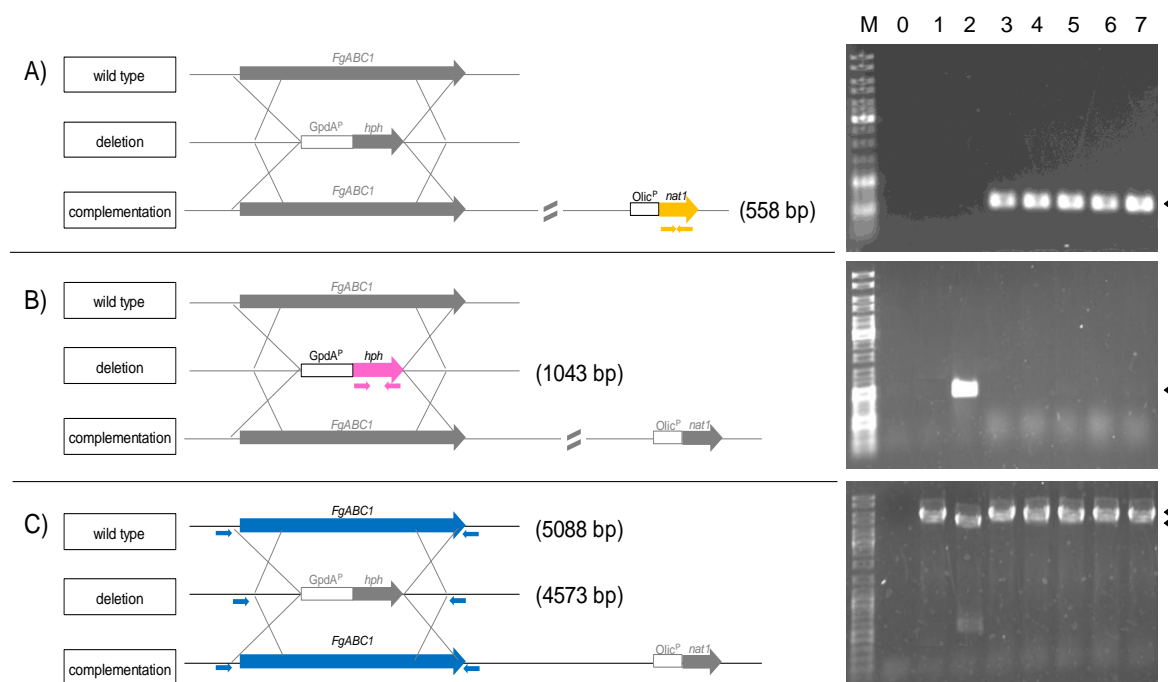


Figure 17. PCR test of the complementation strains of *FgABC1*. A) PCR targeting the *nat1* marker. B) PCR targeting the *hph* marker. C) PCR targeting the WT allele. Whereas the WT and complementation strains show a band of 5,088 bp, the deletion strain shows a band of 4,573 bp. Lane M: GeneRuler DNA ladder Mix; lane 0: negative water control; lane 1: NRRL 13383; lane 2: $\Delta FgABC1$.NRRL.4; lane 3-7 clones no. 5, 7, 8, 15, 18. Yellow, pink and blue arrows show primer positions to amplify *nat1*, *hph*, and WT genes, respectively. Black arrow heads point to the anticipated bands.

A similar strategy was applied in the complementation of a *FgABC4* deletion mutant. The nourseothricin resistance cassette in $\Delta FgABC4$.NRRL.2 mutant was replaced with the native *FgABC4* allele that was amplified from genomic DNA of NRRL 13383 resulting in a product of 6,658 bp. A co-transformation was conducted with a hygromycin resistance cassette that was amplified from pAN7-1 yielding a product of 2,095 bp. Subsequently, the *FgABC4* DNA and the hygromycin cassette were co-transformed into protoplasts of strain $\Delta FgABC4$.NRRL.2 applying the same procedures as for *FgABC1*. The transformation resulted in 13 transformants that grew on RM amended with 100 $\mu\text{g}/\mu\text{L}$ hygromycin. Three of them did not grow on PDA supplemented with 100 $\mu\text{g}/\mu\text{L}$ nourseothricin. These candidates were tested with three PCR assays as described above. All three clones produced a band of 1,043 bp in the PCR for the hygromycin resistance cassette (Figure 18-A), but showed no band in the PCR for the nourseothricin resistance cassette (Figure 18-B), which confirmed the observed phenotypes on the corresponding selective media. Additionally, the

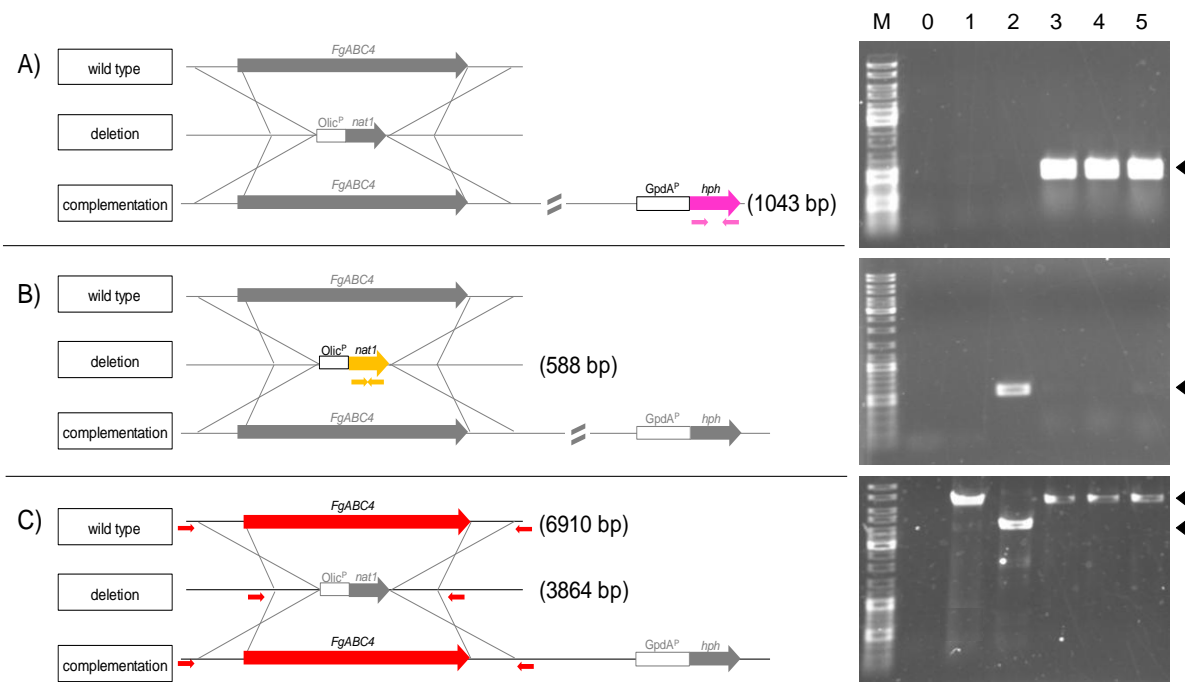


Figure 18. PCR test of the complementation strains of *FgABC4*. A) PCR targeting the *hph* marker. B) PCR targeting the *nat1* marker. C) PCR targeting the WT allele. Whereas the WT and complementation strains show a band of 6,910 bp, the deletion strain shows a band of 3,864 bp. Lane M: GeneRuler DNA ladder Mix; lane 0: negative water control; lane 1: NRRL 13383; lane 2: $\Delta FgABC4$.NRRL.2; lane 3-5 clones no. 3, 7, 8. Pink, yellow and red arrows show primer positions to amplify *hph*, *nat1* and WT genes, respectively. Black arrow heads point to the anticipated bands.

third PCR using primers that bind in the flanks of the *FgABC4* locus amplified a product of 6,910 bp (Figure 18-C). This band had the same size as in NRRL 13383 but was different from that of the deletion strain, which was 3,864 bp. Thus, the three PCRs confirmed that the three clones had the anticipated genotype. These strains were cFgABC4.NRRL.2.3, cFgABC4.NRRL.2.7, cFgABC4.NRRL.2.8.

As performed previously for the deletion mutants, vegetative fitness of the complementation strains was assessed by determining the *in vitro* growth rates and the frequencies of conidial germination. All complementation strains showed similar *in vitro* growth rates as the deletion mutants $\Delta FgABC1$.NRRL.4, $\Delta FgABC4$.NRRL.2 and the WT NRRL 13383 (Figure 19-A). In addition, all complementation strains showed similar conidial germination rates as the deletion mutants $\Delta FgABC1$.NRRL.4, $\Delta FgABC4$.NRRL.2 and the WT NRRL 13383 (Figure 19-B). This result confirmed that the ectopic integration of the new resistance cassette did not impaired vegetative fitness of the complementation strains.

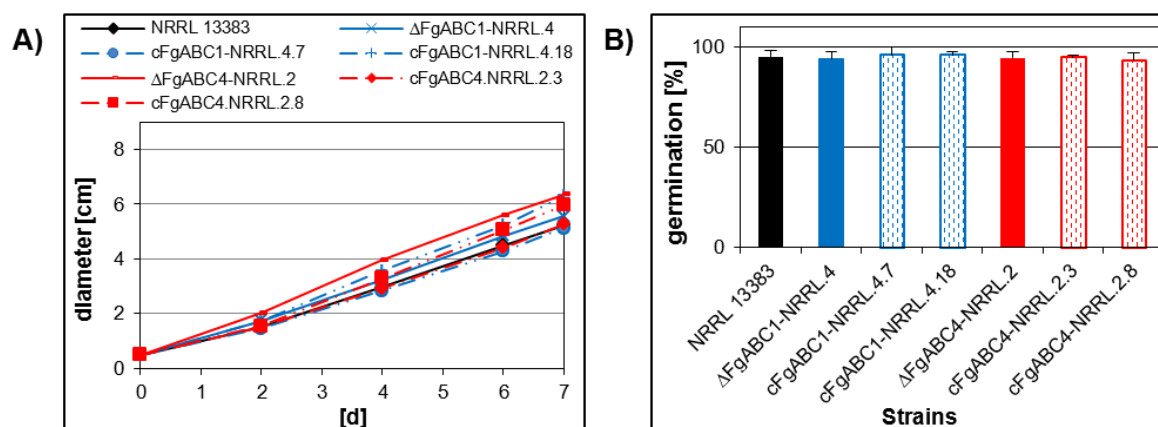


Figure 19. Fitness assays of complementation strains. A) The kinetics of *in vitro* growth on PDA at 23°C during seven days. B) Percentage of conidia germination.

Since the deletion strains of *FgABC1* had a significantly reduced virulence on different hosts, the complementation strains of *FgABC1* were tested by the wheat head and maize stem assays used before for a reversion to wild type NRRL 13383. In wheat, the two complementation strains caused typical FHB symptoms in 20% of the spikelets, which was close to the results observed in NRRL 13383 (Figure 20-A). Similarly, these strains produced areas of necrotic tissue of 90-100 mm² in cross sections of maize stems, thus almost reaching the same levels observed in NRRL 13383 (Figure 20-B). Therefore, the virulence defects exhibited by the deletion mutant Δ*FgABC1*.NRRL.4 were restored in the two complementation strains. This formally confirmed that the phenotype previously observed in the deletion mutants was indeed caused by a loss of function of *FgABC1*, and not by any artifacts that might have occurred in the transformation.

III.4. Deletion of *FgABC4* in strain P1-11

III.4.1. Generation and validation of deletion mutants

Above, it was shown that *FgABC4* provides a certain level of azole tolerance to strains PH-1 and NRRL 13383. The observed effects were stronger in NRRL 13383 than in PH-1 (see III.2.4). Since strain P1-11 is a descendant of NRRL 13383 that has acquired a higher level of tolerance to azole (Becher et al. 2010), this study then investigated the role of *FgABC4* in P1-11.

The azole-resistant strain P1-11, which had been isolated in a previous work by selection on 10 mg/L tebuconazole (Becher et al. 2010), was transformed with the same DNA construct that has been used above to generate deletion mutants of *FgABC4* in the PH-1 and

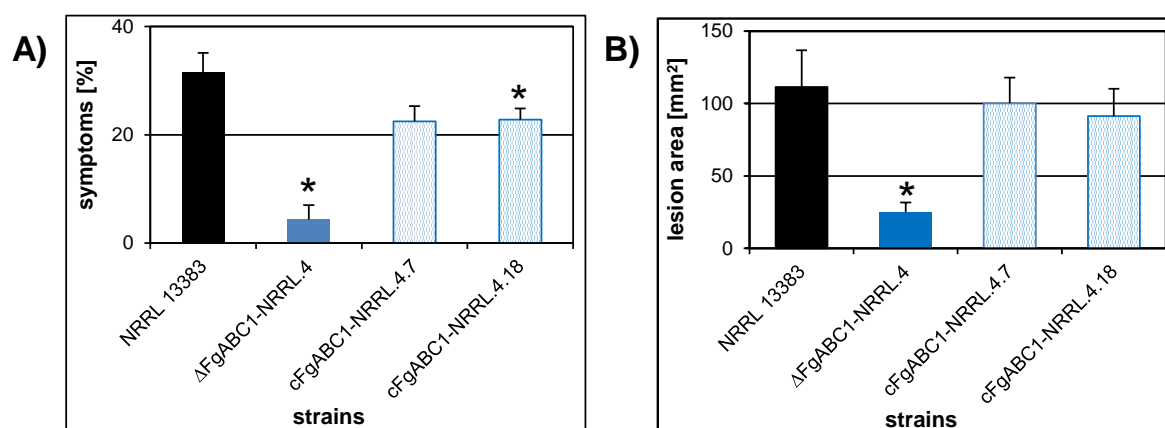


Figure 20. Virulence assays of complementation strains on wheat heads (A) and maize stems (B). An asterisk (*) indicates a significant difference between NRRL 13383 and a mutant. Significance level was determined using Student's T-Test ($P \leq 0.05$).

NRRL 13383 backgrounds (Figure 21-A). This resulted in 10 transformants that were tested by PCR targeting the coding region of *FgABC4* using primers Fg17058.F8 and Fg4.Rv3 (Table 9). This PCR test indicated that seven out of 10 transformants had lost the WT allele, while the remaining three strains and NRRL 13383 and P1-11 showed a 979 bp band, predicted for the resident ORF. This result was supported by another PCR test which detected the nourseothricin resistance cassette using primers uni.nours.Fw and uni.nours.Rv (Table 9), producing a 1,473 bp band (Figure 21-B) in all ten transformants.

The Fg4.probe.Fw and Fg4.probe.Rv, and respectively, uni.nours.Fw and uni.nours.Rv primer pairs were used to generate a DIG-labeled *FgABC4* probe from genomic DNA of NRRL 13383 and a *nat1* probe from pNR1, respectively. Two different restriction enzymes were used to digest genomic DNAs of the clones analyzed, which were then transferred onto two Nylon membranes that were hybridized with the *FgABC4* and *nat1* probes. *Pst*I was used to digest genomic DNA to be probed with *FgABC4*, which resulted in NRRL 13383 in a signal corresponding to a DNA-fragment of 9.454 bp. *Xba*I was used to digest genomic DNA to be probed with *nat1*, which resulted in case of a successful deletion in a signal corresponding to a DNA-fragment of 5.392 bp. Both Southern blots indicated that three deletion mutants were obtained that had a single integration of the *nat1* cassette replacing the WT allele (Figure 21-C). These mutants were named Δ FgABC4-P11.1, Δ FgABC4-P11.4 and Δ FgABC4-P11.7. The ectFgABC4-P11.8 strain was used in later experiments as an ectopic integration mutant.

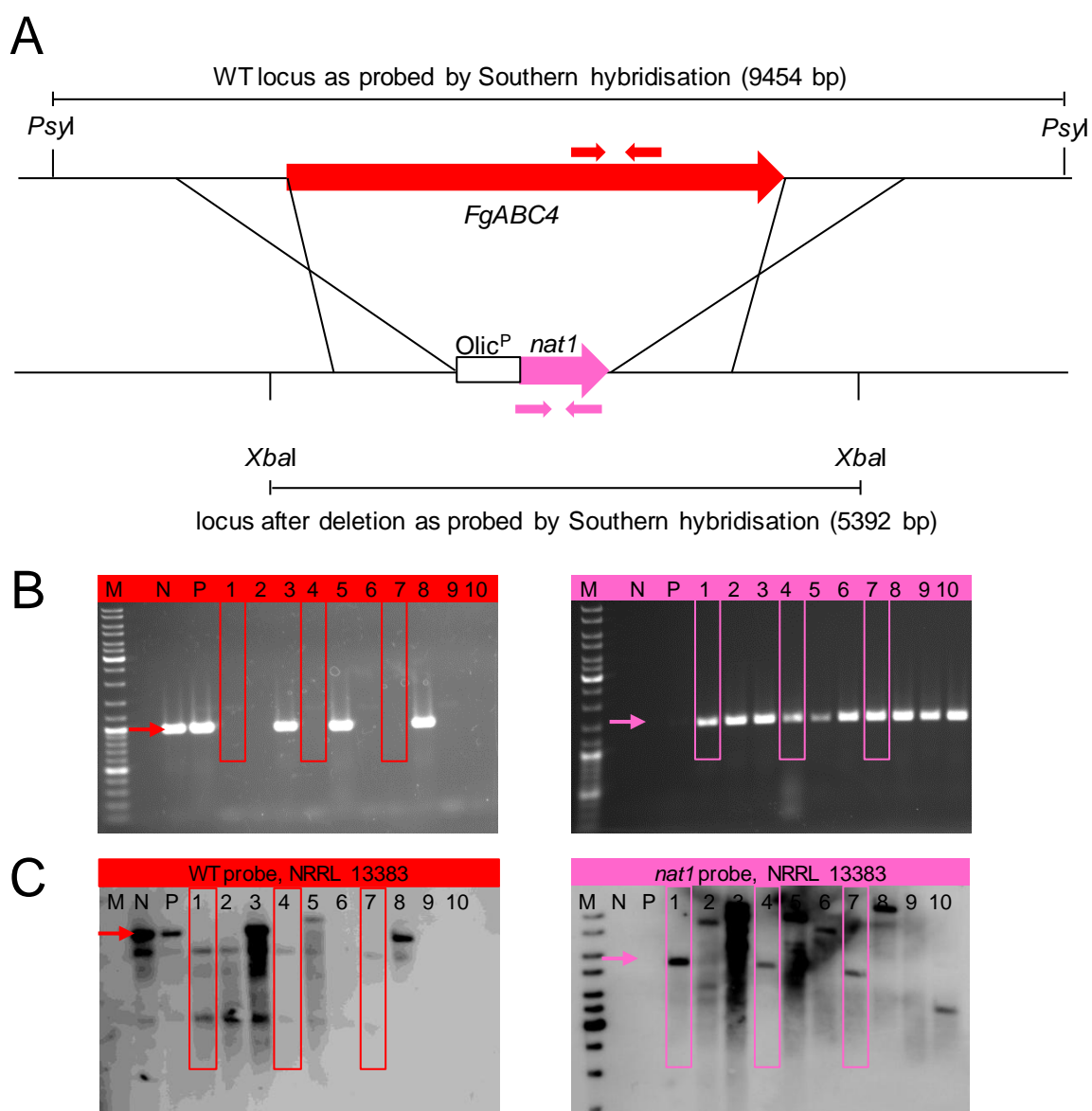


Figure 21. A) Strategy to delete *FgABC4* in the background of P1-11. Red arrows show the positions of primers used to detect the WT type locus by PCR and to generate a DIG-labelled hybridisation probe for the detection of the gene. Pink arrows indicate the respective primers to detect the nourseothricin resistance cassette (*nat1*) and to generate a *nat1* probe. B) Results of PCR targeting the WT locus (left) and *nat1* cassette (right). C) Results of Southern hybridisation detecting the WT locus (left) and *nat1* cassette (right). Arrows indicate the expected band. Boxed lanes indicate clones used for subsequent analyses. N=NRRL 13383, P = P1-11, 1 to 10= name of transformants.

III.4.2. Vegetative fitness

As has been conducted before with the deletion mutants of the PH-1 and NRRL 13383 backgrounds, vegetative fitness assays of three deletion and an ectopic mutants in the

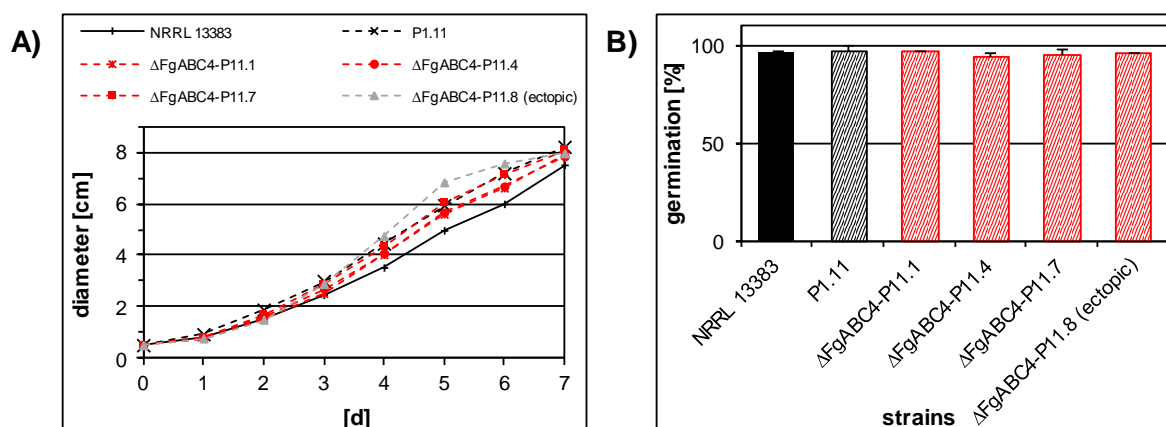


Figure 22. A) Growth kinetics *in vitro* on PDA for seven days. B) Percentage of conidia germination of NRRL 13383, P1-11, three deletion mutants and one ectopic strain in the background of P1-11.

background of P1-11 were done. This was performed to assess whether any essential vegetative parameters were changed by transformation.

P1-11, three deletion mutants ($\Delta FgABC4$ -P11.1, $\Delta FgABC4$ -P11.4 and $\Delta FgABC4$ -P11.7) and one ectopic (ectFgABC4-P11.8) mutants exhibited growth kinetics on PDA plates at 23°C for seven days that were similar to NRRL 13383 (Figure 22-A). This indicates that the deletion of *FgABC4* in the background of P1-11 did not interfere with vegetative growth of the mutants.

Also conidial germination of P1-11, the three deletion mutants and the ectopic mutant were similar to NRRL 13383 (Figure 22-B). All strains exhibited > 90% conidial germination indicating that the deletion of *FgABC4* in the background of P1-11 did not affect conidial germination.

III.4.3. Fungicide sensitivities

Fungicide sensitivity assays were performed for deletion mutants in the background of the azole-adapted strain P1-11 to determine their resistance levels against azoles and to compare them to those of the deletion mutants obtained in the background of the wild type strain NRRL 13383 (see III.3.3). Four triazole and one pyrimidine fungicides were tested here (Table 12). In the control treatment (no fungicide), all strains including the WT and the mutants showed growth that was similar to P1-11. An interesting phenotype was observed when azole was amended. For example, in the presence of 3 µg/mL prothioconazole, the growth rates of three deletion mutants and the ectopic mutant in the background of P1-11, were not significantly different from P1-11. This means that the loss of *FgABC4* in P1-11 did

Table 12. List of fungicides used in the sensitivity test of mutants in P1-11 background.

No	Active ingredient	Chemical group	FRAC code	Provider
1	prothioconazole	triazole	3	Bayer Inc.
2	epoxyconazole	triazole	3	Sigma-Aldrich
3	tebuconazole	triazole	3	(Folicur, BASF)
4	prochloraz	imidazole	3	(Sportak, BASF)
5	fenarimol	pyrimidines	3	Sigma-Aldrich

FRAC: Fungicide Resistance Action Committee (Fungicide Resistance Action Committee 2012); n.a: not available; provider with bracket indicates the respective active ingredient was derived as formulated substance, while the others were derived as pure substance

not alter the resistance to azole. In contrast, as seen above (see III.3.3), the same mutation when introduced in the wild type background caused a significant decrease of tolerance to the fungicide. Corresponding results were obtained when using 2, 3, 0.1 and 3 $\mu\text{g/mL}$ of epoxyconazole, tebuconazole, prochloraz and fenarimol for the treatment, respectively (Figure 23).

III.4.4. Virulence levels

The deletion and ectopic mutants in the P1-11 background were tested using the maize stem assay (see II.8.2) to assess the effect of the deletion on virulence. Three deletion mutants and one ectopic mutant, P1-11 and for comparison, NRRL 13383 and two deletion mutants in this background were included in this assay.

The virulence of P1-11 in maize stems was not significantly different from its WT progenitor, NRRL 13383. Likewise, three deletion and one ectopic *FgABC4* mutants in the P1-11 background exhibited similar virulence levels in comparison with P1-11 and NRRL 13383 (Figure 24). These results confirmed data obtained before for the deletion mutants of *FgABC4* in the PH-1 and NRRL 13383 backgrounds that showed no significant virulence reduction (see III.3.5). This indicates that the deletion of *FgABC4* did not alter virulence in any of the genetic backgrounds tested.

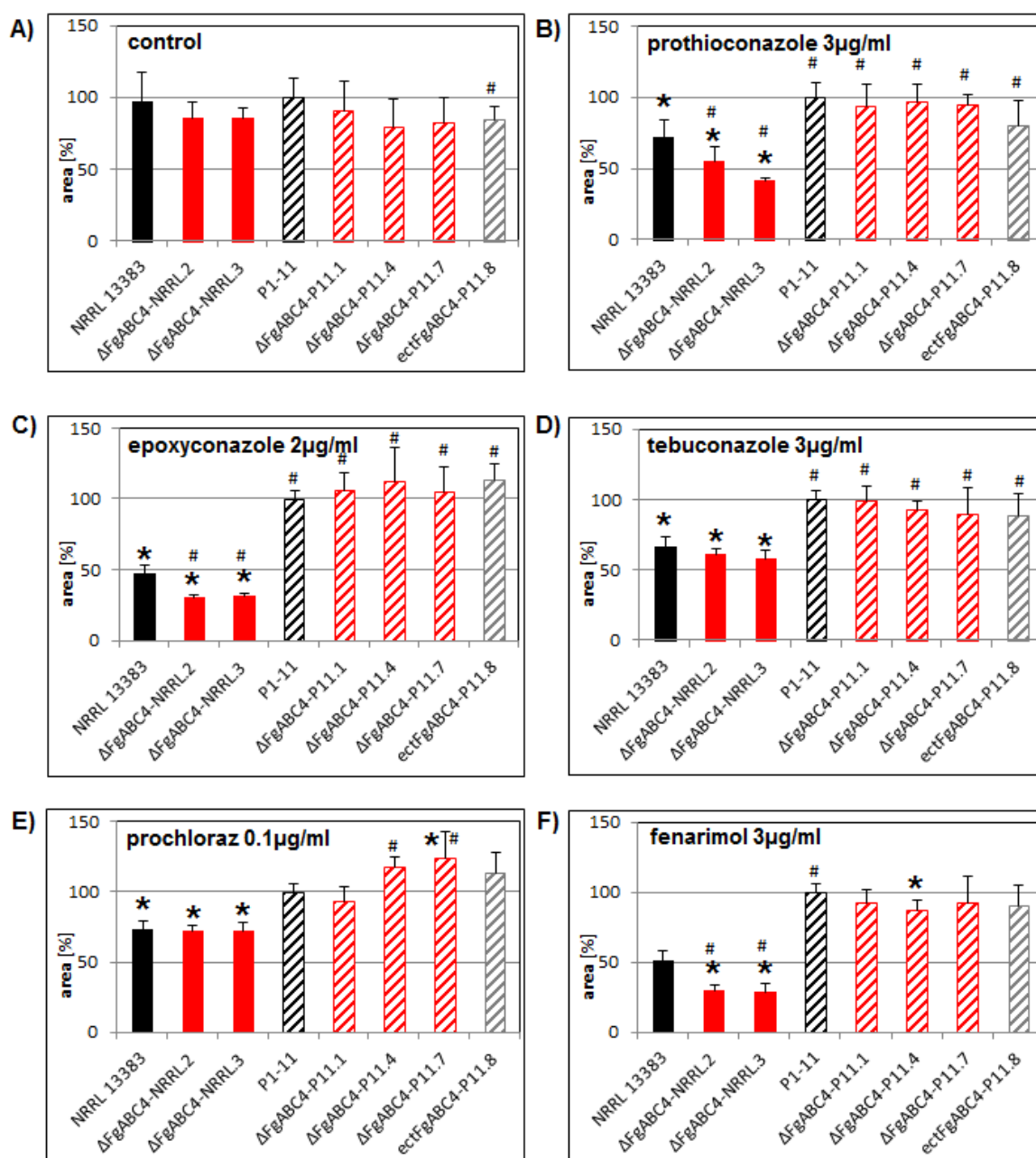


Figure 23. Azole sensitivity assay. A) Control treatment – no fungicide added. B) Prothioconazole 3 μ g/mL. C) Epoxyconazole 3 μ g/mL. D) Tebuconazole 3 μ g/mL. E) Prochloraz 0.1 μ g/mL. F) Fenarimol 3 μ g/mL. Error bars represent SD. An asterisk indicates a significant difference between P1-11 against each tested strain. A hashtag indicates a significant difference between NRRL 13383 against each tested strain. Significance level was determined using Student's T-Test ($P \leq 0.05$).

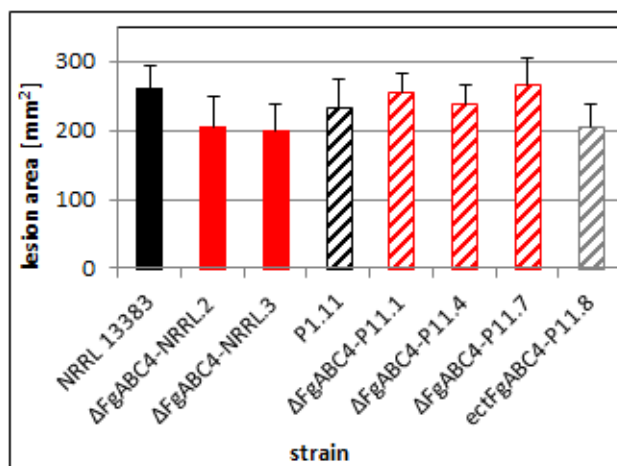


Figure 24. Virulence assay of NRRL 13383, two *FgABC4* deletion mutants in NRRL 13383 background, adapted strain P1-11, three *FgABC4* deletion mutants in P1-11 background and one ectopic mutants in the P1-11 background on maize stem. No significant differences existed between NRRL 13383 and the other strains using Student's T-Test ($P \leq 0.05$).

IV. Discussion

IV.1. The lineage and chemotype of the PH-1 and NRRL 13383 strains

This study used two WT strains of *F. graminearum* i.e. PH-1 and NRRL 13383 because these strains represented two distinct chemotypes. In addition, PH-1 was used as a reference strain for Fusarium Genome Database. Both strains were confirmed as *F. graminearum* lineage 7 based on the sequences of *TEF-1 α* (FGSG_08811) and *RED* (FGSG_03224) genes that encode translation elongation factor 1 alpha and a reductase, respectively. Additional single copy nuclear genes encoding ammonia ligase, 3-*O*-acetyltransferase, phosphate permase, β -tubulin were previously used to differentiate lineages within *F. graminearum* (O'Donnell et al. 2000). This earlier study discovered that this species is in fact a species complex, the so called species complex (FGSC), and described seven lineages all able to cause FHB. Those species were *F. autroamericanum* (lineage 1), *F. meridionale* (lineage 2), *F. boothii* (lineage 3), *F. mesoamericanum* (lineage 4), *F. acaciae-mearnsii* (lineage 5), *F. asiaticum* (lineage 6) and *F. graminearum* (lineage 7) (O'Donnell et al. 2000). Follow-up studies included genes encoding MAT1-1-1, MAT1-1-2, MAT1-1-3, MAT1-2-1 and Histone H3 in phylogenetic analyses (O'Donnell et al. 2004). Currently at least 16 distinct species have been described to exist within the FGSC (Aoki et al. 2012). The *TEF-1 α* and *RED* genes were chosen because they provided a tool for lineage identification that is well documented in the literature (O'Donnell et al. 2000).

PH-1 and NRRL 13383 are strains within *F. graminearum* that show slightly different characteristics. In North America PH-1 is known as an aggressive strain that attacks wheat. This strain was first isolated from an infected wheat head in Michigan (USA) and it had been used in the *F. graminearum* whole genome sequencing project (Hallen and Trail 2008; Cuomo et al. 2007). In contrast, there is little information available for strain NRRL 13383. It was isolated from an infected maize ear in Iran (Becher et al. 2010). *In vitro* growth characteristics of both strains such as colony growth and conidia germination rates are slightly different. PH-1 grows faster *in vitro* than NRRL 13383 (Abou Ammar et al. 2013). On the other hand, NRRL 13383 produces more conidia under the conditions tested.

One aspect used to distinguish both strains is the chemotype, which is a variation between strains within the FGSC with respect to the type B trichothecenes produced. There exist three chemotypes, 3-ADON, 15-ADON and NIV (Wang et al. 2011; Pasquali and Migheli 2014). In addition to DON, strains exhibiting the 3-ADON chemotype produce 3-acetyldeoxynivalenol. In contrast, strains of the 15-ADON chemotype produce 15-

acetyldeoxynivalenol. Strains exhibiting the NIV chemotype produce nivalenol instead of DON (Kimura et al. 2007). The differences between the chemotypes result from differences in the genes *TRI13* and *TRI7*. The DON producing strains, i.e. the 3-ADON and 15-ADON chemotypes, lack the function of *TRI13* and *TRI7* (T. Lee et al. 2002; Alexander, Proctor, and McCormick 2009).

Calonectrin is an intermediate product of trichothecene biosynthesis, from which either DON or NIV will be made (Alexander, Proctor, and McCormick 2009). In the DON pathway, synthesis proceeds directly from calonectrin to 7,8-dihydroxycalonectrin, a reaction that is catalysed by a cytochrome P450 monooxygenase (encoded by *TRII*) (Alexander, Proctor, and McCormick 2009). The latter compound goes through an oxidation of the 8-OH group by unknown oxidoreductases to give 3,15-acetyldeoxynivalenol (3,15-diADON) (Fruhmann et al. 2014). Then, one of the acetyl groups either at C-3 or C-15 is removed by an esterase encoded by *TRI8* to either form 3-ADON or 15-ADON (Figure 25) (McCormick et al. 2011). Differential activity of this esterase is caused by DNA sequence variation at *TRI8* (Alexander, McCormick, and Proctor 2011). In contrast, *TRI13* and *TRI7* gene products are required for the production of NIV. *TRI13* encodes a 3-acetyltrichothecene C-4 hydroxylase that catalyses the C-4 hydroxylation of calonectrin to form 3,15-diacetoxyscirpenol. *TRI7* encodes 4-*O*-acetyltransferase that catalyzes C-4 acetylation of 3,15-diacetoxyscirpenol to form 3,4,15-triacetoxyscirpenol (Foroud and Eudes 2009). Afterwards, *TRII* and *TRI8* gene products continue to generate 4-acetylnivalenol and nivalenol at the last step.

PCR assays have been developed to identify the chemotype of *F. graminearum* strains based on sequence variations found in genes *TRI3*, *TRI7*, *TRII2* and *TRI13* (Pasquali and Migheli 2014). Specific primers were designed for *TRI7* that rendered single bands at 180 bp for DON and 160 bp for NIV producers. Similarly, using a primer pair targeting *TRI13* resulted in single bands at 470 bp for DON and 760 bp for NIV producers (H.-S. Kim et al. 2003). Another primer pair was designed targeting *TRI13* to differentiate 3ADON, 15ADON and NIV based on amplicon fragment sizes of 583, 644 and 859 bp, respectively (Wang et al. 2008). In addition, a multiplex PCR was developed based on *TRI3* and *TRII2* (Starkey et al. 2007; Tateishi et al. 2010). The PCR products of *TRI3* have sizes of 243 bp, 610 bp or 840 bp to represent the 3ADON, 15ADON and NIV chemotypes, respectively. The PCR products of *TRII2* have sizes of 410 bp, 670 bp and 840 bp for 3ADON, 15ADON and NIV, respectively (Starkey et al. 2007). Thus, this multiplex PCR is able to consistently determine the chemotype of a *F. graminearum* strain.

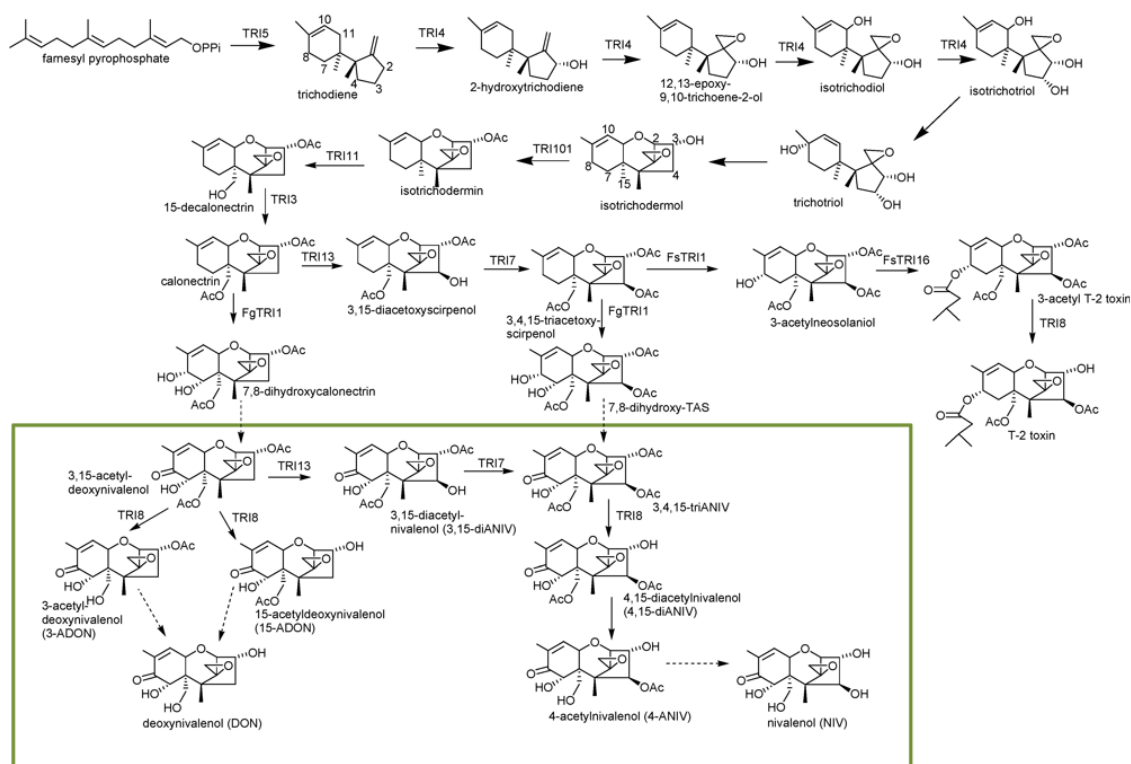


Figure 25. Trichothecene biosynthetic pathway as proposed by (McCormick et al. 2011). The box highlights the type B trichothecenes.

This study adopted the multiplex PCR of *TRI3* and *TRI12* to determine the chemotype of PH-1 and NRRL 13383 strains (Starkey et al. 2007). PH-1 used in this study was confirmed as a 15-ADON producer, while our NRRL 13383 isolate was confirmed as an NIV producer. This difference might be due to the origin of each isolate since PH-1 was isolated in the USA and NRRL 13383 in Iran. Historically, most North American isolates of *F. graminearum* have been determined as 15-ADON producers (Goswami and Kistler 2004). However, in recent years, the 3-ADON chemotype strain originally restricted to eastern Canada started to replace the 15-ADON chemotype westwards across Canada, and into the upper Midwest of the United States (Ward et al. 2008). This shift is likely due to changes in agricultural practices or environmental conditions allowing the 3-ADON strain to take the advantage (Ward et al. 2008). On the other side, the majority of isolates collected from Iran are of the NIV chemotype (Malihipour et al. 2012). Out of 100 *F. graminearum* isolates that were isolated from wheat kernels in Golestan province (Iran), 72 strains were NIV, 10 were 3-ADON and 18 were 15-ADON chemotypes (Abedi-Tizaki and Sabbagh 2013). This highlights that different regions might have different population structures, chemotype diversity and potential chemotype shifting within *F. graminearum* (Guo, Fernando, and Seow-Brock 2008).

IV.2. The role of FgCYP51A, FgCYP51B and FgCYP51C in azole resistance

Azole is a class of antifungal compounds that is widely used in clinical and agricultural practice to control fungal pathogens (Musiol and Kowalczyk 2012). Its basic structure is a heterocyclic ring of five atoms attached by carbon or nitrogen bonds to other aromatic rings (Saag and Dismukes 1988; Shapiro, Robbins, and Cowen 2011). Triazole and imidazole are the two largest subclasses of azole having three and two nitrogen atoms, respectively (Sheehan, Hitchcock, and Carol 1999; Maertens 2004; Fera and Sarro 2009). These nitrogen atoms were located at 1,2,3- or 1,2,4-triazole (Faro 2010) and 1,3- or 1,4-imidazole (Troesken 2005). One nitrogen atom at position N-3 or N-4 of the heterocyclic ring binds to the heme iron of lanosterol 14- α -demethylase encoded by *Erg11* (=CYP51) thereby inhibiting the enzyme (Saag and Dismukes 1988). This results in depletion of ergosterol and the accumulation of 14 α -methylergosta-8,24-dien-3,6-diol, which is a toxic product formed by the Δ 5,6-desaturase encoded by the *ERG3* gene (Lupetti et al. 2002; Lo et al. 2005). The toxicity comes from the polar 6-OH group of the diol that interferes with the sterol-phospholipid packing in the plasma membrane (Lupetti et al. 2002). Consequently, the fluidity of fungal cell membranes is disturbed and impedes fungal growth (Maertens 2004).

In azole resistant fungi, two possible mechanisms involving *CYP51* are known to occur. One is its mutation, the other is its transcriptional up-regulation (Cowen 2008; Cowen and Steinbach 2008). Mutations in *CYP51* cause an alteration in the enzyme structure that avoid the binding of azole and thus lowers sensitivity to this fungicide (Becher and Wirsal 2012). For example, in *M. graminicola* these alterations affect the size and accessibility of the binding pocket, and the localization of residues interacting with azoles (Mullins et al. 2011). Other examples of *CYP51* nucleotide variation associated with azole resistance can be seen in clinical and agricultural fungal pathogens such as *Candida albicans*, *Aspergillus fumigatus*, *Histoplasma capsulatum*, *Candida neoformans*, *Mycosphaerella graminicola*, *Erysiphe necator* and *Blumeria graminis* (Becher and Wirsal 2012; Leroux, Walker, and Schrot 2010). Furthermore, it is also possible that a mutation in the promoter region of *CYP51* leads to the up-regulation of *CYP51* transcription and this in turn to increased azole tolerance. This had been demonstrated in *M. graminicola* (Cools et al. 2012).

This study supports the notion that increased resistance of six *F. graminearum* strains to some azoles and amines (Becher et al. 2010) is not caused by nucleotide alterations in any of the three *FgCYP51* genes. The DNA sequences of the coding regions, as well as those of the upstream and downstream regions of *FgCYP51A*, *FgCYP51B* and *FgCYP51C* of all six

adapted strains are identical to those of their WT progenitor NRRL 13383. This result aligned with a previous study that found no correlation between *FgCYP51* sequence variations observed in field isolates of *F. graminearum* collected in China and levels of azole tolerance. Among 41 isolates tested, the HN8 isolate showed an EC₅₀ value of 6.24 mg/L and 4.575 mg/L for tebuconazole and prochloraz, respectively, which is significantly higher than those of other isolates. This isolate showed 99.94 and 99.89% similarity of *CYP51A* and *CYP51B* genes to those of the published PH-1 sequence. Nevertheless these nucleotide variations were not associated with azole resistance (Yin et al. 2009). A similar result was obtained for clinical isolates of *C. glabrata* that were recovered from hospital patients during three years of antifungal treatment. Silent mutations occurred, however but no variations associated with fluconazole-resistant isolates were found when compared to the published sequence (Sanguinetti et al. 2005). This suggests that increased resistance in these isolates is not caused by a mutation in *CYP51*.

Nonetheless, nucleotide variations in *FgCYP51* do occur among strains and species of *Fusarium*. For example, it was reported that *FgCYP51A* and *FgCYP51B* sequences can differentiate *F. graminearum* and *F. asiaticum* (Yin et al. 2009). The former gene exhibited higher variation between the two species than the latter. That study also suggested that sequence variation existed in *FgCYP51A* in a given species, but there was no evidence for any correlation with the levels of sensitivity to tebuconazole and prochloraz. This finding was however only based on the analysis of three field isolates for each species. In this study, variations were also found between strains PH-1 and NRRL 13383 for the genes *FgCYP51A* and *FgCYP51C*. However, the sequences of the three *FgCyp51* genes in six adapted strains exhibiting increased tolerance to azoles (Becher et al. 2010) were exactly the same as in their progenitor strain NRRL 13383. This provided additional evidence that mutations in *FgCyp51* genes may be not the principal cause of azole resistance in *F. graminearum*.

Beside mutations in *CYP51*, another possibility to acquire azole resistance is its transcriptional up-regulation, which may lead to enhanced ergosterol biosynthesis. Microarray and RT-qPCR analyses of the transcript levels of *FgCYP51A*, *FgCYP51B* and *FgCYP51C* indicated significant increases for all three genes in strain PH-1 after a treatment with 5 µg/mL tebuconazole for 12 hours. In that study, 163 and 121 fold increased transcript levels were demonstrated for *FgCYP51A* using microarrays and RT-qPCR, respectively (Becher et al. 2011). Similarly, DeepSAGE analysis indicated that transcript levels of *FgCYP51A* and *FgCYP51B* increased 58 and 53 fold after a treatment with 2.5 µg/mL tebuconazole for 6 hours (Liu et al. 2010). Unfortunately, *FgCYP51C* transcription was not analysed in that

study. A similar result was obtained for two homologous *CYP51* genes in *M. oryzae*, *MoCYP51A* and *MoCYP51B*, using qRT-PCR. Transcript abundance of *MoCYP51A* increased 117, 102 and 90 fold after treatment with 1.09 ppm propiconazole, 0.31 ppm tebuconazole and 0.08 ppm prochloraz, respectively (Yan et al. 2011). Meanwhile, transcript abundance of *MoCYP51B* increased only moderately at 6, 7 and 4 fold for the same treatments (Yan et al. 2011). This suggests an important role for *CYP51A* genes in providing azole resistance in both fungal species.

Another way to examine the role of *FgCYP51* in azole resistance is to delete each of the genes individually, and then to evaluate the resulting mutants for azole sensitivity. This was performed by two research groups (Liu et al. 2011; Fan et al. 2013). The first group showed that $\Delta FgCYP51A$ and $\Delta FgCYP51C$ mutants were more sensitive to tebuconazole, diniconazole, difenoconazole, flutriafol, prochloraz, triadimefon, propiconazole, except for triadimefon and propiconazole in the $\Delta FgCYP51C$ mutants. In contrast, $\Delta FgCYP51B$ mutants showed sensitivities to these substances that resembled those of the WT control (Liu et al. 2011). An inconsistency in this result was highlighted by the second research group. $\Delta FgCYP51A$ mutants showed higher sensitivity to tebuconazole, epoxiconazole, propiconazole, imazalil, metconazole, prochloraz and difenoconazole. On the other hand, $\Delta FgCYP51B$ mutants showed higher sensitivity only to the last three azoles compound, while $\Delta FgCYP51C$ mutants again were like the WT control (Fan et al. 2013). Additional experiments suggested that *FgCYP51A* may encode a sterol 14 α -demethylase, which is essential for ergosterol synthesis and which determines azole sensitivity (Fan et al. 2013). *FgCYP51B* encodes a primary sterol 14 α -demethylase that plays an essential role in ascospore formation (Fan et al. 2013). In contrast, *FgCYP51C* is unlikely to function as a sterol 14 α -demethylase, because it has substitutions in the conserved substrate recognition site. However, the protein is required for full virulence on wheat ears (Fan et al. 2013). These *in vitro* studies suggested that of the three genes probably *FgCYP51A* is most important in influencing azole sensitivity in *F. graminearum*.

Taken together, current knowledge suggests that in *F. graminearum*, it is possible that azole resistance may not arise in the field by mutation of the *CYP51* genes. On the other hand, transcriptional up-regulation of these genes has been shown to occur when the fungus is exposed to azoles. However, CYP51 is not the only protein known to contribute to azole resistance. Specifically, membrane-bound efflux transporters such as the major facilitator superfamily (MFS) and the ATP-binding cassette (ABC) transporters are well-established in other organisms as contributing to azole resistance (Cowen 2008; Cowen and Steinbach

2008). ABC transporters are a large protein family that have diverse functions, including that of a xenobiotic efflux pump. This aspect has been well studied in fungal clinical isolates that commonly arise from mutation and / or over-expression of efflux transporters (Cannon et al. 2009). In plant pathogenic fungi far less research has been conducted on the contribution of ABC transporters to fungicide resistance.

IV.3. The role of FgABC1 and FgABC4 in azole resistance

MRP (=ABCC) is a subfamily of ABC transporters in which some of their members have been shown to contribute to various xenobiotic resistances in cancer cells, human and plant fungal pathogens. In human tumor cells, ABCB1 (MDR) together with ABCC1 (MRP) transporters are highly expressed to protect the tissue from clinical drugs (Grant et al. 1994), and for more rapid efflux and clearing of the drug agent (Brodeur 2011). The substrate binding pocket of these transporters interacts with drugs via flexible hydrophobic and H-bond interactions to transport the drugs to the outside of the cell (Sharom 2008). The activity of these transporters was shown to be suppressed through inhibition of ionic and hydrogen bonds by plant phenolic compounds that disturb the 3D structure of the transporters (Wink, Ashour, and El-Readi 2012).

In the human fungal pathogen *C. albicans*, a MRP member called *CaMLT1* was intensively studied. Its transcript level was highly induced by Cadmium chloride and 1-chloro-2,4-dinitrobenzene, which are toxic to fungi (Theiss et al. 2002; Coleman and Mylonakis 2009). In *S. cerevisiae*, the MRP subfamily is the second largest subfamily of ABC transporters and contains six members, i.e. ScYCF1, ScYOR1, YKR, YLL015, YHL035 and YLL048 (Rea 1999). ScYCF1 contributes to resistance to Cadmium salts and heavy metals, while ScYOR1 contributes to oligomycin and multidrug resistance (Rea 1999; Del Sorbo, Schoonbeek, and De Waard 2000; Paumi et al. 2009). YKR, YLL015, YHL035 and YLL048 had been sequenced but their function remains to be revealed.

Arabidopsis thaliana has become a model for ABC transporter studies in plants. This plant's genome encodes 130 ABC transporters putatively acting as importers as well as exporters of various substances (Kang et al. 2011). The subfamily ABCC (=MRP) comprises 15 members (12%) (Kang et al. 2011). They function primarily as phototoxic metal or metalloid transporters conferring resistance to these substances. In addition, they also function as folate and / or chlorophyll catabolite transporters (Kang et al. 2011). In maize, *ZmMRP1* acts as glutathione transporter involved in the detoxification of xenobiotics (Pang, Duan, et al. 2012). Semi-quantitative RT-PCR showed that the transcript levels of *ZmMRP1* were induced

by atrazine, 2,4-D, primisulfuron, dichlormid or metolachlor herbicides 48 h after treatment (Pang, Duan, et al. 2012; Pang, Ran, et al. 2012). Again, this indicates a role of MRP in xenobiotic resistance.

In fungal plant pathogens, only few MRP transporter members have been characterized for fungicide resistance. This is different from PDR transporters, which represent another subfamily of ABC transporters shown to contribute to azole resistance. For example, in *C. albicans*, *PDR5* has been confirmed as having an important role in azole resistance (Kontoyiannis 1999). A paralog of *PDR5* in *N. crassa*, *NcCDR4*, has been characterized as playing a key role in azole resistance (Y. Zhang et al. 2012). Another PDR member characterized in azole resistance is *BcatrD* of *B. cinerea*. The transcript level of this transporter was strongly induced by a treatment with 30 mg/L oxpoconazole after 30 minutes (Hayashi et al. 2001).

The higher contribution of PDR transporters to azole resistance is possibly due to different topologies of both proteins. MRP consists of an N-terminal extension and two TMDs and two NBDs that make up a NTE-[TMD-NBD]₂ structure (Honorat, Dumontet, and Payen 2009; Kovalchuk and Driessen 2010). On the other side, PDR has a unique structure since all other subfamilies arrange as TMD-NBD instead of NBD-TMD. It consists of two NBDs and two TMDs to form a [NBD-TMD]₂ structure (Lamping et al. 2010; Kovalchuk and Driessen 2010). The TMD segment is responsible for the specificity of the substrate being pumped out, while the NBD is responsible for ATP binding and energy-driven substrate translocation (Higgins 2001; Higgins and Linton 2004). Basically, the specificity of an ABC transporter is dependent on the compatibility of the substrate-binding site at the TMD and the chemical nature of the transported substrates (Schmitt and Tampé 2002). Several amino acid residues at the TMD of a yeast PDR ABC transporter (*Cdr1p*) were identified as substrate-binding sites responsible for the translocation of a substrate (Prasad and Goffeau 2012; Prasad and Rawal 2014). Meanwhile the physicochemical basis of the substrate such as hydrophobicity or hydrophilicity affects its transport by ABC transporter (Cuthbertson, Kos, and Whitfield 2010).

Even though PDR transporters have been shown more often to be involved in azole resistance, several MRP transporters have been reported also to contribute to this phenomenon. A study assessed a contribution of MRP and other ABC subfamilies in *F. graminearum* using microarray analysis in response to 5 ppm tebuconazole after 12 hours (Becher et al. 2011). Two MDRs, two PDRs and three MRP (including *FgABC1* and *FgABC4*) were found to exceed the significance threshold with changes in excess of log₂-

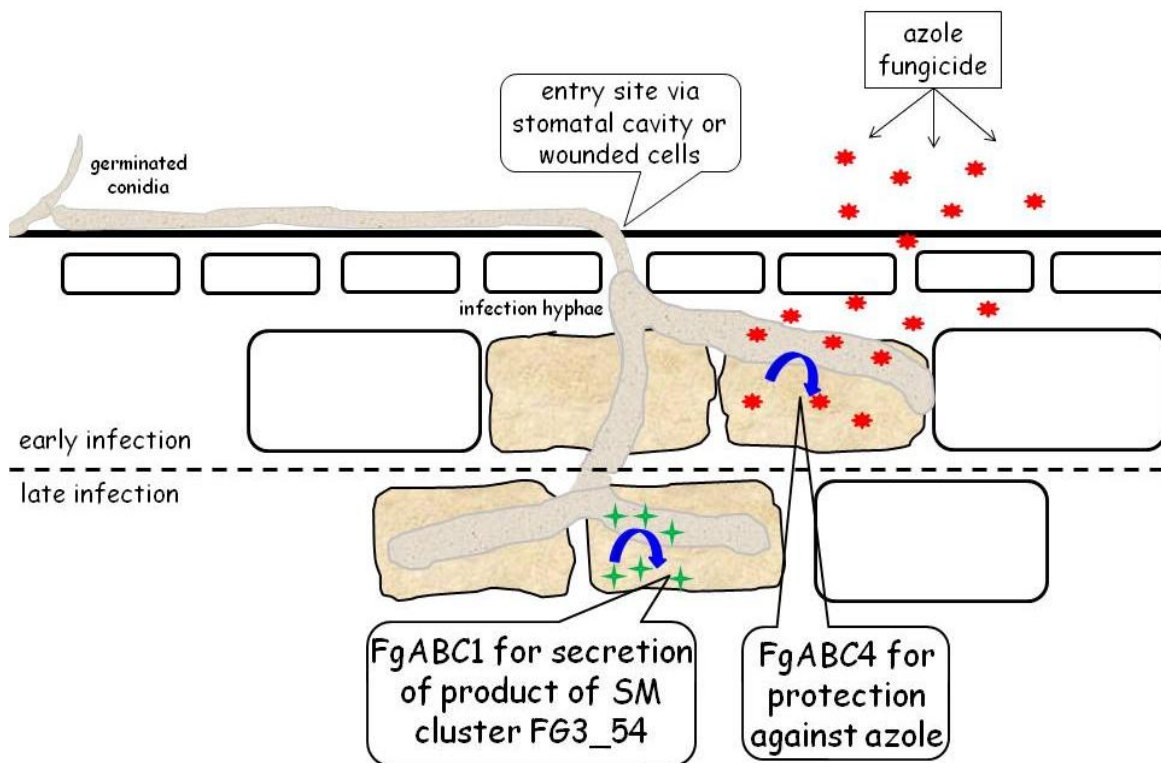


Figure 26. Model for the proposed roles of FgABC1 in virulence and FgABC4 in azole resistance.

fold. This was confirmed with RT-qPCR data showing that *FgABC1* and *FgABC4* increased 2.46 and 10.63 fold, respectively (Becher et al. 2011). Both genes are close paralogs of one another, which provided an ideal opportunity to study whether they retained similar roles and / or specificities during their evolution.

Even though both genes share high sequence similarity, their encoded protein functionality has diverged (Figure 26). This study, as shown by the deletion mutants (see III.3.3) demonstrates a contribution of FgABC4 to azole tolerance but not of FgABC1. As stated above, this study did not find any mutations in the three *CYP51* genes in six azole resistant strains that had been generated previously *in vitro* (Becher et al. 2010). Therefore, *FgABC4* was sequenced in those six strains to examine whether a mutation might have occurred during the adaptation process that might explain their acquired azole resistance. However, sequence analysis of the ORF, the up-, and down-stream regions of *FgABC4* did not reveal any mutation in any adapted strain when compared with their wild type progenitor, NRRL 13383. This shows that neither the amino acid sequence of the encoded transporter nor the cis-regulatory sequence of *FgABC4* is changed in the adapted strains. Therefore, other factors must be responsible for the increased azole tolerance observed. Indeed, several transcription factors are up-regulated in response to 5 ppm tebuconazole after 12 hours

(Becher et al. 2011). Such transcription factors may regulate amongst others *FgABC4* and thus may affect indirectly azole sensitivity levels.

One of the characterized transcription factors involved in azole resistance is CRZ1 in yeast. It is a transcription factor that has a Cys₂His₂ (C₂H₂) zinc finger domain that specifically binds to a calcineurin-dependent response element (CDRE) at the promoter region of gene(s) being dependently-expressed (Stathopoulos and Cyert 1997). CDRE had been identified in *S. cerevisiae* as CCGTGGCTGTGTGC (Stathopoulos and Cyert 1997) and in *A. nidulans* as G[T/G]GGC[T/A]G[T/G]G (Hagiwara et al. 2008). Unfortunately, such a CDRE motif has not been determined in *F. graminearum*, yet. Thus the role of a CRZ1-like transcription factor in regulating *FgABC4* and other dependently regulated genes remains to be revealed. The genome of *F. graminearum* encodes three proteins with similarity to CRZ1-like transcription factors, i.e. FGSG_01341, FGSG_10470 and FGSG_13711 (Becher et al. 2011). Using microarray analysis, the transcript abundances of FGSG_01341, FGSG_10470 and FGSG_13711 were determined to be up-regulated by factors of 3, 27 and 4 after treatment with 5 ppm tebuconazole for 12 hours (Becher et al. 2011). Deletion mutants of FGSG_01341 had defective conidial germination, and were more sensitive to tebuconazole and prochloraz, respectively (Kowriga 2012). This may be an indication of a role of CRZ1 in response to azole stress.

IV.4. The role of FgABC1 and FgABC4 in virulence

As mentioned above, this thesis revealed that FgABC1 and FgABC4 are two similar MRP proteins that have not only different roles in azole resistance, but also in virulence. FgABC1 is needed to confer full virulence on all three hosts tested but it does not contribute to azole resistance. Contrary, FgABC4 is not involved in virulence, however it does contribute to azole resistance. A role of MRPs in fungal virulence is possibly due to the extrusion of toxic host defense compounds (Y. Kim et al. 2013) or the secretion of fungal virulence compounds such as the products of polyketide synthases (PKS) or non-ribosomal-peptide synthases (NRPS) (X.-W. Zhang et al. 2012).

In human fungal pathogens, an explanation for the contribution of MRPs to fungal virulence was provided through the detoxification of toxic host metabolites as illustrated by *MLT1* in *C. albicans*. This protein localizes at the vacuolar membrane and it is involved in the compartmentalisation of toxic metabolites in that organelle. The transcript of *MRP1* is inducible by poisonous metabolic compounds that might originate from the host. Homologous gene replacement mutants show a virulence defect in a mouse peritonitis model (Theiss et al.

2002; Coleman and Mylonakis 2009). This phenotype was restored in complementation mutants.

In plant fungal pathogens, extrusion of toxic host metabolites by MRP was shown for *M. oryzae*. In this fungi, 11 of the 50 ABC transporter proteins putatively encoded by its genome have been categorized as members of the MRP subfamily (Y. Kim et al. 2013). The expression of all 11 genes was inducible by a treatment with 8 mg/mL Iprobenfos for four hours. Iprobenfos acts as a choline biosynthesis inhibitor which is toxic to fungal growth. Based on their expression patterns, three genes were selected for a deletion study, i.e. *Moabc5* (MGG_05009), *Moabc6* (MGG_05044), and *Moabc7* (MGG_04855). Δ *Moabc5* mutants showed normal conidia germination and appressorium formation, but lost the ability to infect susceptible rice cultivars. This phenotype was restored in complementation mutants. An *in vivo* expression study showed that transcript levels of *Moabc5* were up-regulated 10 fold at 72 hpi and then gradually decreased until 168 hpi. In addition, this gene is up-regulated *in vitro* after treatment with iprobenfos and isoprothiolane (fungal choline biosynthesis inhibitors) and H₂O₂ which may suggest that *Moabc5* may promote the efflux of host defense metabolites to overcome plant defenses at an earlier stage (Y. Kim et al. 2013). In contrast, Δ *Moabc6* and Δ *Moabc7* mutants exhibited similar virulence levels as the WT strain (Y. Kim et al. 2013).

Considering the results of assays testing the sensitivities against plant metabolites it may be doubted that FgABC1 has a role in the extrusion of plant defence compounds. None of five compounds tested affected the Δ FgABC1 mutants in an extent that differed from the WT strain (III.3.3.). However, likely there exist additional defence compounds in the host plants tested, whose impact on the fungus could not be tested because they are not commercially available. Therefore, it cannot be ruled out that FgABC1 transports for example phytoalexins. On the other hand, an alternative explanation for the contribution of MRPs to fungal virulence could be the secretion of essential virulence factors in infected host tissues.

FgABC1 is located in a secondary metabolite biosynthesis cluster called FG3_54 (W. Lee 2010; X.-W. Zhang et al. 2012). This cluster comprises eight genes, FGSG_17487 (related to non-ribosomal peptide synthetase or NPS5), FGSG_10989 (conserved hypothetical protein), FGSG_10990 (related to AM-toxin synthetase or NPS9), FGSG_10991 (related to benzoate 4-monooxygenase), FGSG_10992 (related to polysaccharide deacetylase / PSDA), FGSG_10993 (related to selenocysteine lyase), FGSG_10994 (conserved hypothetical protein) and FGSG_10995 (related to multidrug resistance protein or FgABC1) (X.-W. Zhang et al. 2012). Deletion of *NPS9*, *PSDA* or *FgABC1* caused strongly reduced virulence in different hosts suggesting that the substance produced by the enzymes encoded by NRPS

cluster FG3_54 is essential for pathogenesis of *F. graminearum* in wheat, barley and maize (X.-W. Zhang et al. 2012; Abou Ammar et al. 2013). Therefore, it is likely that FgABC1 acts as an efflux pump for this substance. Deletion of *FgABC1* prevents the formation of the encoded transporter, which would lead to an accumulation of the currently unknown metabolite present in the fungal cell. It remains to be shown whether such cells counteract this accumulation by down-regulating the whole pathway.

The function of the secondary metabolite formed by the enzymes of cluster FG3_54 remains unknown. *NPS9* encodes a NRPS, which is related to AM-toxin synthetase (W. Lee 2010). AM-toxin is known from *Alternaria alternata* as a virulence factor on apple (Johnson et al. 2000; Harimoto et al. 2007). In *F. graminearum*, there exist two additional genes encoding proteins with similarity to AM-toxin synthetase. These are FGSG_11395 (*NPS14*) located in cluster FG1_57 and FGSG_02394 (*NPS15*) in the zearalenone cluster. Microarray data suggest that of these three NRPS only *NPS9* and *NPS14* are expressed during infection. *NPS9* was expressed in wheat after 64 hpi (X.-W. Zhang et al. 2012) while *NPS14* was expressed in wheat from 24 hpi to 96 h hpi and in barley from 96 hpi to 144 hpi (Lysøe et al. 2011). Unfortunately, no further analysis was performed to determine the roles of these secondary metabolites in virulence.

Often, genes for a given biosynthetic pathway, which are combined in a cluster, are co-coordinately regulated by a specific transcription factor whose gene may or may not be located in that cluster. The gene product of FGSG_02398 (FgZeb2) is an example of a transcription factor regulating the expression of the genes in the zearalenone secondary metabolite biosynthesis cluster (Y.-T. Kim et al. 2005). Other examples are *FgTri6* and *FgTri10* regulating the trichothecene biosynthesis cluster (Seong et al. 2009) and *FgGIP2* controlling aurofusarin biosynthesis (J.-E. Kim et al. 2006). Inspection of cluster FG3_54 and its flanking genes provided no evidence of a transcription factor that may regulate the expression of the genes located in this cluster. Probably, this assumed transcription factor may locate somewhere else in the genome (Lawler et al. 2013). There are 709 genes encoding transcription factors in *F. graminearum* (Son et al. 2011). One or more of these transcription factors may act as a regulatory protein for the co-expression of the genes in cluster FG3_54. Indeed, a transcription factor containing *GTII/PAC2* domains that is called *FGPI* (annotated as FGSG_12164) regulates expression of PKS and NPS genes across several clusters (Jonkers et al. 2012). Its deletion mutants showed greatly reduced virulence and loss of trichothecene accumulation in wheat and *in vitro*. Additionally, transcription levels of *NPS9*, *NPS12*, *NPS14*, *PKS7* and *PKS15* during wheat infection are much reduced in the deletion mutants of

FGP1 compared to the WT (Jonkers et al. 2012). In the future, it needs to be shown whether a pathway-specific transcription factor regulating the genes in cluster FG3_54 does exist, in addition to FGP1.

V. Conclusion

Two *F. graminearum* WT isolates were used as wild type reference strains in this study, PH-1 and NRRL 13383. Sequences of *FgRED* and *FgTEF1- α* were determined in both strains, which confirmed their identity since they exactly matched those of PH-1 and NRRL 13383 deposited in the NCBI database. Both, PH-1 and NRRL13383 belong to lineage 7 of the *Fusarium graminearum* species complex (FGSC), but have different chemotypes. Based on multiplex PCR targeting *FgTRI3* and *FgTRI2*, the PH-1 isolate used in this study was confirmed to represent the 15-ADON chemotype, whereas the NRRL 13383 isolate represented the NIV chemotype.

Previously, six adapted strains were derived from NRRL 13383 that had acquired higher tolerance levels to azoles by unknown mechanisms (Becher et al. 2010). Three paralogs of lanosterol 14- α demethylase-encoding-genes in *F. graminearum* (*FgCYP51A*, *-B* and *-C*) were sequenced in the adapted strains, and compared with those of their progenitor NRRL 13383. No variation existed between the adapted strains and NRRL 13383 in any of the three ORFs. This shows that the increased azole tolerance of the adapted strains was not caused by a structural alteration of lanosterol 14- α demethylase, which is the molecular target of azoles. Furthermore, sequencing of the up- and down-stream regions of the three *FgCyp51* genes did neither retrieve any difference between the adapted strains and their progenitor. Thus, mutations in cis-regulatory elements are not responsible for increased transcript levels that were observed for the *FgCyp51* genes in earlier microarray experiments (Becher et al. 2011). Nevertheless, several sequence variations existed between PH-1 and NRRL 13383. One silent substitution was found in *FgCYP51A*, none in *FgCYP51B* and six in *FgCYP51C*. In the latter, five of the six changed the amino acid sequence.

Since no mutation in any of the three CYP51 existed in any of the adapted strains another mechanism should be responsible for azole resistance in these strains. From other fungal species it was known that ABC transporters may contribute also to azole resistance by removing the fungicide from the cell (Cowen 2008). Therefore, *FgABC4*, which affects azole tolerance (see below), was also sequenced, adopting the same strategy as for *FgCYP51*. Similarly, no alteration was found in this gene between the six adapted strains and NRRL 13383. In contrast, 11 variations existed between PH-1 and NRRL 13383. One substitution existed in an intron, while the remaining 10 existed in exons, all affecting the amino acid sequences.

Alterations of the structure of FgABC4, which might affect its substrate specificity, do not exist in the adapted strains and thus cannot explain their increased azole tolerance. However, it has been shown that several ABC transporter genes were transcriptionally up-regulated in *F. graminearum* in response to an azole treatment. Among them were two members of the MRP subfamily, *FgABC1* and *FgABC4* (Becher et al. 2011). These encode multidrug-related resistance proteins sharing similar sequences. Even though, using a gene deletion approach this study revealed that they have distinct functions. Both genes were deleted individually in both, the PH-1 and the NRRL 13383 backgrounds. This demonstrated that FgABC1 is required for full virulence in three host species tested, whereas FgABC4 contributes to azole tolerance. This result was consistent in both backgrounds.

This study provides evidence that FgABC4 contributes to azole tolerance. For fungal phytopathogens, this is a relatively new finding for MRP subfamily members. The deletion mutants of this gene were significantly more sensitive to some azole fungicides than the corresponding WT strains. Moreover, *FgABC4* was transcriptionally up-regulated in response to azole treatment suggesting that another regulatory gene may be involved. A corresponding situation has been shown in yeast, where the transcription factor *CRZI* was activated by azole treatment to regulate the transcription of other genes reducing the effect of azole in the fungal cell. Three *CRZI* yeast paralogs were found in *F. graminearum*, FGSG_01341, FGSG_10470 and FGSG_13711. Deletion mutants created for FGSG_01341 were more sensitive to tebuconazole and prochloraz, which suggested a role for the encoded *CRZ*-like transcription factor to azole resistance (Kowriga 2012). However, whether these genes have influence on the transcription of *FgABC4* was needed to be revealed in the future study.

In contrast to *FgABC4*, for *FgABC1* no evidence was found for a contribution to azole tolerance. However, FgABC1 is required for full virulence in *F. graminearum*, probably because it exports an essential fungal secondary metabolite (SM) during late infection. In support of this notion, *FgABC1* locates in the SM cluster FG3_54. Transcript levels of genes within this cluster are up-regulated during later stages of infection (Zhang et al. 2012). Furthermore, the deletion of a gene encoding an enzyme needed to make the unknown SM resulted in mutants that were as impeded in virulence as the Δ FgABC1 mutants (Zhang et al. 2012).

Overall, this study identified functions of two similar MRP transporters. While *FgABC1* is necessary for full virulence, *FgABC4* mediates azole tolerance. This information will be helpful for researchers working on the emergence of azole resistance in *F. graminearum*.

VI. References

- Abedi-Tizaki, Mostafa, and Sayed Kazem Sabbagh. 2013. "Detection of 3-Acetyldeoxynivalenol, 15-Acetyldeoxynivalenol and Nivalenol-Chemotypes of *Fusarium graminearum* from Iran Using Specific PCR Assays." *Plant Knowledge Journal* 2: 38–42.
- Abou Ammar, Ghada, Reno Tryono, Katharina Döll, Petr Karlovsky, Holger B. Deising, and Stefan G. R. Wirsal. 2013. "Identification of ABC Transporter Genes of *Fusarium graminearum* with Roles in Azole Tolerance And/or Virulence." *PloS One* 8: 1–13.
- Akallal, Rachida, Daniele Debieu, Catherine Lanen, Marie-Josée Daboussi, René Fritz, Christian Malosse, Jocelyne Bach, and Pierre Leroux. 1998. "Inheritance and Mechanisms of Resistance to Tebuconazole, a Sterol C14-Demethylation Inhibitor, in *Nectria haematococca*." *Pesticide Biochemistry and Physiology* 60: 147–166.
- Alexander, Nancy J., Susan P. McCormick, and Robert H. Proctor. 2011. "The Genetic Basis for 3-ADON and 15-ADON Trichothecene Chemotypes in *Fusarium*." *Fungal Genetics and Biology* 48: 485–495.
- Alexander, Nancy J., Robert H. Proctor, and Susan P. McCormick. 2009. "Genes, Gene Clusters, and Biosynthesis of Trichothecenes and Fumonisin in *Fusarium*." *Toxin Reviews* 28: 198–215.
- Aoki, Takayuki, Todd J. Ward, H. Corby Kistler, and Kerry O'Donnell. 2012. "Systematics, Phylogeny and Trichothecene Mycotoxin Potential of *Fusarium* Head Blight Cereal Pathogens." *Mycotoxins* 62: 91–102.
- Bai, Gui-Hua, and Gregory Shaner. 2004. "Management and Resistance in Wheat and Barley to *Fusarium* Head Blight." *Annual Review of Phytopathology* 42: 135–161.
- Becher, Rayko, Ursula Hettwer, Petr Karlovsky, Holger B. Deising, and Stefan G. R. Wirsal. 2010. "Adaptation of *Fusarium graminearum* to Tebuconazole Yielded Descendants Diverging for Levels of Fitness, Fungicide Resistance, Virulence, and Mycotoxin Production." *Phytopathology* 100: 444–453.
- Becher, Rayko, Fabian Weihmann, Holger B. Deising, and Stefan G. R. Wirsal. 2011. "Development of a Novel Multiplex DNA Microarray for *Fusarium graminearum* and Analysis of Azole Fungicide Responses." *BMC Genomics* 12: 1–17.
- Becher, Rayko, and Stefan G. R. Wirsal. 2012. "Fungal Cytochrome P450 Sterol 14 α -Demethylase (CYP51) and Azole Resistance in Plant and Human Pathogens." *Applied Microbiol Biotechnol* 95: 825–840.
- Bellamine, Aouatef, Galina I. Lepesheva, and Michael R. Waterman. 2004. "Fluconazole Binding and Sterol Demethylation in Three CYP51 Isoforms Indicate Differences in Active Site Topology." *Journal of Lipid Research* 45: 2000–2007.

-
- Beyer, Marco, M. B. Klix, H. Klink, and Verreet Joseph-Alexander. 2006. "Quantifying the Effects of Previous Crop, Tillage, Cultivar and Triazole Fungicides on the Deoxynivalenol Content of Wheat Grain – a Review." *Journal of Plant Diseases and Protection* 113: 241–246.
- Beyer, Marco, and Joseph-Alexander Verreet. 2005. "Germination of *Gibberella zeae* Ascospores as Affected by Age of Spores after Discharge and Environmental Factors." *European Journal of Plant Pathology* 111: 381–389.
- Blake, Jonathan, Sarah Wynn, and Lise Nistrup Jørgensen. 2011. "Evaluation of the Benefits Provided by the Azole Class of Compounds in Wheat, and the Effect of Losing All Azoles on Wheat and Potato Production in Denmark, France and the UK. Report 1 – Impact of the Loss of All Azoles". ADAS UK Ltd. Wolverhampton: 1-23.
- Blandino, Massimo, Luca Minelli, and Amedeo Reyneri. 2006. "Strategies for the Chemical Control of Fusarium Head Blight: Effect on Yield, Alveographic Parameters and Deoxynivalenol Contamination in Winter Wheat Grain." *European Journal of Agronomy* 25: 193–201.
- Blandino, Massimo, Michelangelo Pascale, Miriam Haidukowski, and Amedeo Reyneri. 2011. "Influence of Agronomic Conditions on the Efficacy of Different Fungicides Applied to Wheat at Heading: Effect on Flag Leaf Senescence, Fusarium Head Blight Attack, Grain Yield and Deoxynivalenol Contamination." *Italian Journal of Agronomy* 6: 204–211.
- Boddu, Jayanand, Seungho Cho, Warren M. Kruger, and Gary J. Muehlbauer. 2006. "Transcriptome Analysis of the Barley – *Fusarium graminearum* Interaction." *Molecular Plant-Microbe Interactions* 19: 407–417.
- Boyacioglu, D., N. S. Hettiarachchy, and R. W. Stacks. 1992. "Effect of Three Systemic Fungicides on Deoxynivalenol (vomitoxin) Production by *Fusarium graminearum* in Wheat." *Canadian Journal of Plant Science* 72: 93–101.
- Brodeur, Garrett M. 2011. "Knowing Your ABCCs: Novel Functions of ABCC Transporters." *Journal of the National Cancer Institute* 103: 1207–1208.
- Brown, Neil A., Martin Urban, Allison M. L. Van de Meene, and Kim E. Hammond-Kosack. 2010. "The Infection Biology of *Fusarium graminearum*: Defining the Pathways of Spikelet to Spikelet Colonisation in Wheat Ears." *Fungal Biology* 114: 555–571.
- Cannon, Richard D., Erwin Lamping, Ann R. Holmes, Kyoko Niimi, Philippe V. Baret, Mikhail V. Keniya, Koichi Tanabe, Masakazu Niimi, Andre Goffeau, and Brian C. Monk. 2009. "Efflux-Mediated Antifungal Drug Resistance." *Clinical Microbiology Reviews* 22: 291–321.
- Coleman, Jeffrey J., and Eleftherios Mylonakis. 2009. "Efflux in Fungi: La Pièce de Résistance." *PloS Pathogens* 5: 1–7.

-
- Cools, H. J., B. A. Fraaije, S. H. Kim, and J. A. Lucas. 2006. "Impact of Changes in the Target P450 CYP51 Enzyme Associated with Altered Triazole-Sensitivity in Fungal Pathogens of Cereal Crops." *Biochemical Society Transactions* 34: 1219–1222.
- Cools, Hans J, Carlos Bayon, Sarah Atkins, John A Lucas, and Bart A Fraaije. 2012. "Overexpression of the Sterol 14 α -Demethylase Gene (MgCYP51) in *Mycosphaerella graminicola* Isolates Confers a Novel Azole Fungicide Sensitivity Phenotype." *Pest Management Science* 68: 1034–1040.
- Cools, Hans J., and Bart A. Fraaije. 2013. "Update on Mechanisms of Azole Resistance in *Mycosphaerella graminicola* and Implications for Future Control." *Pest Management Science* 69: 150–155.
- Cools, Hans J., Bart A. Fraaije, Tim P. Bean, John Antoniw, and John A. Lucas. 2007. "Transcriptome Profiling of the Response of *Mycosphaerella graminicola* Isolates to an Azole Fungicide Using cDNA Microarrays." *Molecular Plant Pathology* 8: 639–651.
- Cowen, Leah E. 2008. "The Evolution of Fungal Drug Resistance: Modulating the Trajectory from Genotype to Phenotype." *Nature Reviews Microbiology* 6: 187–98.
- . 2009. "Hsp90 Orchestrates Stress Response Signaling Governing Fungal Drug Resistance." *PloS Pathogens* 5: 1–3.
- Cowen, Leah E., Anne E. Carpenter, Oranart Matangkasombut, Gerald R. Fink, and Susan Lindquist. 2006. "Genetic Architecture of Hsp90-Dependent Drug Resistance." *Eukaryotic Cell* 5: 2184–2188.
- Cowen, Leah E., and William J. Steinbach. 2008. "Stress, Drugs, and Evolution: The Role of Cellular Signaling in Fungal Drug Resistance." *Eukaryotic Cell* 7: 747–764.
- Cuomo, Christina A., Gueldener Ulrich, Jin-Rong Xu, Frances Trail, B. Gillian Turgeon, Antonio Di Pietro, Jonathan D. Walton, Li-Jun Ma, Scott E. Baker, Martijn Rep, Gerhard Adam, John Antoniw, Thomas Baldwin, Sarah Calvo, Yueh-Long Chang, David DeCaprio, Liane R. Gale, Sante Gnerre, Rubella S. Goswami, Kim Hammond-Kosack, Linda J. Harris, Karen Hilburn, John C. Kennell, Scott Kroken, Jon K. Magnuson, Gertrud Mannhaupt, Evan Mauceli, Hans-Werner Mewes, Rudolf Mitterbauer, Gary Muehlbauer, Martin Münsterkötter, David Nelson, Kerry O'Donnell, Thérèse Ouellet, Weihong Qi, Hadi Quesneville, M. Isabel G. Roncero, Kye-Yong Seong, Igor V. Tetko, Martin Urban, Cees Waalwijk, Todd J. Ward, Jiqiang Yao, Bruce W. Birren, H. Corby Kistler. 2007. "The *Fusarium graminearum* Genome Reveals a Link between Localized Polymorphism and Pathogen Specialization." *Science* 317: 1400–1402.
- Cuthbertson, Leslie, Veronica Kos, and Chris Whitfield. 2010. "ABC Transporters Involved in Export of Cell Surface Glycoconjugates." *Microbiology and Molecular Biology Reviews* 74: 341–362.
- De Waard, Maarten A. 1997. "Significance of ABC Transporters in Fungicide Sensitivity and Resistance." *Pesticide Science* 51: 271–275.

-
- De Waard, Maarten A., Alan C. Andrade, Keisuke Hayashi, Henk-Jan Schoonbeek, Ioannis Stergiopoulos, and Lute-Harm Zwiars. 2006. "Impact of Fungal Drug Transporters on Fungicide Sensitivity, Multidrug Resistance and Virulence." *Pest Management Science* 62: 195–207.
- Del Sorbo, Giovanni, Henk-Jan Schoonbeek, and Maarten A. De Waard. 2000. "Fungal Transporters Involved in Efflux of Natural Toxic Compounds and Fungicides." *Fungal Genetics and Biology* 30: 1–15.
- Desjardins, Anne E., and Robert H. Proctor. 2011. "Genetic Diversity and Trichothecene Chemotypes of the *Fusarium graminearum* Clade Isolated from Maize in Nepal and Identification of a Putative New Lineage." *Fungal Biology* 115: 38–48.
- Fan, Jieru, Martin Urban, Josie E. Parker, Helen C. Brewer, Steven L. Kelly, Kim E. Hammond-Kosack, Bart A. Fraaije, Xili Liu, and Hans J. Cools. 2013. "Characterization of the Sterol 14 a-Demethylases of *Fusarium graminearum* Identifies a Novel Genus-Specific CYP51 Function." *New Phytologist* 198: 821–835.
- Faro, Lilian R. Ferreira. 2010. "Neurotoxic Effects of Triazole Fungicides on Nigrostriatal Dopaminergic Neurotransmission." In *Fungicides*, edited by Odile Carisse. InTech Publisher: 405–420.
- Fera, Maria Teresa, and Angelina De Sarro. 2009. "New Triazoles and Echinocandins: Mode of Action, in Vitro Activity and Mechanisms of Resistance." *Expert Review of Anti-Infective Therapy* 7: 981–998.
- Foroud, Nora A, and François Eudes. 2009. "Trichothecenes in Cereal Grains." *International Journal of Molecular Sciences* 10: 147–173.
- Foroud, Nora Afsaneh. 2011. "Investigating the Molecular Mechanisms of Fusarium Head Blight Resistance in Wheat". PhD thesis, University of Lethbridge: 1-314.
- Francis, R.G., and L.W. Burgess. 1977. "Characteristics of Two Populations of *Fusarium roseum* 'graminearum' in Eastern Australia." *Transactions of the British Mycological Society* 68: 421–427.
- Fruhmann, Philipp, Christian Hametner, Hannes Mikula, Gerhard Adam, Rudolf Krska, and Johannes Fröhlich. 2014. "Stereoselective Luche Reduction of Deoxynivalenol and Three of Its Acetylated Derivatives at C8." *Toxins* 6: 325–336.
- Fungicide Resistance Action Committee. 2007. "Mode of Action of Fungicides". FRAC Switzerland: 1.
- . 2012. "FRAC List of Fungicide Common Names". FRAC Switzerland: 1-9
- Golkari, Saber, Jeannie Gilbert, Suvira Prashar, and J. Douglas Procnier. 2007. "Microarray Analysis of *Fusarium graminearum*-Induced Wheat Genes: Identification of Organ-Specific and Differentially Expressed Genes." *Plant Biotechnology Journal* 5: 38–49.

- Goswami, Rubella S., and H. Corby Kistler. 2004. "Heading for Disaster: *Fusarium graminearum* on Cereal Crops." *Molecular Plant Pathology* 5: 515–525.
- Gottwald, Sven, Birgit Samans, Stefanie Lück, and Wolfgang Friedt. 2012. "Jasmonate and Ethylene Dependent Defence Gene Expression and Suppression of Fungal Virulence Factors: Two Essential Mechanisms of *Fusarium* Head Blight Resistance in Wheat?" *BMC Genomics* 13: 1–22.
- Grant, Caroline E., Gunnar Valdimarsson, David R. Hipfner, Kurt C. Aimquist, Susan P. C. Cole, and Roger G. Deeley. 1994. "Overexpression of Multidrug Resistance-Associated Protein (MRP) Increases Resistance to Natural Product Drugs Resistance to Natural Product Drugs I." *Cancer Research* 54: 357–361.
- Guo, X. W., W. G. D. Fernando, and H. Y. Seow-Brock. 2008. "Population Structure, Chemotype Diversity, and Potential Chemotype Shifting of *Fusarium graminearum* in Wheat Fields of Manitoba." *Plant Disease* 92: 756–762.
- Guo, Xiaoxian, Jingkai Li, Tanjun Wang, Zhenhua Liu, Xin Chen, Yudong Li, Zhenglong Gu, Wenjun Guan, and Yongquan Li. 2012. "A Mutation in Intracellular Loop 4 Affects the Drug-Efflux Activity of the Yeast Multidrug Resistance ABC Transporter Pdr5p." *PloS One* 7: 1–9.
- Hagiwara, Daisuke, Atsushi Kondo, Tomonori Fujioka, and Keietsu Abe. 2008. "Functional Analysis of C2H2 Zinc Finger Transcription Factor CrzA Involved in Calcium Signaling in *Aspergillus nidulans*." *Current Genetics* 54: 325–338.
- Haidukowski, Miriam, Michelangelo Pascale, Giancarlo Perrone, Davide Pancaldi, Claudio Campagna, and Angelo Visconti. 2005. "Effect of Fungicides on the Development of *Fusarium* Head Blight, Yield and Deoxynivalenol Accumulation in Wheat Inoculated under Field Conditions with *Fusarium graminearum* and *Fusarium culmorum*." *Journal of the Science of Food and Agriculture* 85: 191–198.
- Haidukowski, Miriam, Angelo Visconti, Giancarlo Perrone, Sebastiano Vanadia, Davide Pancaldi, Lorenzo Covarelli, Roberto Balestrazzi, and Michelangelo Pascale. 2012. "Effect of Prothioconazole-Based Fungicides on *Fusarium* Head Blight, Grain Yield and Deoxynivalenol Accumulation in Wheat under Field Conditions." *Phytopathologia Mediterranea* 51: 236–246.
- Hallen, Heather E., and Frances Trail. 2008. "The L-Type Calcium Ion Channel *cch1* Affects Ascospore Discharge and Mycelial Growth in the Filamentous Fungus *Gibberella zeae* (anamorph *Fusarium graminearum*)." *Eukaryotic Cell* 7: 415–424.
- Harimoto, Yoshiaki, Rieko Hatta, Motoichiro Kodama, Mikihiro Yamamoto, Hiroshi Otani, and Takashi Tsuge. 2007. "Expression Profiles of Genes Encoded by the Supernumerary Chromosome Controlling AM-Toxin Biosynthesis and Pathogenicity in the Apple Pathotype of *Alternaria alternata*." *Molecular Plant-Microbe Interactions* 20: 1463–1476.

-
- Hayashi, Keisuke, H. Schoonbeek, H. Sugiura, and Maarten A. De Waard. 2001. "Multidrug Resistance in *Botrytis cinerea* Associated with Decreased Accumulation of the Azole Fungicide Oxpoconazole and Increased Transcription of the ABC Transporter Gene BcatrD." *Pesticide Biochemistry and Physiology* 70: 168–179.
- Hayashi, Keisuke, Henk Jan Schoonbeek, and Maarten A. De Waard. 2002. "Expression of the ABC Transporter BcatrD from *Botrytis cinerea* Reduces Sensitivity to Sterol Demethylation Inhibitor Fungicides." *Pesticide Biochemistry and Physiology* 73: 110–121.
- Higgins, Christopher F. 2001. "ABC Transporters: Physiology, Structure and Mechanism - An Overview." *Research in Microbiology* 152: 205–210.
- Higgins, Christopher F., and Kenneth J. Linton. 2004. "The ATP Switch Model for ABC Transporters." *Nature Structural and Molecular Biology* 11: 918–926.
- Honorat, Mylene, Charles Dumontet, and Lea Payen. 2009. Multidrug Resistance-Associated Protein (MRP/ABCC Proteins). In *ABC Transporters and Multidrug Resistance*, edited by Ahcene Boumendel, Jean Boutonnat, and Jacques Robert. A John Wiley & Sons, Inc.: 47-82.
- Howley, Peter M., Mark A. Israel, Ming-Fan Law, and Malcom A. Martin. 1979. "A Rapid Method for Detecting and Mapping Homology between Heterologous DNAs Evaluation of Polyomavirus Genomes." *The Journal of Biological Chemistry* 254: 4876–4883.
- Jansen, Carin, Diter von Wettstein, Wilhelm Schäfer, Karl-Heinz Kogel, Angelika Felk, and Frank J. Maier. 2005. "Infection Patterns in Barley and Wheat Spikes Inoculated with Wild-Type and Trichodiene Synthase Gene Disrupted *Fusarium graminearum*." *Proceedings of the National Academy of Sciences* 102: 16892–16897.
- Johnson, R. D., L. Johnson, Y. Itoh, M. Kodama, H. Otani, and K. Kohmoto. 2000. "Cloning and Characterization of a Cyclic Peptide Synthetase Gene from *Alternaria alternata* Apple Pathotype Whose Product Is Involved in AM-Toxin Synthesis and Pathogenicity." *Molecular Plant-Microbe Interactions* 13: 742–753.
- Jonkers, Wilfried, Yanhong Dong, Karen Broz, and H. Corby Kistler. 2012. "The Wor1-like Protein Fgp1 Regulates Pathogenicity, Toxin Synthesis and Reproduction in the Phytopathogenic Fungus *Fusarium graminearum*." *PloS Pathogens* 8: 1–18.
- Kang, Joohyun, Jiyoung Park, Hyunju Choi, Bo Burla, Tobias Kretschmar, Youngsook Lee, and Enrico Martinoia. 2011. "Plant ABC Transporters." *The Arabidopsis Book* 9. The American Society of Plant Biologists: 1–25.
- Kim, Hye-Seon, Theresa Lee, Mamtaz Dawlatana, Sung-Hwan Yun, and Yin-Won Lee. 2003. "Polymorphism of Trichothecene Biosynthesis Genes in Deoxynivalenol- and Nivalenol-Producing *Fusarium graminearum* Isolates." *Mycological Research* 107: 190–197.

-
- Kim, Jung-Eun, Jianming Jin, Hun Kim, Jin-Cheol Kim, Sung-Hwan Yun, and Yin-Won Lee. 2006. "GIP2, a Putative Transcription Factor That Regulates the Aurofusarin Biosynthetic Gene Cluster in *Gibberella zeae* GIP2, a Putative Transcription Factor That Regulates the Aurofusarin Biosynthetic Gene Cluster in *Gibberella zeae*." *Applied and Environmental Microbiology* 72: 1645–1652.
- Kim, Yongnam, Sook-Young Park, Dongyoung Kim, Jaeyoung Choi, Yong-Hwan Lee, Jong-Hwan Lee, and Woobong Choi. 2013. "Genome-Scale Analysis of ABC Transporter Genes and Characterization of the ABCC Type Transporter Genes in *Magnaporthe oryzae*." *Genomics* 101: 354–361.
- Kim, Yong-Tae, Ye-Ryun Lee, Jianming Jin, Kap-Hoon Han, Hun Kim, Jin-Cheol Kim, Theresa Lee, Sung-Hwan Yun, and Yin-Won Lee. 2005. "Two Different Polyketide Synthase Genes Are Required for Synthesis of Zearalenone in *Gibberella zeae*." *Molecular Microbiology* 58: 1102–1113.
- Kimura, Makoto, Takeshi Tokai, Kerry O'Donnell, Todd J. Ward, Makoto Fujimura, Hiroshi Hamamoto, Takehiko Shibata, and Isamu Yamaguchi. 2003. "The Trichothecene Biosynthesis Gene Cluster of *Fusarium graminearum* F15 Contains a Limited Number of Essential Pathway Genes and Expressed Non-Essential Genes." *Federation of European Biochemical Societies Letters* 539: 105–110.
- Kimura, Makoto, Takeshi Tokai, Naoko Takahashi-Ando, Shuichi Ohsato, and Makoto Fujimura. 2007. "Molecular and Genetic Studies of *Fusarium* Trichothecene Biosynthesis: Pathways, Genes, and Evolution." *Bioscience, Biotechnology, and Biochemistry* 71: 2105–2123.
- Klix, Melanie B., Joseph Alexander Verreet, and Marco Beyer. 2007. "Comparison of the Declining Triazole Sensitivity of *Gibberella zeae* and Increased Sensitivity Achieved by Advances in Triazole Fungicide Development." *Crop Protection* 26: 683–690.
- Kontoyiannis, D. P. 1999. "Genetic Analysis of Azole Resistance by Transposon Mutagenesis in *Saccharomyces cerevisiae*." *Antimicrobial Agents and Chemotherapy* 43: 2731–2735.
- Kovalchuk, Andriy, and Arnold J. M. Driessen. 2010. "Phylogenetic Analysis of Fungal ABC Transporters." *BMC Genomics* 11: 1–21.
- Kowriga, Wladislaw. 2012. "Deletionsanalyse Azol-Responsiver Gene Für Transkriptionsfaktoren in *Fusarium graminearum*". Master thesis, Martin Luther University: 1-80.
- Lamping, Erwin, Philippe V. Baret, Ann R. Holmes, Brian C. Monk, Andre Goffeau, and Richard D. Cannon. 2010. "Fungal PDR Transporters: Phylogeny, Topology, Motifs and Function." *Fungal Genetics and Biology* 47: 127–142.
- Langevin, François, François Eudes, and Andre Comeau. 2004. "Effect of Trichothecenes Produced by *Fusarium graminearum* during *Fusarium* Head Blight Development in Six Cereal Species." *European Journal of Plant Pathology* 110: 735–746.

-
- Lawler, Katherine, Kim Hammond-Kosack, Alvis Brazma, and Richard Coulson. 2013. “Genomic Clustering and Co-Regulation of Transcriptional Networks in the Pathogenic Fungus *Fusarium graminearum*.” *BMC Systems Biology* 7: 1–16.
- Lee, Theresa, You-Kyoung Han, Kook-Hyung Kim, Sung-Hwan Yun, and Yin-Won Lee. 2002. “Tri13 and Tri7 Determine Deoxynivalenol- and Nivalenol-Producing Chemotypes of *Gibberella zeae*.” *Applied and Environmental Microbiology* 68: 2148–2154.
- Lee, Wanseon. 2010. “Comprehensive Discovery of Fungal Gene Clusters: Unexpected Co-Work Reflected at the Genomic Level”. PhD thesis, Technische Universitaet Muenchen: 1-119.
- Leroux, Pierre, Anne-Sophie Walker, and J. Schrot. 2010. “Multiple Mechanisms Account for Resistance to Sterol 14 A-Demethylation Inhibitors in Field Isolates of *Mycosphaerella graminicola*.” *Pest Management Science* 2028: 1–16.
- Leslie, John F., and Brett A. Summerell. 2006. *The Fusarium Laboratory Manual*. Blackwell Publishing Ltd: 1-388.
- Li, Ze-Sheng, Mark Szczyпка, Yu-Ping Lu, Dennis J. Thiele, and Philip A. Rea. 1996. “The Yeast Cadmium Factor Protein (YCF1) Is a Vacuolar Glutathione S-Conjugate Pump.” *The Journal of Biological Chemistry* 271: 6509–6517.
- Liu, Weihong, and David A. Saint. 2002. “A New Quantitative Method of Real Time Reverse Transcription Polymerase Chain Reaction Assay Based on Simulation of Polymerase Chain Reaction Kinetics.” *Analytical Biochemistry* 302: 52–59.
- Liu, Xin, Jinhua Jiang, Jiaofang Shao, and Yanni Yin. 2010. “Gene Transcription Profiling of *Fusarium graminearum* Treated with an Azole Fungicide Tebuconazole.” *Applied Microbiol Biotechnol* 85: 1105–1114.
- Liu, Xin, Fangwei Yu, Guido Schnabel, Jianbing Wu, Zhengyi Wang, and Zhonghua Ma. 2011. “Paralogous cyp51 Genes in *Fusarium graminearum* Mediate Differential Sensitivity to Sterol Demethylation Inhibitors.” *Fungal Genetics and Biology* 48: 113–123.
- Lo, Hsiu-Jung, Jang-Shiun Wang, Chih-Yang Lin, Chia-Geun Chen, Ting-Yin Hsiao, Chia-Tung Hsu, Chia-Li Su, Ming-Ji Fann, Yu-Tai Ching, and Yun-Liang Yang. 2005. “Efg1 Involved in Drug Resistance by Regulating the Expression of ERG3 in *Candida albicans*.” *Antimicrobial Agents and Chemotherapy* 49: 1213–1215.
- Lupetti, Antonella, Romano Danesi, Mario Campa, Mario Del Tacca, and Steven Kelly. 2002. “Molecular Basis of Resistance to Azole Antifungals.” *Trends in Molecular Medicine* 8: 76–81.
- Lysøe, Erik, Matias Pasquali, Andrew Breakspear, and H. Corby Kistler. 2011. “The Transcription Factor FgStuAp Influences Spore Development, Pathogenicity, and

- Secondary Metabolism in *Fusarium graminearum*.” *Molecular Plant-Microbe Interactions* 24: 54–67.
- Lysøe, Erik, Kye-Yong Seong, and H. Corby Kistler. 2011. “The Transcriptome of *Fusarium graminearum* During the Infection of Wheat.” *Molecular Plant-Microbe Interactions* 24: 995–1000.
- Ma, Li-Jun, David M. Geiser, Robert H. Proctor, Alejandro P. Rooney, Kerry O. Donnell, Frances Trail, Donald M. Gardiner, John M. Manners, and Kemal Kazan. 2013. “Fusarium Pathogenomics.” *Annual Review of Microbiology* 67: 399–416.
- Maertens, J. A. 2004. “History of the Development of Azole Derivatives.” *Clinical Microbiology Infection* 10: 1–10.
- Maier, Frank J., Thomas Miedaner, Birgit Hadel, Angelika Felk, Siegfried Salomon, Marc Lemmens, Helmut Kassner, and Wilhelm Schäfer. 2006. “Involvement of Trichothecenes in Fusarioses of Wheat, Barley and Maize Evaluated by Gene Disruption of the Trichodiene Synthase (Tri5) Gene in Three Field Isolates of Different Chemotype and Virulence.” *Molecular Plant Pathology* 7: 449–461.
- Malihipour, Ali, Jeannie Gilbert, Michele Piercey-Normore, and Sylvie Cloutier. 2012. “Molecular Phylogenetic Analysis, Trichothecene Chemotype Patterns, and Variation in Aggressiveness of *Fusarium* Isolates Causing Head Blight in Wheat.” *Plant Disease* 96: 1016–1025.
- Malonek, Stefan, Maria C. Rojas, Peter Hedden, Paul Gaskin, Paul Hopkins, and Bettina Tudzynski. 2004. “The NADPH-Cytochrome P450 Reductase Gene from *Gibberella fujikuroi* Is Essential for Gibberellin Biosynthesis.” *The Journal of Biological Chemistry* 279: 25075–2584.
- McCormick, Susan P., April M. Stanley, Nicholas A. Stover, and Nancy J. Alexander. 2011. “Trichothecenes: From Simple to Complex Mycotoxins.” *Toxins* 3: 802–814.
- McMullen, Marcia, S. Halley, B. Schatz, S. Meyer, J. Jordahl, and J. Ransom. 2008. “Integrated Strategies for *Fusarium* Head Blight Management in the United States.” *Cereal Research Communications* 36: 563–568.
- Menke, Jon. 2011. “A Study of *Fusarium graminearum* Virulence Factors”. PhD thesis, University of Minnesota: 1-211.
- Mullins, Jonathan G. L., Josie E. Parker, Hans J. Cools, Roberto C. Togawa, John A. Lucas, A. Bart, Diane E. Kelly, and Steven L. Kelly. 2011. “Molecular Modelling of the Emergence of Azole Resistance in *Mycosphaerella graminicola*.” *PloS One* 6: 1–11.
- Musiol, R., and W. Kowalczyk. 2012. “Azole Antimycotics – A Highway to New Drugs or a Dead End?” *Current Medicinal Chemistry* 19: 1–11.

-
- Nakajima, Takashi. 2010. "Fungicides Application against Fusarium Head Blight in Wheat and Barley for Ensuring Food Safety." In *Fungicides*, edited by Odile Carisse. InTech Publisher: 140–156.
- Nowaczyk, Alicja, and Bożena Modzelewska-Banachiewicz. 2008. "Triazole Derivatives with Antifungal Activity: A Pharmacophore Model Study." *Acta Poloniae Pharmaceutica - Drug Research* 65: 795–798.
- O'Donnell, Kerry, H. Corby Kistler, Beth K. Tacke, and Howard H. Casper. 2000. "Gene Genealogies Reveal Global Phylogeographic Structure and Reproductive Isolation among Lineages of *Fusarium graminearum*, the Fungus Causing Wheat Scab." *Proceedings of the National Academy of Sciences* 97: 7905–7910.
- O'Donnell, Kerry, Todd J. Ward, Dereje Aberra, H. Corby Kistler, Takayuki Aoki, Nathane Orwig, Makoto Kimura, Åsmund Bjørnstad, and Sonja S. Klemsdal. 2008. "Multilocus Genotyping and Molecular Phylogenetics Resolve a Novel Head Blight Pathogen within the *Fusarium graminearum* Species Complex from Ethiopia." *Fungal Genetics and Biology* 45: 1514–1522.
- O'Donnell, Kerry, Todd J. Ward, David M. Geiser, H. Corby Kistler, and Takayuki Aoki. 2004. "Genealogical Concordance between the Mating Type Locus and Seven Other Nuclear Genes Supports Formal Recognition of Nine Phylogenetically Distinct Species within the *Fusarium graminearum* Clade." *Fungal Genetics and Biology* 41: 600–623.
- Onyewu, Chiatogu, Jill R. Blankenship, Maurizio Del Poeta, and Joseph Heitman. 2003. "Ergosterol Biosynthesis Inhibitors Become Fungicidal When Combined with Calcineurin Inhibitors against *Candida albicans*, *Candida glabrata*, and *Candida krusei*." *Antimicrobial Agents and Chemotherapy* 47: 956–964.
- Osborne, Lawrence, and Jeff Stein. 2007. *Wheat Fungicide Recommendations*. South Dakota University Extension Service: 1-4.
- Pang, Sen, Liusheng Duan, Zhiqian Liu, Xiaoyu Song, Xuefeng Li, and Chengju Wang. 2012. "Co-Induction of a Glutathione-S-Transferase, a Glutathione Transporter and an ABC Transporter in Maize by Xenobiotics." *PloS One* 7: 1–5.
- Pang, Sen, Zhaojin Ran, Zhiqian Liu, Xiaoyu Song, Liusheng Duan, Xuefeng Li, and Chengju Wang. 2012. "Enantioselective Induction of a Glutathione-S-Transferase, a Glutathione Transporter and an ABC Transporter in Maize by Metolachlor and Its (S)-Isomer." *PloS One* 7: 1–4.
- Pasquali, Matias, and Corby Kistler. 2006. "*Gibberella zeae* Ascospore Production and Collection for Microarray Experiments." *Journal of Visualized Experiments* 115: 1-2.
- Pasquali, Matias, and Quirico Migheli. 2014. "Genetic Approaches to Chemotype Determination in Type B-Trichothecene Producing Fusaria." *International Journal of Food Microbiology* 189: 164–182.

-
- Paumi, Christian M., Matthew Chuk, Jamie Snider, Igor Stagljar, and Susan Michaelis. 2009. "ABC Transporters in *Saccharomyces cerevisiae* and Their Interactors: New Technology Advances the Biology of the ABCC (MRP) Subfamily." *Microbiology and Molecular Biology Reviews* 73: 577–593.
- Pirgozliev, Stoyan R., Simon G. Edwards, Martin C. Hare, and Peter Jenkinson. 2003. "Strategies for the Control of Fusarium Head Blight in Cereals." *European Journal of Plant Pathology* 1980: 731–742.
- Prasad, Rajendra, and Andre Goffeau. 2012. "Yeast ATP-Binding Cassette Transporters Conferring Multidrug Resistance." *Annual Review of Microbiology* 66: 39–63.
- Prasad, Rajendra, and Manpreet K. Rawal. 2014. "Efflux Pump Proteins in Antifungal Resistance." *Frontiers in Pharmacology* 5: 1–13.
- Prasad, Tulika, Sunesh Sethumadhavan, and Zeeshan Fatima. 2011. "Altered Ergosterol Biosynthetic Pathway - an Alternate Multidrug Resistance Mechanism Independent of Drug Efflux Pump in Human Pathogenic Fungi *C. Albicans*." In *Science against Microbial Pathogens: Communicating Current Research and Technological Advances*. Formatex Research Center: 757-768.
- Pritsch, C., G. J. Muehlbauer, W. R. Bushnell, D. A. Somers, and C. P. Vance. 2000. "Fungal Development and Induction of Defense Response Genes during Early Infection of Wheat Spikes by *Fusarium graminearum*." *Molecular Plant-Microbe Interactions* 13: 159–169.
- Procko, Erik, Megan L. O. Mara, W. F. Drew Bennett, D. Peter Tieleman, and Rachelle Gaudet. 2009. "The Mechanism of ABC Transporters: General Lessons from Structural and Functional Studies of an Antigenic Peptide Transporter." *The Federation of American Societies for Experimental Biology Journal* 23: 1287–1302.
- Punt, P. J., R. P. Oliver, M. A. Dingemanse, P. H. Pouwels, and C. A. van den Hondel. 1987. "Transformation of *Aspergillus* Based on the Hygromycin B Resistance Marker from *Escherichia coli*." *Gene* 56: 2280.
- Rea, Philip A. 1999. "MRP Subfamily ABC Transporters from Plants and Yeast." *Journal of Experimental Botany* 50: 895–913.
- Rees, Douglas C., Eric Johnson, and Oded Lewinson. 2009. "ABC Transporters: The Power to Change." *Nature Reviews Molecular Cell Biology* 10: 218–227.
- Reimann, Sven, and Holger B. Deising. 2005. "Inhibition of Efflux Transporter-Mediated Fungicide Resistance in *Pyrenophora tritici-repentis* by a Derivative of 4'-Hydroxyflavone and Enhancement of Fungicide Activity." *Applied and Environmental Microbiology* 71: 3269–3275.
- Rekanović, Emil, Milica Mihajlović, and Ivana Potočnik. 2011. "In Vitro Sensitivity of *Fusarium graminearum* (Schwabe) to Difenoconazole, Prothioconazole and Thiophanate-Methyl." *Pesticide Phytomedicine* 25: 325–333.

-
- Saag, Michael S., and William E. Dismukes. 1988. "Azole Antifungal Agents: Emphasis on New Triazoles." *Antimicrobial Agents and Chemotherapy* 32: 1–8.
- Sanguinetti, Maurizio, Brunella Posteraro, Barbara Fiori, Stefania Ranno, Riccardo Torelli, and Giovanni Fadda. 2005. "Mechanisms of Azole Resistance in Clinical Isolates of *Candida glabrata* Collected during a Hospital Survey of Antifungal Resistance." *Antimicrobial Agents and Chemotherapy* 49: 668–679.
- Sarver, Brice A. J., Todd J. Ward, Liane R. Gale, Karen Broz, H. Corby Kistler, Takayuki Aoki, Paul Nicholson, Jon Carter, and Kerry O'Donnell. 2011. "Novel Fusarium Head Blight Pathogens from Nepal and Louisiana Revealed by Multilocus Genealogical Concordance." *Fungal Genetics and Biology* 48: 1096–1107.
- Scauflaire, Jonathan, and Olivier Mahieu. 2011. "Biodiversity of Fusarium Species in Ears and Stalks of Maize Plants in Belgium." *European Journal of Agronomy* 131: 59–66.
- Schmitt, Lutz, and Robert Tampé. 2002. "Structure and Mechanism of ABC Transporters." *Current Opinion in Structural Biology* 12: 754–760.
- Seong, Kye-Yong, Matias Pasquali, Xiaoying Zhou, Jongwoo Song, Karen Hilburn, Susan McCormick, Yanhong Dong, Jin-Rong Xu, and H. Corby Kistler. 2009. "Global Gene Regulation by Fusarium Transcription Factors Tri6 and Tri10 Reveals Adaptations for Toxin Biosynthesis." *Molecular Microbiology* 72: 354–367.
- Shapiro, Rebecca S., Nicole Robbins, and Leah E. Cowen. 2011. "Regulatory Circuitry Governing Fungal Development, Drug Resistance, and Disease." *Microbiology and Molecular Biology Reviews* 75: 213–267.
- Sharma, Vandana, and Rakesh Bhatia. 2011. "Triazoles in Antifungal Therapy: A Review." *International Journal of Research in Pharmaceutical and Biomedical* 2: 417–427.
- Sharom, Frances J. 2008. "ABC Multidrug Transporters: Structure, Function and Role in Chemoresistance." *Pharmacogenomics* 9: 105–127.
- Sheehan, Daniel J., Christopher A. Hitchcock, and M. Carol. 1999. "Current and Emerging Azole Antifungal Agents Current and Emerging Azole Antifungal Agents." *Clinical Microbiology Reviews* 12: 40–79.
- Smith, Steven J., and Leo W. Parks. 1993. "The ERG3 Gene in *Saccharomyces cerevisiae* Is Required for the Utilization of Respiratory Substrates and in Heme-Deficient Cells." *Yeast* 9: 1177–1187.
- Son, Hokyong, Young-Su Seo, Kyunghun Min, Ae Ran Park, Jungkwan Lee, Jian-Ming Jin, Peijian Cao, Sae-Yeon Hong, Eun-Kyung Kim, Seung-Ho Lee, Aram Cho, Seunghoon Lee, Myung-Gu Kim, Jung-Eun kim, Jin-Cheol Kim, Hyung Ja Choi, Sung-hwan Yun, Jae Yun Lim, Minkyun Kim, Yong-Hwan Lee, Yang-Do Choi, Yin-Won Lee. 2011. "A Phenome-Based Functional Analysis of Transcription Factors in the Cereal Head Blight Fungus, *Fusarium graminearum*." *PLoS Pathogens* 7: 1–10.

-
- Spolti, Pierri, Emerson M. Del Ponte, Jaime A. Cummings, and Gary C. Bergstrom. 2014. "Triazole Sensitivity in a Contemporary Population of *Fusarium graminearum* from New York Wheat and Competitiveness of a Tebuconazole-Resistant Isolate." *Plant Disease* 98: 607–613.
- Starkey, David E., Todd J. Ward, Takayuki Aoki, Liane R. Gale, H. Corby Kistler, David M. Geiser, Haruhisa Suga, Beáta Tóth, János Varga, and Kerry O'Donnell. 2007. "Global Molecular Surveillance Reveals Novel *Fusarium* Head Blight Species and Trichothecene Toxin Diversity." *Fungal Genetics and Biology* 44: 1191–1204.
- Stathopoulos, Angelike M., and Martha S. Cyert. 1997. "Calcineurin Acts through the CRZ1/TCN1-Encoded Transcription Factor to Regulate Gene Expression in Yeast." *Genes Development* 11: 3432–3444.
- Stergiopoulos, Ioannis, Lute-Harm Zwiers, and Maarten A. De Waard. 2002. "Secretion of Natural and Synthetic Toxic Compounds from Filamentous Fungi by Membrane Transporters of the ATP-Binding Cassette and Major Facilitator Superfamily." *European Journal of Plant Pathology* 108: 719–734.
- Tateishi, Hideaki, Taiji Miyake, Masaru Mori, Rie Kimura, Yoneko Sakuma, and Toshihide Saishoji. 2010. "Sensitivity of Japanese *Fusarium graminearum* Species Complex Isolates to Metconazole." *Journal of Pesticide Science* 35: 419–430.
- Theiss, Stephanie, Marianne Kretschmar, Thomas Nichterlein, Herbert Hof, Nina Agabian, Jörg Hacker, and Gerwald a Köhler. 2002. "Functional Analysis of a Vacuolar ABC Transporter in Wild-Type *Candida albicans* Reveals Its Involvement in Virulence." *Molecular Microbiology* 43: 571–584.
- ThermoScientific. 2013. "pJET1.2/blunt Cloning Vector." CloneJET PCR Cloning Kit Manual: 1-2.
- Trail, Frances. 2009. "For Blighted Waves of Grain: *Fusarium graminearum* in the Postgenomics Era." *Plant Physiology* 149: 103–110.
- Trail, Frances, Iffa Gaffoor, and Steven Vogel. 2005. "Ejection Mechanics and Trajectory of the Ascospores of *Gibberella zeae* (anamorph *Fusarium graminearum*)." *Fungal Genetics and Biology* 42: 528–533.
- Troesken, Eva-Regina. 2005. "Toxicological Evaluation of Azole Fungicides in Agriculture and Food Chemistry". PhD thesis, University of Wuerzburg: 1-133.
- Wang, Jian-Hua, He-Ping Li, Bo Qu, Jing-Bo Zhang, Tao Huang, Fang-Fang Chen, and Yu-Cai Liao. 2008. "Development of a Generic PCR Detection of 3-Acetyldeoxynivalenol-, 15-Acetyldeoxynivalenol- and Nivalenol-Chemotypes of *Fusarium graminearum* Clade." *International Journal of Molecular Sciences* 9: 2495–2504.

-
- Wang, Jian-Hua, Mbacke Ndoeye, Jing-Bo Zhang, He-Ping Li, and Yu-Cai Liao. 2011. "Population Structure and Genetic Diversity of the *Fusarium graminearum* Species Complex." *Toxins* 3: 1020–1037.
- Wang, Shuangchao, Hideki Kondo, Liang Liu, Lihua Guo, and Dewen Qiu. 2013. "A Novel Virus in the Family Hypoviridae from the Plant Pathogenic Fungus *Fusarium graminearum*." *Virus Research* 174: 69–77.
- Wanjiru, Wanyoike Mary, Kang Zhensheng, and Heinrich Buchenauer. 2002. "Importance of Cell Wall Degrading Enzymes Produced by *Fusarium graminearum* during Infection of Wheat Heads." *European Journal of Plant Pathology* 108: 803–810.
- Ward, Todd J., Randall M. Clear, Alejandro P. Rooney, Kerry O'Donnell, Don Gaba, Susan Patrick, David E. Starkey, Jeannie Gilbert, David M. Geiser, and Tom W. Nowicki. 2008. "An Adaptive Evolutionary Shift in *Fusarium* Head Blight Pathogen Populations Is Driving the Rapid Spread of More Toxicogenic *Fusarium graminearum* in North America." *Fungal Genetics and Biology* 45: 473–484.
- Wegulo, Stephen N., Tamra A. Jackson, P. Stephen Baenziger, Michael P. Carlson, and John Hernandez Nopsa. 2008. *Fusarium Head Blight of Wheat*. Extension of the Institute of Agricultural and Natural Resources at the University of Nebraska-Lincoln: 1-8.
- Wink, Michael, Mohamed L. Ashour, and Mahmoud Zaki El-Readi. 2012. "Secondary Metabolites from Plants Inhibiting ABC Transporters and Reversing Resistance of Cancer Cells and Microbes to Cytotoxic and Antimicrobial Agents." *Frontiers in Microbiology* 3: 1–15.
- Woolley, D. W. 1944. "Some Biological Effects Produced By Benzimidazole And Their Reversal By Purines." *The Journal of Biological Chemistry* 152: 225–232.
- Yan, Xia, Wei-Bin Ma, Ya Li, Hong Wang, Ya-Wei Que, Zhong-Hua Ma, Nicholas J Talbot, and Zheng-Yi Wang. 2011. "A Sterol 14 a-Demethylase Is Required for Conidiation, Virulence and for Mediating Sensitivity to Sterol Demethylation Inhibitors by the Rice Blast Fungus *Magnaporthe oryzae*." *Fungal Genetics and Biology* 48: 144–153.
- Yin, Y., X. Liu, B. Li, and Z. Ma. 2009. "Characterization of Sterol Demethylation Inhibitor-Resistant Isolates of *Fusarium asiaticum* and *F. graminearum* Collected from Wheat in China." *Phytopathology* 99: 487–497.
- Yli-Mattila, Tapani, Tatiana Gagkaeva, Todd J. Ward, Takayuki Aoki, H. Corby Kistler, and Kerry O'Donnell. 2009. "A Novel Asian Clade within the *Fusarium graminearum* Species Complex Includes a Newly Discovered Cereal Head Blight Pathogen from the Russian Far East." *Mycologia* 101: 841–852.
- Yoshida, Megumi, Takashi Nakajima, Kenta Tomimura, Fumihiko Suzuki, Michiyoshi Arai, and Atsushi Miyasaka. 2012. "Effect of the Timing of Fungicide Application on *Fusarium* Head Blight and Mycotoxin Contamination in Wheat." *Plant Disease* 96: 845–851.

- Yu, Jae-Hyuk, Zsuzsanna Hamari, Kap-hoon Han, and Jeong-Ah Seo. 2004. "Double-Joint PCR: A PCR-Based Molecular Tool for Gene Manipulations in Filamentous Fungi." *Fungal Genetics and Biology* 41: 973–981.
- Zhang, Xiao-Wei, Lei-Jie Jia, Yan Zhang, Gang Jiang, Xuan Li, Dong Zhang, and Wei-Hua Tang. 2012. "In Planta Stage-Specific Fungal Gene Pro Fi Ling Elucidates the Molecular Strategies of *Fusarium graminearum* Growing inside Wheat Coleoptiles." *Plant Cell*: 1–18.
- Zhang, Yu, Zhenying Zhang, Xinyu Zhang, Hanxing Zhang, Xianyun Sun, Chengcheng Hu, Shaojie Li, and Michael Lorenz. 2012. "CDR4 Is the Major Contributor to Azole Resistance among Four Pdr5p-like ABC Transporters in *Neurospora crassa*." *Fungal Biology* 116: 848–854.

Acknowledgements

I would like to express my heartfelt thanks to my supervisor, Dr. Stefan G. R. Wirsal (MLU), for his guidance and knowledge in producing a research paper and my dissertation. Furthermore, I thank him for his motivation and his experiences on how we should act as professional scientists.

My sincere thanks go to Prof. Dr. H. B. Deising (MLU) who gave me the opportunity to pursue my PhD study in his research group. I also thank him for creating and managing a constructive academic atmosphere that allows students to focus on their research and achieve their goals.

I sincerely thank also the Deutscher Akademischer Austausch Dienst (DAAD = German Academic Exchange Service) for my scholarship. The knowledge I gained while studying in Germany will allow me to make valuable contributions to my research institution in Indonesia. In addition, my time in Germany has left me with many pleasant memories that will surely last a life time.

Many thanks are also dedicated to my working institute, PT. SMART, Tbk, especially to Mr. Jo Daud Dharsono, who as the chairman permitted me to study at MLU and who financed my German course at the Goethe Institute in Jakarta. Furthermore, I thank Dr. Tony Liwang and Dr. Condro Utomo who supported the administration process during my study. I am especially thankful also to Dr. William Henderson and Ms. Lisa Muliani who assisted me with the English proofreading of my dissertation.

I also gratefully appreciate working together with my colleague, Ms. Ghada Abou Ammar, for the frequent discussions and the sharing of valuable knowledge. Many thanks go also to the entire Phytopathology group at MLU, especially to Dr. Rayko Becher, Dr. Jorrit-Jan Krijger for their ideas, suggestions and constructive criticism provided. To Mrs. Andrea Beutel, Mrs. Doris Jany and Mrs. Elke Vollmer, thank you for your kind assistance in the laboratory and in the green house.

To my parents, parents in law, and my family, my heartfelt thanks for all your support. Finally a very special thank you to my wife Anna Safarrida who has been so very patient and supportive, and for our son, Azka Raffanno Rafiulshidqi, the greatest joy and motivation in our life.

Curriculum Vitae

Personal Data

Name: Reno Tryono
Date of birth: 18th March 1982
Place of birth: Jakarta, Indonesia
Nationality: Indonesian
Family status: Married, one child

Professional experience

2007 – Today: Research officer at the Plant Production and Biotechnology Division of PT. SMART, Tbk., Sentul, Indonesia.

Educational background

2010 – 2014: Doctoral studies at the Institute of Agricultural and Nutritional Sciences, Martin-Luther-University Halle-Wittenberg, Germany.
2004 – 2006: Master studies at the Department of Entomology and Phytopathology, Bogor Agricultural University, Bogor, Indonesia.
1999 – 2004: Bachelor studies at Department of Plant Pest and Disease Science, Brawijaya University, Malang, Indonesia.

List of Scientific Publications

- Ammar, G. A., **Tryono, R.**, Döll, K., Karlovsky, P., Deising, H. B., Wirsal, S. G. R. 2013. Identification of ABC transporter genes of *Fusarium graminearum* with roles in azole tolerance and/or virulence. *Plos One* 8(11): 1-13.
- Abou Ammar G., **Tryono R.**, Becher R., Deising H.B., Wirsal S.G.R. 2014. Contribution of ABC transporters to azole resistance and virulence in *Fusarium graminearum*. IN: Modern Fungicides and Antifungal Compounds, eds.: Dehne H.W., Deising H.B., Gisi U., Fraaije B., Hermann, D., Mehl, A., Oerke, E.C., Russell P.E., Stammler, G., Kuck K.H., Lyr H., Vol. VII, pp 117-122. DPG, Braunschweig.

Declaration

Hereby, I declare that the work in this dissertation is the original work of the author and that no other than the quoted references or resources have been used. This work has not been submitted entirely or partially to any other institution for any other academic award.

I further declare that there are no legal proceedings instituted against me.

Halle (Saale), December 2015

Reno Tryono